UNIVERSIDAD AUTÓNOMA DE MADRID

PROGRAMA DE DOCTORADO EN BIOCIENCIAS MOLECULARES

Regulation of leg development by '*dysfusion*' in *Drosophila melanogaster*: From pattern formation to morphogenesis

Sergio Córdoba Casado

Madrid, 2018

DEPARTAMENTO DE BIOLOGÍA MOLECULAR
FACULTAD DE CIENCIAS

UNIVERSIDAD AUTÓNOMA DE MADRID

Regulation of leg development by '*dysfusion*' in *Drosophila melanogaster*: From pattern formation to morphogenesis

Tesis Doctoral presentada por:

Sergio Córdoba Casado, Licenciado en Biología

Director y Tutor:

Dr. Carlos Estella Sagrado

Tesis Realizada en el *Departamento de Desarrollo y Regeneración*
Centro de Biología Molecular Severo Ochoa (CBMSO)

Madrid, 2018

'To think that heredity will build organic beings without mechanical means is a piece of unscientific mysticism'

Wilhelm His, 1988

A Ana

A mi familia

INDEX

SUMMARY

Development relies on the sequential deployment of different morphogenetic mechanisms that operates at the level of cells, tissues and organs to shape the body of living organisms. Morphogenesis is the result of the implementation of cellular behaviors, such as proliferation, apoptosis or cell movements, that are directed by an underlying patterning network that subdivides the tissue in territories of distinctive gene expression. This regulatory network arises as the result of the hierarchical interactions of transcription factors, which expression is tightly controlled in time and space. Nevertheless, despite pattern formation and morphogenesis are widely studied separately, much less is known about how they are coordinated. In this work, we use *Drosophila* leg joint development as a model to study how genetic patterning directs the formation of biological structures.

We have found that the gene *dysfusion* (*dysf*), which encodes for a bHLH-PAS transcription factor is expressed specifically at the four tarsal joints of the *Drosophila* leg, and is completely required for their formation. We demonstrated that the Notch signaling pathway directly regulates *dysf* expression, which is restricted to the tarsal region of the leg by the presence of a secondary regulatory input. Two processes, regulation of Rho GTPase activity and programmed cell death have been previously implicated in tarsal joint morphogenesis, and Dysf transcriptionally controls the expression of both Rho GTPase regulators and pro-apoptotic genes at the presumptive tarsal joints. We show here that Dysf promotes apical localization and activation of the Rho1 GTPase, a key regulator of acto-myosin cytoskeleton dynamics and apical constriction, to form epithelial folds and adult joints in the tarsal region of the leg. Surprisingly, we do not observe joint defects when apoptosis is inhibited, a result that opposes previous models for joint development. Moreover, ectopic activation of Dysf, Rho1, or Rho1 downstream effectors is sufficient to generate folds in the wing disc epithelium, a phenotype that is independent of cell death. Our results highlight the coordination between a patterning transcription factor and the cellular processes that cause the cell shape changes necessary to sculpt a flat epithelium into a three dimensional structure.

El desarrollo se vale del despliegue secuencial de distintos mecanismos morfogenéticos, que operan al nivel de las células, los tejidos y los órganos para dar forma al cuerpo de los organismos vivos. La morfogénesis es el resultado de la acción coordinada de diferentes comportamientos celulares, tales como proliferación, apoptosis o movimientos celulares, los cuales son dirigidos por un mecanismo subyacente de formación de patrón que subdivide el tejido en territorios con expresión génica diferencial. Esta red de regulación emerge como resultado de las interacciones jerárquicas entre factores de transcripción, cuya expresión es finamente regulada en el tiempo y el espacio. Sin embargo, a pesar de que los procesos de formación de patrón y morfogénesis han sido ampliamente estudiados por separado, se sabe poco acerca de cómo se coordinan. En este trabajo, utilizamos el desarrollo de las articulaciones de la pata de *Drosophila* como modelo para estudiar cómo la regulación genética dirige la formación de estructuras biológicas.

El gen *dysfusion* (*dysf*), que codifica para un factor de transcripción de tipo bHLH-PAS, se expresa específicamente en las cuatro articulaciones tarsales de la pata de *Drosophila*, y es completamente necesario para su formación. Hemos demostrado que la actividad de Notch regula directamente la expresión de *dysf*, que es restringida a la región tarsal de la pata por la presencia de un elemento regulador adicional. Dos procesos, la regulación de la actividad de Rho GTPasas y la muerte celular programada han sido previamente relacionados con la morfogénesis de las articulaciones tarsales. Dysf controla transcripcionalmente tanto la expresión de reguladores de Rho GTPasas como la de genes pro-apoptóticos en las articulaciones tarsales en desarrollo. En este trabajo demostramos que Dysf promueve la localización apical y la activación de la GTPasa Rho1, un regulador clave de la dinámica del citoesqueleto de acto-miosina y de la constricción apical, para dirigir la formación de pliegues epiteliales y las articulaciones adultas en la región tarsal de la pata. Sorprendentemente, no observamos defectos en la formación de las articulaciones cuando inhibimos la muerte celular, un resultado que contrasta con modelos previamente propuestos. Además, la activación ectópica de Dysf, Rho1, o de efectores dependientes de Rho1 es suficiente para generar pliegues en el epitelio del disco de ala, de forma independiente de muerte celular. Nuestros resultados presentan la coordinación entre un factor de transcripción que determina el patrón de la pata y los procesos celulares que causan los cambios de forma necesarios para transformar un epitelio plano en una estructura tridimensional.

ABBREVIATIONS

A-P: Anterior-Posterior (antero-posterior) axis

acto-myosin: relative to F-actin and Myo II interactions, generally to generate contractility force

APF: After Puparium Formation

Bab: Bric-à-brac

Bib: Big brain

bp: base pairs

Bowl: Brother of odd with entrails limited

Chr.: Chromosome

Ci: Cubitus interruptus

CRM: *cis*-regulatory module

D-V: Dorsal-Ventral (dorso-ventral) axis

Dac: Dachshund

Dcp1: Death caspase 1

Dia: Diaphanous

Diap1: Death-associated inhibitor of apoptosis 1

Dl: Delta

Dlg: Discs-large

Dll: Distalless

DNA: Deoxyribonucleic acid

Dpp: Decapentaplegic

Drak: Death-associated protein kinase related

Drm: Drumstick

Dronc: Death regulator Nedd2-like caspase

Dysf: Dysfusion

E(spl)mβ: Enhancer of split mβ

F-actin: Filamentous Actin

Fog: Folded gastrulation

FRT: Frequent Recombination Targets

GEF: Guanine nucleotide exchange factor

GAP: GTPase-activating protein

Hh: Hedgehog

Hid: Head involution defective

Hth: Homothorax

Imaginal discs: epithelial sac-like structures that will give rise to most of the cuticular structures of the adult (wings, legs, genitalia, etc.). The term *'disc'* is usually used instead of *'imaginal disc'*

JNK: c-Jun N-terminal Kinase

Myo II: Nonmuscle Myosin Type II

N: Notch

$Notch^{ECD}$: Notch Extracellular Domain

$Notch^{ICD}$: Notch Intracellular Domain

Odd: Odd skipped

P-D: Proximal-Distal (proximo-distal) axis

P-Mad: Phosphorylated form of the Mother against Dpp protein

PCP: Planar Cell Polarity

Phal: Phalloidin

Ptc: Patched

RNA: Ribonucleic acid

RNAi: Interference RNA

Rpr: Reaper

RHG: Reaper, Hid and Grim

Rn: rotund

Rok: Rho kinase

Ser: Serrate

Sna: Snail

Sob: Sister of odd and bowl

Sqh: Spaghetti squash

Ss: Spineless

Su(H): Supressor of Hairless

Tgo: Tango

TUNEL: Terminal deoxynucleotidyl transferase dUTP nick end labeling

TFs: Transcription Factors

Trh: Trachealess

TOPRO: TO-PRO™-3 Iodide (642/661)

Twi: Twist

Zip: Zipper

INTRODUCTION

1. From Pattern formation to Morphogenesis

The plans and directions that guide the formation of an organism are encoded in its genome. The goal of developmental biology is to unravel the mechanisms through which this genetic information is translated into cellular and tissue behaviors that are coordinated to form an organism from a single egg cell. The processes that shape organisms during development, such as cell proliferation, cell differentiation, cell shape changes and cell movements, are ultimately regulated by underlying genetic networks (WOLPERT AND TICKLE 2011). The acquisition of form, morphogenesis, is a central topic in developmental biology. Through morphogenesis, that requires the integration of genetic networks and cellular behaviors, tissues and organisms acquire their correct shape.

1.1. Genetic regulation of pattern formation

Pattern formation refers to the acquisition of different cell fates in a developing tissue according to the relative position that cells occupy within it. This process requires the precise regulation of gene expression in time and space. The progressive generation of different cell fates is the prerequisite for the implementation of coordinated cellular behaviors in distinct groups of cells. Importantly, the genetic patterning of the embryo or of any given organ is usually carried out by transcription factors (TFs), DNA binding proteins that are capable of regulating gene expression.

One of the best-known examples of pattern formation is the specification of the embryonic body plan of the fruit fly, *Drosophila melanogaster* (reviewed in WOLPERT AND TICKLE 2011). During *Drosophila* embryogenesis, cascades of gene expression pattern the two main body axes, giving positional identity to the cells that form the early embryo (Figure I-1A). The formation of the anterior-posterior (A-P) axis is initiated by positional cues already present in the egg. These lead to the expression, in a sequence in which each step depends on the previous one, of 'Gap genes', 'Paired-rule genes' and 'Segment polarity genes' (NUSSLEIN-VOLHARD AND WIESCHAUS 1980; HULSKAMP AND TAUTZ 1991). The final result of this process is the division of the embryo in a succession of repeated developmental units or parasegments (GARCIA-BELLIDO *et al.* 1973; MARTINEZ-ARIAS AND LAWRENCE 1985) (Figure I-1B). The segmentation genes also regulate the expression of the *homeobox-containing* (*Hox*) genes that provide segmental identity along the A-P axis (*e.g.* thoracic, abdominal, etc.) (LAWRENCE AND MORATA 1977) (MANN AND MORATA 2000). Similarly, maternally provided positional cues determine the localized activity of the Dorsal protein, which in turn organize the dorsal-ventral (D-V) axis of the early embryo (ANDERSON 1998) (Figure I-1C). Nevertheless, the genetic control of pattern formation is not only important to establish the body axes, it is a general process required to organize any developing tissue, as described for the formation of the veins in the *Drosophila* wing or in the development of the vertebrate neural cord (DE CELIS 2003; LE DREAU AND MARTI 2012).

1.2. Morphogenetic processes shape developing tissues

One of the most prominent processes regulated by pattern formation is morphogenesis. In particular, epithelial morphogenesis is of special interest for developmental biology for its contribution to organ formation and overall body shaping. This process generates three-dimensional structures out of more simple, two-dimensional layers of cells, thus incrementing the morphological complexity in the developing animal. Changes of form are caused by different events that include cell shape modifications, cell intercalation, cell migration, cell division and cell death (SCHOCK AND PERRIMON 2002). Importantly, cell adhesion plays a fundamental role in the maintenance of epithelial integrity and allowing force transmission between neighboring cells during morphogenesis (WOLPERT AND TICKLE 2011; GILMOUR *et al.* 2017). The cytoskeleton is essential for the generation of forces within the cell and the transmission of these forces across the epithelium to drive morphogenesis. The actin filaments (F-actin) are especially relevant in this context: polymerization of F-actin occurs at the leading edge of migrating cells, and the interaction between F-actin and the nonmuscle Myosin II (MyoII) motor protein leads to acto-myosin contractility, a process that generates force and is required for multiple morphogenetic events (YOUNG *et al.* 1993; RIDLEY *et al.* 2003; QUINTIN *et al.* 2008; VASQUEZ AND MARTIN 2016; GILMOUR *et al.* 2017).

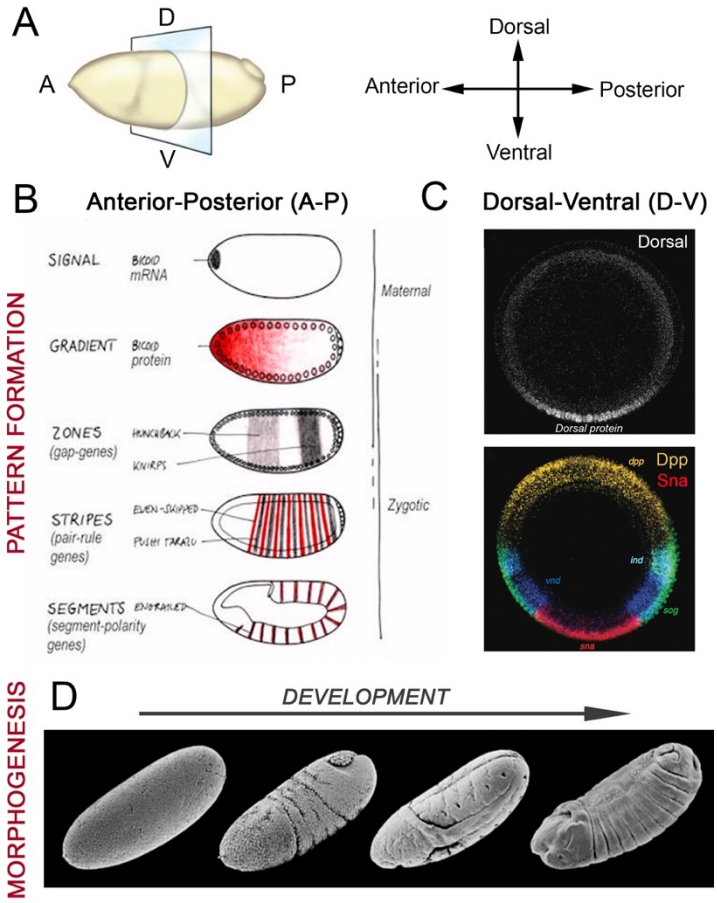

Figure I-1: Early patterning and morphogenesis in the *Drosophila* embryo. (A) Representation of the main body axes of the *Drosophila* embryo: Anterior, A; Posterior, P; Dorsal, D; and Ventral, V. **(B)** The hierarchical cascade of TFs that regulates A-P segmentation of the early embryo. **(C)** Induction of D-V axis patterning is initiated by the localization of Dorsal protein in the ventral region of the embryo (REEVES AND STATHOPOULOS 2009). **(D)** Pattern formation is a prerequisite for the implementation of the morphogenetic processes that cause shape changes in the embryo.

Collective tissue behaviors then emerge as the result of the integration and transmission of the forces generated by individual cell shape changes across the epithelium (SCHOCK AND PERRIMON 2002; KELLER 2012; HEISENBERG AND BELLAICHE 2013; GILMOUR *et al.* 2017). The main players and mechanisms that carry out epithelial morphogenesis are highly conserved, as demonstrated by numerous studies in different model organisms; from seminal early studies in Amphibian gastrulation and mammalian neurulation to the genetic approach that can

be achieved using *Drosophila melanogaster* (NUSSLEIN-VOLHARD AND WIESCHAUS 1980; GORDON 1985; KELLER 2012) and reviewed in GILMOUR *et al.* 2017).

However, and despite the extensive knowledge we have regarding the mechanisms that control tissue patterning and cell behavior separately, much less is known about how these two processes are coordinated (GILMOUR *et al.* 2017). In this context, the studies carried out in the past two decades by the groups of Maria Leptin and Eric Wieschaus, among others, regarding the genetic control of *Drosophila* gastrulation are helping to understand how patterning and morphogenesis are linked. During *Drosophila* gastrulation, peak levels of Dorsal activate the *twist* (*twi*) and *snail* (*sna*) genes in the ventral region of the embryo. Subsequently, these transcription factors regulate Rho1 activity, leading to apical constriction that cause the ventral furrow cells to invaginate (BARRETT *et al.* 1997; HACKER AND PERRIMON 1998; DAWES-HOANG *et al.* 2005; KOLSCH *et al.* 2007; MARTIN *et al.* 2009) (Figure I-9).

In the present work we aim to understand the connection between patterning signals and cell behaviors that drive tissue morphogenesis using the development of tarsal joints in the leg of *Drosophila melanogaster* as a model.

2. *Drosophila melanogaster* as a model for development

From a genetic perspective, *Drosophila* is one of the best-characterized model organisms for developmental studies. Its genome is entirely sequenced and a great fraction of its genes are functionally and molecularly annotated thanks to the contributions of generations of researchers dating back to Thomas Hunt Morgan, who first established *Drosophila* as a model for genetics in the early 1900s (ADAMS *et al.* 2000; RUBIN AND LEWIS 2000; BELLEN *et al.* 2010). The wide availability of mutants, the tools that allow clonal analysis, and the two-components systems to perform ectopic gene expression are among the most useful resources that *Drosophila* presents, and allow precise genetic manipulations (KORNBERG AND KRASNOW 2000; DEL VALLE RODRIGUEZ *et al.* 2012) and see Materials and Methods). In addition, basic cellular functions as well as complex processes (*e.g.* development, cell signaling pathways, innate immunity, etc.) are conserved between the fly and mammals, including humans, and many *Drosophila* genes have mammalian orthologs. Moreover, the genetic complement of *Drosophila* is relatively small (~14.000 genes) and presents few duplicated genes, which has proven useful to unveil regulatory pathways in humans and assign gene functions based on their *Drosophila* counterparts (KORNBERG AND KRASNOW 2000; WANGLER *et al.* 2015). Last but not least, other characteristics of the fly such as its inexpensiveness, elevated progeny and short life cycle further helps *Drosophila*'s case as a suitable model organism.

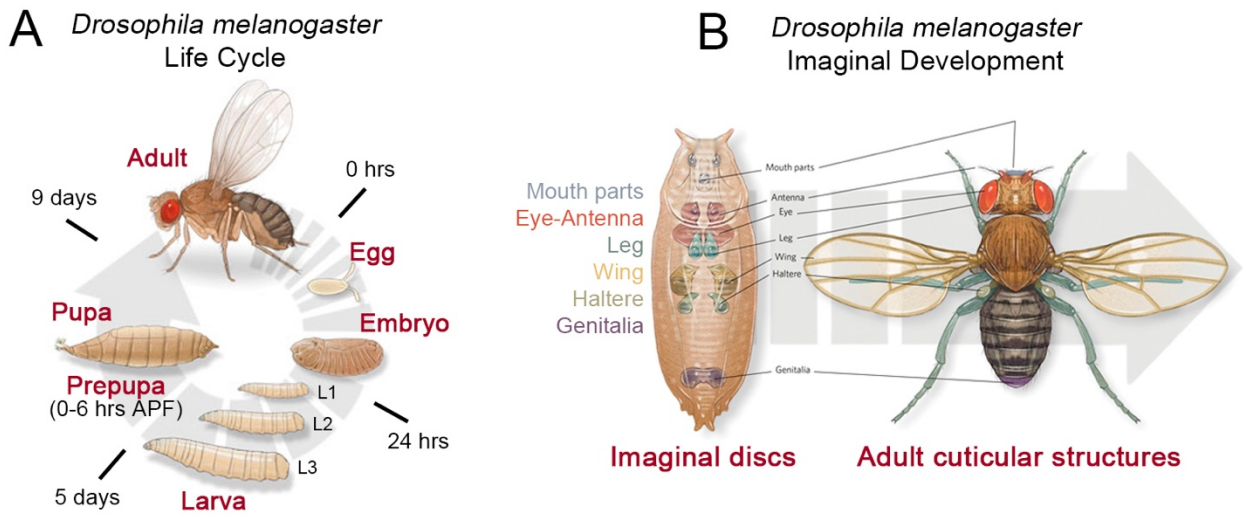

Figure I-2: *Drosophila* life cycle and imaginal development. (A) Life cycle of *Drosophila* depicting its four life stages (Adult, Embryo, Larva and Pupa) and the developmental time when change of stage occurs (raising *Drosophila* in standard conditions, at 25°C). **(B)** The imaginal discs in the larval and prepupal stages prefigure the adult cuticular structures. The colors of the imaginal discs matches the corresponding adult body parts.

Drosophila is a holometabolous insect with four distinct life stages (embryo, larva, pupae and adult) and a relative short life cycle that lasts ~10 days at 25°C (Figure I-2A). After fertilization, the egg is laid and starts embryonic development, where the main body plan is established and the three germ layers are formed. Importantly, at this stage the primordia of the imaginal discs are specified from the embryonic ectoderm (BATE AND ARIAS 1991; COHEN *et al.* 1993; WOLPERT AND TICKLE 2011). Imaginal discs are epithelial sac-like structures that will give rise, after metamorphosis, to most of the cuticular structures of the adult (wings, legs, genitalia, etc.). The imaginal discs are named after the adult structure they form, *e.g.* the wing disc, the leg disc or the eye-antenna disc (VON KALM *et al.* 1995; WOLPERT AND TICKLE 2011) (Figure I-2B). There are 19 imaginal discs, 9 pairs and the genitalia, that grow during larval development and, are progressively patterned by the restricted expression of transcription factors. TFs confer specific identities to each presumptive parts of the adult structures (BEIRA AND PARO 2016). A pulse of the steroid hormone ecdysone triggers pupation, where metamorphosis takes place: larval tissues are eliminated and the imaginal discs evert and fuse to each other to form the adult body (PASTOR-PAREJA *et al.* 2004; ALDAZ *et al.* 2010; WOLPERT AND TICKLE 2011).

3. Leg development in *Drosophila*

Appendages are all the structures that projects out from the body wall, and in invertebrates include antennae, genitalia, legs and wings, among others. They allow the implementation of diverse biological functions such as reproduction, environment sensing, locomotion or flight (SHUBIN *et al.* 1997). The vast morphological diversity of their appendages has contributed to the evolutionary success of arthropods, and especially of insects, the more diverse animal group representing over three quarters of all the living species (ENGEL 2015; JOCKUSCH 2017). The possibility to articulate these appendages by the presence of movable joints is key for

appendage function. Indeed, the presence of joints is what gives arthropods their name (from Greek *árthron*, 'joint' and *pous*, 'foot'). Specifically in the legs, specialized appendages for terrestrial locomotion, the articulation provided by flexible joints is fundamental for their function. In our model organism, *Drosophila melanogaster*, the leg is composed by 10 segments (from proximal to distal: *coxa*, *trochanter*, *femur*, *tibia*, five *tarsal* segments (*t1-t5*) and *pretarsus*), which are separated by the presence of flexible joints.

3.1 Genetic patterning of the *Drosophila* leg

All appendages require the formation of a proximo-distal (P-D) axis that must be established *de novo* orthogonally to the preexisting A-P and D-V main body axes. Leg appendages are specified during embryogenesis, and the expression of an intricate code of transcription factors along the P-D axis of the developing limb determines the identity of the future adult segments of the leg. This information is later interpreted to localize bands of Notch activity that would direct the formation of the joints that separate each segment from the adjacent ones.

3.1.1. Establishment of the proximo-distal axis of the leg

Drosophila legs are specified during embryogenesis as ventral appendage primordia by the expression of the homeobox gene *Distalless* (*Dll*) and the two paralogous genes *buttonhead* (*btd*) and *Sp1* (COHEN 1990; COHEN *et al.* 1993; ESTELLA *et al.* 2003; MCKAY *et al.* 2009; ESTELLA AND MANN 2010; CORDOBA *et al.* 2016) (Figure I-3A). The newly formed leg primordium is divided in anterior (A) and posterior (P) compartments by the function of *engrailed* (*en*), which specifies posterior identity. Hedgehog (Hh), a short-range ligand, is produced and secreted by cells of the P compartment and induces the expression of two long-range signaling molecules, Decapentaplegic (Dpp) and Wingless (Wg), in cells of the A compartment that are adjacent to the A-P boundary (BASLER AND STRUHL 1994). Hh activates *dpp* expression in the dorsal half of the leg disc and *wg* expression in the ventral half to determine dorsal and ventral identities, respectively (STRUHL AND BASLER 1993; WILDER AND PERRIMON 1995; JOHNSTON AND SCHUBIGER 1996; MORIMURA *et al.* 1996; THEISEN *et al.* 1996; SVENDSEN *et al.* 2015).

Wg and Dpp inputs act combinatorially to establish the P-D axis by activating the expression of *Dll* and *dachshund* (*dac*) in concentric rings in the leg disc to determine distal and medial fates, respectively (CAMPBELL *et al.* 1993; DIAZ-BENJUMEA *et al.* 1994; LECUIT AND COHEN 1997; ESTELLA AND MANN 2008; ESTELLA *et al.* 2008; GIORGIANNI AND MANN 2011). Cells at the periphery of the disc that receive low levels of combined Wg and Dpp activate the expression of *homothorax* (*hth*), and are fated as the proximal region of the leg disc (GONZÁLEZ-CRESPO AND MORATA 1996; ABU-SHAAR AND MANN 1998; GONZALEZ-CRESPO *et al.* 1998). Thus, the P-D axis is broadly defined by the expression domains of *hth*, *dac* and *Dll*, which are collectively known as the 'leg gap genes' (reviewed in ESTELLA *et al.* 2012) (Figure I-3B).

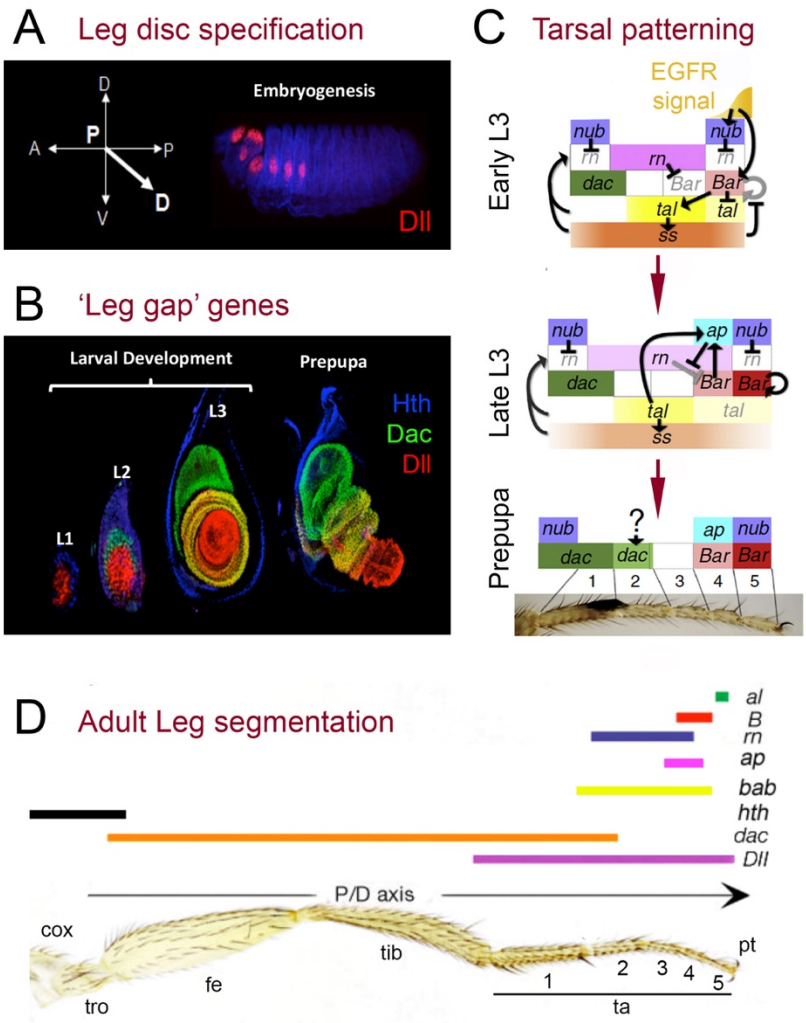

Figure I-3: Leg patterning in *Drosophila*. (A) Specification of the leg disc primordia is initiated by the expression of *Dll* (red) during embryogenesis. **(B)** Expression of the 'leg gap' genes *Hth* (blue), *Dac* (green) and *Dll* (red) through the three instars of larval development (L1, L2 and L3) and in a prepupal leg disc. **(C)** Genetic network patterning the tarsal region of the leg in response to EGFR signaling (yellow) through L3 and prepupal development. Note the complex genetic interactions that subdivide the tarsal region into five differentiated segments (modified from KOJIMA 2017). **(D)** Expression of different TFs (color bars above the leg) in nested domains along the P-D axis of the leg determine the identity of each future adult segment (modified from (CAMPBELL 2002). From proximal to distal: *coxa* (cox), *trochanter* (tro), *femur* (fe), *tibia* (tib), five *tarsal* segments (ta 1-5) and *pretarsus* (pt).

The tarsal region of the leg is further subdivided by a complex genetic network that is initiated by the activation of the Epidermal Growth Factor Receptor (EGFR) pathway. The EGFR ligand Vein is expressed in the distal-most tip of the leg disc and form a distal to proximal morphogen gradient to promote nested domains of target gene expression (CAMPBELL 2002; GALINDO *et al.* 2002) (Figure I-3C). High levels of the EGFR pathway activate the expression of *clawless* (*cl*, also known as *C15*), *aristalless* (*al*) and *Lim1*, in the distal-most tip of the leg disc that will form the pretarsus (CAMPBELL 2005). *BarH1* and *BarH2* (collectively referred as *Bar*) homeobox genes and *apterous* (*ap*) are expressed in response to EGFR in a more proximal region (KOJIMA *et al.* 2000; PUEYO *et al.* 2000). Early during third instar stage *Bar* expression abuts proximally with that of *dac*, and as the disc grows *Bar* and *dac* expression domains become separated by a gap that enables the expression of *rotund* (*rn*) (NATORI *et al.* 2012). Simultaneously, Bar non-autonomously activates the expression of *tarsal-less* (*tal*) that in turn activate *spineless* (*ss*) transiently in the tarsal region (DUNCAN *et al.* 1998; EMMONS *et al.* 1999; PUEYO AND COUSO 2008). This regulatory network is highly dynamic, due to the constant growth of the leg disc during third instar stage (NATORI *et al.* 2012). Moreover, other inputs such as the expression of the *odd-skipped* family member *brother of odd with entrails limited* (*bowl*), activated by Notch activity, or *bric-à-brac* (*bab*) in response to *rn* also play a role in specification of the tarsal region (GODT *et al.* 1993; COUDERC *et al.* 2002; DE CELIS IBEAS AND BRAY 2003; BAANANNOU *et al.* 2013).

The final result of this complex genetic regulation is the eventual subdivision of the leg disc into discrete regions of gene expression that will determine the identity of each segment of the adult leg (SUZANNE 2016; KOJIMA 2017) (Figure I-3D).

3.1.2 Genetic regulation of joint formation

The P-D subdivision of the leg disc by the restricted expression of transcription factors serves as a blueprint for the positioning of Notch ligands. Thus, *Delta* (*Dl*) and *Serrate* (*Ser*) are expressed in a band of cells located distally in each presumptive segment of the leg. However, how such a complex combination of TFs is integrated at the molecular level to activate *Dl* and *Ser* expression in each segment is mostly unknown (RAUSKOLB 2001; CORDOBA *et al.* 2016). Physical contact between ligands Dl/Ser and their receptor activates the Notch pathway in stripes of cells adjacent and distal to Dl and Ser. Notch activity directs the formation of all the joints and contributes to the growth of the leg disc (DE CELIS *et al.* 1998; BISHOP *et al.* 1999; RAUSKOLB AND IRVINE 1999) (Figure I-4A). Planar cell polarity (PCP) prevents the activation of Notch in the proximal border of the Dl/Ser positive cells. Therefore, in PCP defective legs a double joint phenotype is observed as a consequence of the symmetric activation of Notch at each side of Dl/Ser expressing cells (CAPILLA *et al.* 2012). After all positional information is set, another round of EGFR activation in the proximal end of each segment also contributes to

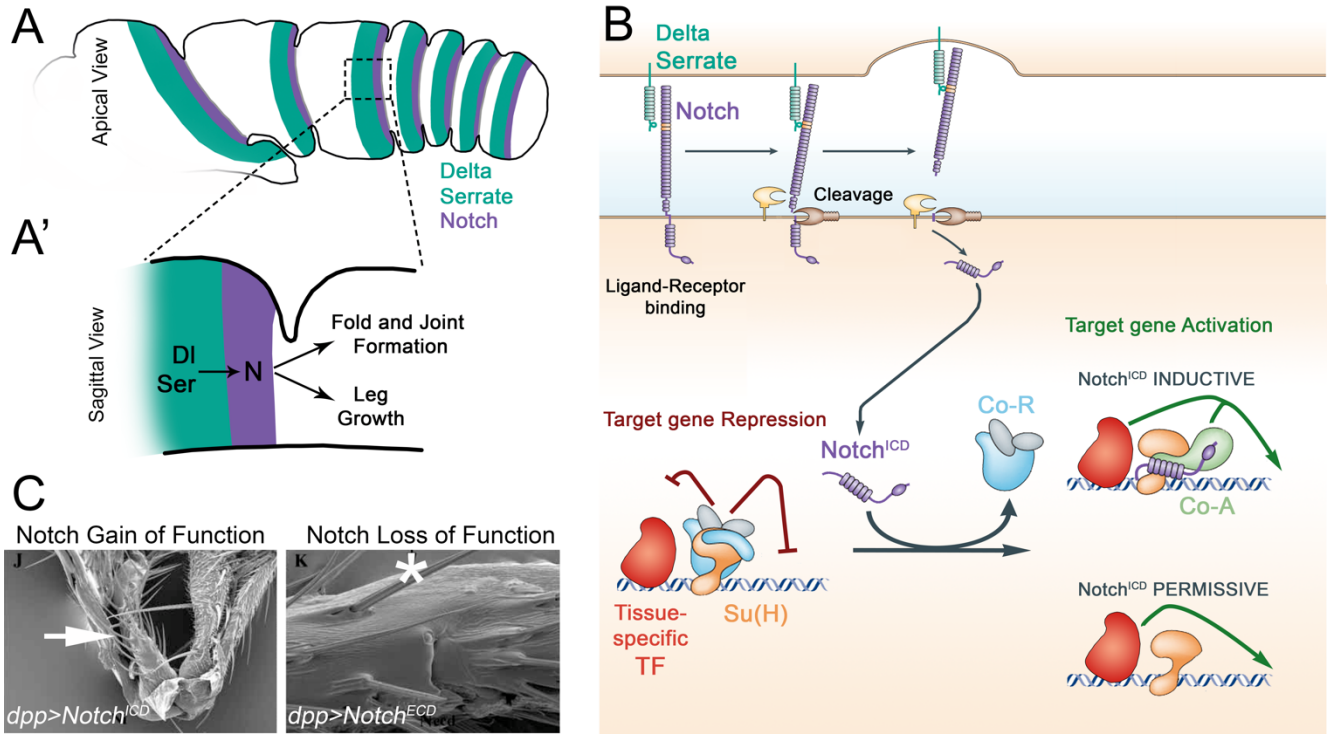

Figure I-4: Notch regulation of leg joint development. (A) Localization of Dl/Ser (green) in rings at the distal part of every leg segment cause Notch activation (purple) in a band of cells distal to Dl/Ser domains. Notch activation is then required for joint formation and leg growth **(A')**. **(B)** Molecular mechanism of Notch pathway activation and regulation of target genes. Notch receptor is cleaved upon ligand binding; Notch^{ICD} translocate into the nucleus where binds Su(H) to regulate target gene expression (details in the main text) (modified from BRAY 2006). **(C)** Ectopic activation of the Notch pathway cause ectopic folds in the leg (arrow), whereas Notch inhibition disrupts endogenous joint formation (asterisk) (DE CELIS *et al.* 1998).

repress Notch targets in the proximal border of the Dl/Ser domain (GALINDO *et al.* 2005). Ligand binding to the Notch receptor cause its proteolitic cleavage and the release of its intracellular domain ($Notch^{ICD}$) that is translocated to the nucleus, where it binds to Supressor of Hairless (Su(H)). $Notch^{ICD}$ cannot directly bind DNA, and therefore Su(H) provides the DNA-binding specificity to the Notch pathway. Su(H) recognizes its binding sites in the regulatory region of target genes, and recruits Co-Repressors (Co-R) to inhibit transcription. $Notch^{ICD}$ can regulate gene transcription in two different ways, depending on the target gene. First, it could play a *permissive* role, simply alleviating the repression exerted by the Su(H)/Co-R complex upon binding to Su(H). Or second, it could also play an additional *instructive* role, recruiting Co-Activators (Co-A) to enhance transcription of target genes. In both models, usually an additional activating regulatory input (Tissue-specific TF) is required to determine the domain where target genes could respond to $Notch^{ICD}$ (reviewed in BRAY AND FURRIOLS 2001; LAI 2002) (Figure I-4B).

The establishment of precise Notch activation domains depends on the TFs that pattern the P-D axis of the leg, and is further refined by feedback regulatory loops that also involve the activity of specific TFs. These feedback loops could act in every leg joint, such as *dAP-2* (KERBER *et al.* 2001; CIECHANSKA *et al.* 2007; AHN *et al.* 2011), be specific for 'true' joints, such as *lines* and *bowl* (GREENBERG AND HATINI 2009; PUEYO AND COUSO 2011), or be restricted to tarsal segments, such as *zfh-2* (GUARNER *et al.* 2014). The resulting combination of localized TF expression and regulatory feedback loops ensure the finely tuned activation of Notch that is completely necessary for the correct formation of all leg joints and for the proper growth of the leg. Accordingly, loss of function of components of the Notch pathway results in segment fusions and reduced leg size (DE CELIS *et al.* 1998; BISHOP *et al.* 1999; RAUSKOLB AND IRVINE 1999; ANGELINI *et al.* 2012; ESTELLA AND BAONZA 2015) (Figure I-4C).

3.2. Functional and developmental divergence between leg joints

Although all leg joints are homologous structures and require Notch activity for their development, not all joints are equivalent. Adult joints could be assigned to two classes, regarding their morphology: the 'true' or proximal joints present an asymmetrical structure and are attached to leg musculature, while the 'tarsal' or distal joints display radially symmetrical ball-and-socket morphology and are not linked to muscles (SNODGRASS 1935; MIRTH AND AKAM 2002) (Figure I-5). Moreover, the evolutionary origins of both types of joints and the developmental mechanisms that shape them are proposed to be different (CASARES AND MANN 2001; DE CELIS IBEAS AND BRAY 2003; MANJON *et al.* 2007; TAJIRI *et al.* 2010).

Therefore, Notch signaling that is essential for the development of all joints should bifurcate into, at least, two different genetic programs to direct the formation of proximal and tarsal joints. Accordingly, transcription factors of the *odd-skipped* family that include *odd*, *drumstick* (*drm*) and *sister of odd and bowl* (*sob*) are expressed exclusively at the proximal joints, and their simultaneous downregulation in the flour beetle

Tribolium castaneum demonstrate that these genes are required for 'true' joint formation (HAO *et al.* 2003; ANGELINI *et al.* 2012). Conversely, other genes such as *deadpan* (*dpn*) or *Pox neuro* (*Poxn*) are restricted to the tarsal joints, yet their function in tarsal joint formation is mostly unknown (AWASAKI AND KIMURA 2001). A direct target of Notch that specifically directs the formation of the tarsal joints is currently missing.

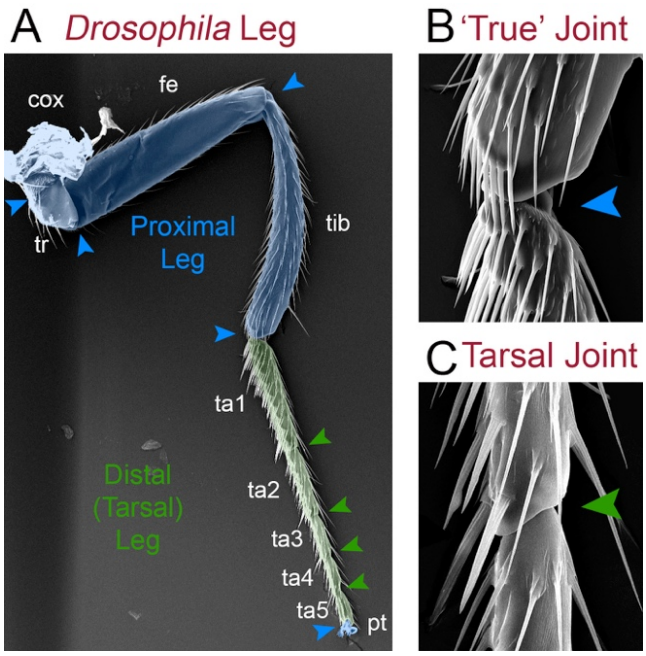

Figure I-5: Divergence between 'true' and tarsal joints. (A) SEM imaging of an adult *Drosophila* leg depicting the proximal (blue) and the distal (green) regions. **(B and C)** Detail of a 'true' joint (blue arrowheads) and a tarsal joint (green arrowheads), respectively.

3.3. Morphogenetic mechanisms that sculpt tarsal joint formation

In the present work, we aim to elucidate both the genetic regulation and the cellular mechanisms that control the morphogenesis of the tarsal joints. Two steps can be distinguished in this process. The first takes place during prepupal development (0-6 hrs after puparium formation, APF) and leads to the formation of four folds transversal to the P-D axis in the distal leg disc epithelium. These folds form just distal to the band of Notch-activating cells and are formed by apical constriction of the cells at the presumptive joints (GREENBERG AND HATINI

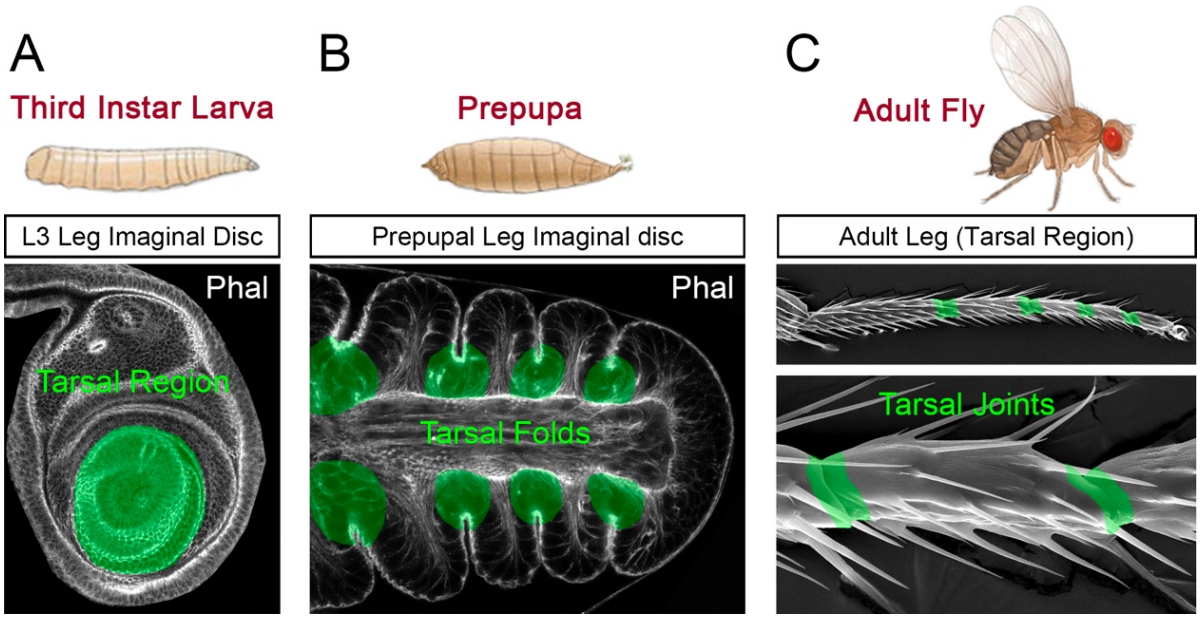

Figure I-6: Prepupal epithelial folds prefigure tarsal joint formation. (A) Third instar leg disc showing the tarsal region (highlighted in green). **(B)** Prepupal leg discs display the characteristic four deep constrictions (tarsal folds, green), characterized by the accumulation of F-actin. **(C)** Adult leg showing the four tarsal joints (green, and see detail below). In **A** and **B**, Phalloidin staining (Phal, grey channel) is used to outline the leg disc.

2011; MONIER *et al.* 2015). Later, during pupal development, the epithelium is again flattened and these constrictions are partially unfolded while the leg elongates, although joint cells retain some degree of apical constriction (MIRTH AND AKAM 2002). A second round of morphogenesis that again relies on Notch activity is required during late pupation to form the ball-and-socket structure of the adult joints (MIRTH AND AKAM 2002; TAJIRI *et al.* 2010; TAJIRI *et al.* 2011; KOJIMA 2017) (Figure I-6). For the shake of clarity, in this work we are referring to the tarsal constrictions as 'folds', and reserve the denomination of 'joint' for the adult structure.

Two morphogenetic mechanisms have been proposed to contribute to tarsal joint formation, namely the regulation of cytoskeleton dynamics by the Rho family of GTPases and programmed cell death or apoptosis (MANJON *et al.* 2007; GREENBERG AND HATINI 2011).

3.3.1. Rho GTPases in tarsal joint development

Rho GTPases are key regulators of cell structure, and thus are required for fundamental cell functions such as maintenance of apico-basal polarity, the organization of epithelial junctions or the regulation of the cell cycle, especially during cytokinesis (BAUSEK AND ZEIDLER 2014; CITI *et al.* 2014; MACK AND GEORGIOU 2014). During morphogenesis, Rho GTPases play a central role coordinating cell shape changes and adhesion properties required during processes of cell migration and apical constriction (MARTIN AND GOLDSTEIN 2014; ZEGERS AND FRIEDL 2014). Rho GTPases act as molecular switches cycling between active (GTP-bound) and inactive (GDP-bound) conformational states. When active, Rho GTPases modulate the activity of target proteins to elicit a wide range of cellular responses. Not surprisingly given the important roles that Rho GTPases play in tissue homeostasis and morphogenesis, their activity is tightly regulated. Rho GTPases are activated by Guanine Exchange Factors (GEFs) that promotes GDP substitution by GTP in the catalytic domain, and are inhibited by GTPase Activating Proteins (GAPs) that promote the hydrolysis of GTP (VAN AELST AND SYMONS 2002; JAFFE AND HALL 2005). The precise balance between Rho GEFs and Rho GAPs is critical to regulate Rho GTPase activity in each morphogenetic context (GREENBERG AND HATINI 2011; GILMOUR *et al.* 2017) (Figure I-7A).

Three canonical Rho GTPases, Rho, Rac and Cdc42, are present both in vertebrates and *Drosophila* and their functions have been thoroughly characterized. All of them are implicated in the organization of cell junctions and their remodeling during morphogenesis and cell movements (CITI *et al.* 2014; MACK AND GEORGIOU 2014). Rac1 and Cdc42 also regulate the organization of the actin cytoskeleton and the formation of lamellipodia and filopodia during cell migration. In this work, we will focus on the activity of Rho, Rho1 in *Drosophila*, which is the main regulator of acto-myosin contractility and directs the process of apical constriction in multiple models of morphogenesis (JAFFE AND HALL 2005; MARTIN AND GOLDSTEIN 2014; ZEGERS AND FRIEDL 2014; GILMOUR *et al.* 2017).

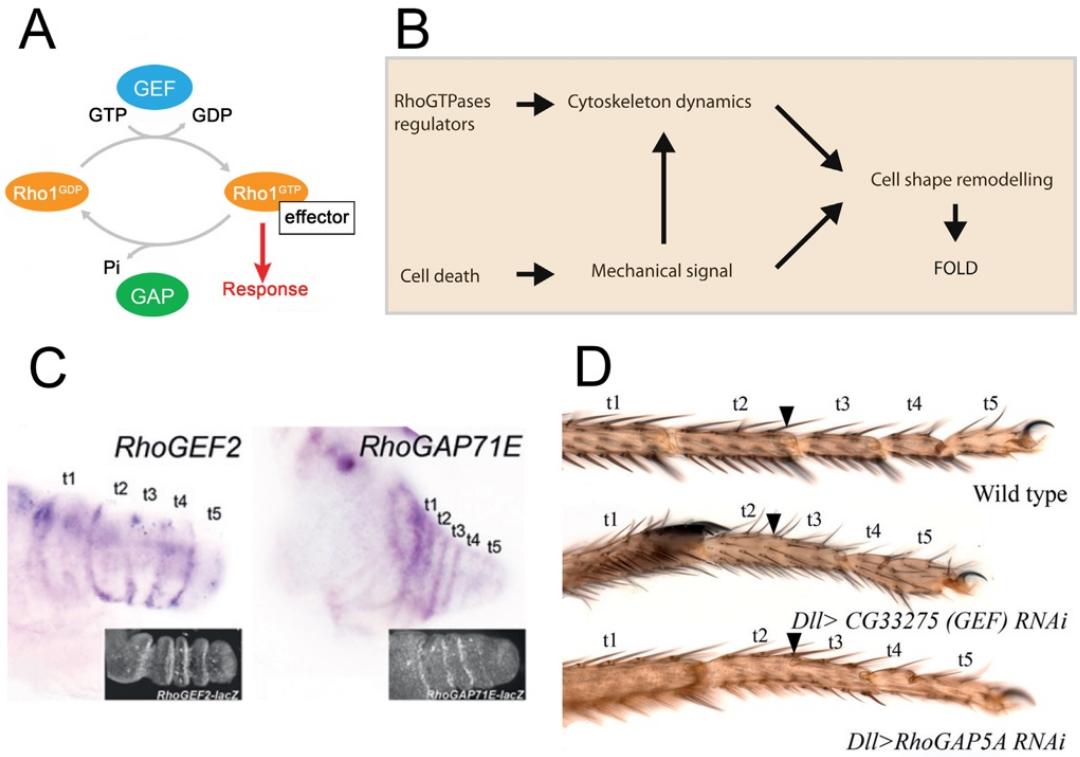

Figure I-7: Rho GTPase regulation in tarsal joint formation. (A) Transition between Rho GTPase 'on' (GTP-bound) and 'off' (GDP-bound) states is modulated by RhoGEFs and RhoGAPs (blue and green, respectively). Rho1 bound to GTP can activate its effectors to elicit different cellular responses (JAFFE AND HALL 2005). **(B)** Proposed model for the coordination between Rho GTPase activity and cell death to regulate prepupal fold and adult tarsal joint formation (details in the main text) (SUZANNE 2016). **(C)** Specific localization of GEFs and GAPs at the presumptive joints of prepupal leg discs, visualized by *'in situ'* hybridization (purple) and *lac-Z* reporters (insets). **(D)** Knockdown of several GEFs and GAPs cause tarsal joint defects (**C** and **D** are modified from GREENBERG AND HATINI 2011).

The role of Rho1 GTPase has not been directly studied in the context of tarsal morphogenesis. Nevertheless, a comprehensive analysis of the expression and requirements of Rho GEFs and Rho GAPs during leg development was performed by GREENBERG AND HATINI in 2011. Interestingly, many Rho GTPase regulators are specifically expressed at the presumptive leg joints, and a subset of them are restricted to the tarsal region and require Notch activity. Moreover, loss of function of several regulators, including the Rho GEF *Pura*, *RhoGAP5A* and *RhoGAP68F* resulted in defects in prepupal fold and adult joint formation. (GREENBERG AND HATINI 2011; DE MADRID *et al.* 2015) (Figure I-7B and C). These results suggest that an intricate regulation of Rho GTPase activity, probably Rho1, is required in order to coordinate joint morphogenesis in the *Drosophila* leg.

3.3.2. Cell death in tarsal joint development

Apoptosis is the most common among different types of programmed cell death, and is a process that kills the cell in a stereotyped and controlled manner in response to apoptotic stimuli. In order to simplify, we use here the terms cell death and apoptosis as synonyms (for further details, see FUCHS AND STELLER 2015). In *Drosophila*, programmed cell death is initiated by the regulated expression of the pro-apoptotic genes *reaper* (*rpr*), *head involution defective* (*hid*) and *grim*, collectively known as RHG. RHG in turn binds to the Death-associated inhibitor of apoptosis 1 (Diap1), causing its degradation (GOYAL *et al.* 2000). In the absence of pro-

apoptotic signals, Diap1 ubiquitinate and sends the initiator caspase Dronc to degradation (WILSON *et al.* 2002). In this manner, apoptosis remains inhibited when the pro-apoptotic signals are not present. When RHG are expressed in response to apoptotic stimuli, the elimination of the repressor Diap1 releases the activity of Dronc, which starts the biochemical cascade of executioner caspases that cause cell death (XU *et al.* 2009). Importantly, the apoptotic cascade is highly conserved between *Drosophila* and mammals (reviewed in FUCHS AND STELLER 2015) (Figure I-8A and B).

Apoptosis has been observed to participate in several processes of tissue remodeling and morphogenesis. A classic example is the role of apoptosis in the individualization of mammalian digits during development (HERNANDEZ-MARTINEZ AND COVARRUBIAS 2011). Apoptosis has also been related to other important developmental process such as mammalian neural tube formation, where its morphogenetic role is controversial (MASSA *et al.* 2009; YAMAGUCHI *et al.* 2011) (Figure I-8D). In *Drosophila*, cell death has been implicated in the rotation of the male genitalia and in the *rpr*-dependent formation of folds between cephalic segments during embryogenesis (LOHMANN *et al.* 2002; SUZANNE *et al.* 2010; and reviewed in SUZANNE AND STELLER

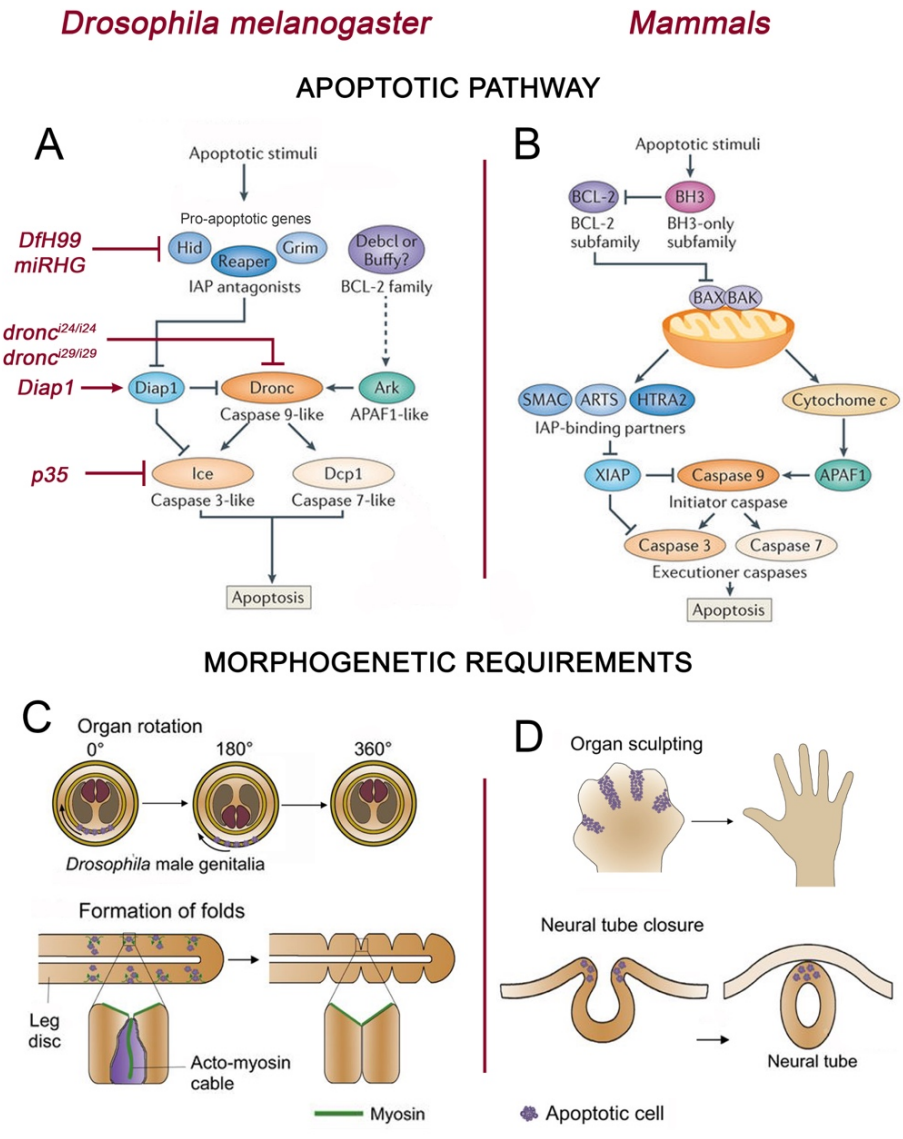

Figure I-8: Cell death pathway and morphogenetic requirements. (A) Schematic representation of the apoptotic pathway in *Drosophila*. Apoptotic stimuli induces the expression of the pro-apoptotic genes *rpr*, *hid* and *grim* (RHG), which blocks Diap1 activity. When Diap1 is degraded, the initiator caspase Dronc activates the executioner caspases Ice and Dcp1 to initiate the apoptotic process. In red (to the left) are shown the different tools used in this work to inhibit apoptosis at four different levels. **(B)** Scheme of the apoptotic pathway in mammals. Note the differences in the upstream regulation of pro-apoptotic gene activation (IAP-binding partners in mammals), and the conservation of the caspase cascade downstream of XIAP that initiates apoptosis (FUCHS AND STELLER 2015). **(C and D)** Morphogenetic requirements of apoptosis in *Drosophila* and mammals, respectively. In *Drosophila* cell death has been implicated in genitalia rotation and in the formation of epithelial folds in the leg disc. In mammals apoptosis is required for the individualization of the digits, and has been observed to take place during neural tube closure (PEREZ-GARIJO AND STELLER 2015).

2013). During leg development, the pro-apoptotic gene *rpr* is expressed at the presumptive joints, accompanied by elevated levels of cell death (MANJON *et al.* 2007). Interestingly, this apoptotic activity only occurs at the presumptive tarsal joints, and is not observed in the proximal ones. The activation of the pro-apoptotic genes depends on the generation of sharp boundaries of Dpp activity at the distal end of each tarsal segment in a c-Jun N-terminal Kinase (JNK) pathway dependent manner (MANJON *et al.* 2007). A similar cell death response has been described in the wing disc when a discontinuity in the Dpp gradient is generated (ADACHI-YAMADA AND O'CONNOR 2002). Moreover, tarsal joint phenotypes have been observed upon cell death inhibition, either in *DfH99* mutants that lack RHG genes or blocking apoptosis by the ectopic expression of the baculovirus p35 protein, an executioner caspase inhibitor (MANJON *et al.* 2007; HAY *et al.* 1994). These observations led to hypothesize an active role of apoptosis in shaping the tarsal folds and adult joints.

More recently, a mechanistic explanation of how cell death could contribute to joint development was provided (MONIER *et al.* 2015). This model implies that apoptotic cells generate apico-basal forces that cause transient invaginations in the surrounding epithelium. This process involves the formation of a MyoII cable in the dying cell and MyoII accumulation in the nearby cells. The combined forces generated by the individual apoptotic events occurring around each presumptive joint would form a stable fold in the epithelium. This challenging model is also supported by the active role that apoptosis play in other morphogenetic events (reviewed in SUZANNE AND STELLER 2013; MONIER AND SUZANNE 2015).

4. Apical constriction drives tarsal fold formation

Regulation of Rho GTPase activity and programmed cell death contribute to the formation of prepupal epithelial folds and tarsal leg joint development. However, how these two processes are spatially regulated, coordinated and implemented in order to dictate the apical constriction of fold-forming cells is mostly unknown.

4.1. Apical constriction in epithelial morphogenesis

Apical constriction is a common morphogenetic mechanism consistent in the shrinkage of the apical domain of the cell, and is used by individual cells or groups of cells to produce tissue shape changes. Individual cells undergo apical constriction for cell delamination (AN *et al.* 2017), while concerted apical constriction of a group of cells leads to invagination or folding of the epithelium (reviewed in MARTIN AND GOLDSTEIN 2014). During *Drosophila* development many morphogenetic processes use coordinated apical constriction: ventral furrow and segmental groove formation, tracheal and salivary gland invagination during embryogenesis or morphogenetic furrow formation in eye imaginal disc development are only some examples (BRODU AND CASANOVA 2006; ESCUDERO *et al.* 2007; MULINARI *et al.* 2008; MARTIN *et al.* 2009; GIRDLER AND ROPER 2014). Two

fundamental elements are required for apical constriction: 1) the generation of force by acto-myosin contraction, and 2) the binding of the F-actin cytoskeleton to the adherens junctions that provides contractile force transmission to neighboring cells. Acto-myosin contractile machinery could form a contractile ring located at the level of adherens junctions (purse-string model of apical constriction) or a dynamic meshwork in the apical cortex of the cell that generate pulses of contraction. These mechanisms could be combined, and the contribution of each of them and the dynamics of the process vary depending on the cellular context (MARTIN AND GOLDSTEIN 2014; VASQUEZ AND MARTIN 2016) (Figure I-9A and B).

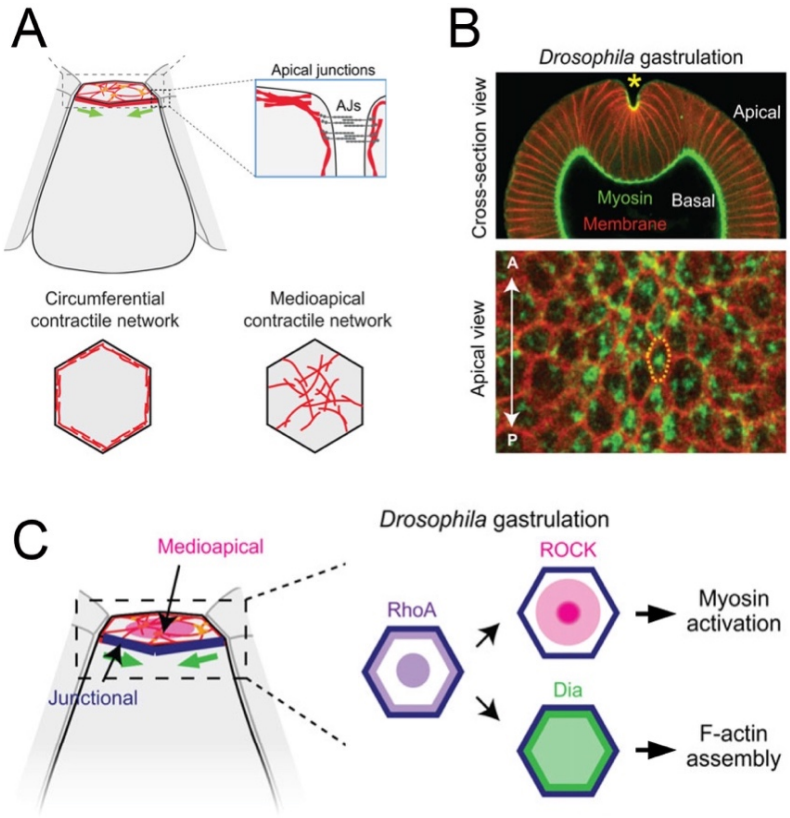

Figure I-9: Apical constriction and ventral furrow formation during *Drosophila* embryogenesis. (A) Distribution of the acto-myosin cytoskeleton (red) in a cell undergoing apical constriction. Two dispositions of acto-myosin could be distinguished, one forming a band at the level of adherens junctions next to the cell membrane (inset and apical view down to the left) and a medioapical network (down to the right). **(B)** Myosin localization in ventral furrow formation. Note the accumulation of MyoII in the apical region of the folds that form the fold. Cross-section on top and apical view below. **(C)** Localization of Rho1 (here termed RhoA, purple) and its downstream effectors Rok (here ROCK, pink) and Dia (green) in a cell undergoing apical constriction. Rok and Dia are activated by Rho1 in different subcellular localizations, and regulate MyoII activation and F-actin assembly at the level of adherens junctions, respectively (MARTIN AND GOLDSTEIN 2014).

Apical constriction is used reiteratively in different developmental processes and in highly divergent organisms throughout the animal kingdom. While the core cytoskeletal and adhesion effector proteins that carry out the process are strikingly conserved, its developmental regulation is specific for each context (SAWYER *et al.* 2010; MARTIN AND GOLDSTEIN 2014; GILMOUR *et al.* 2017). Moreover, the activation of Rho1 appears to be a common theme in the regulation of processes that require acto-myosin contractility, as cell migration, cell intercalation and particularly apical constriction (JAFFE AND HALL 2005; ZIMMERMAN *et al.* 2010; MARTIN AND GOLDSTEIN 2014; GILMOUR *et al.* 2017).

4.2. Regulation of apical constriction by Rho1

In its GTP-bound form, Rho1 binds and activates numerous targets that affect different cellular processes, including the acto-myosin cytoskeleton dynamics. One of the most prominent Rho1 effectors is the Rho-associated protein kinase (Rok) that in turn activates MyoII motor activity (WINTER *et al.* 2001; BOETTNER AND VAN AELST 2002; RIENTO AND RIDLEY 2003; XU *et al.* 2008). MyoII is an hexameric protein composed by two regulatory light chains, encoded in *Drosophila* by the gene *spaghetti squash* (*sqh*), two heavy chains encoded by the gene *zipper* (*zip*) that bind F-actin and provide the motor activity, and two essential light chains encoded by *Myosin light chain cytoplasmic* (*Mlc-c*). The activation of MyoII occurs through the phosphorylation of Sqh by the activated form of Rok (KARESS *et al.* 1991; TAN *et al.* 1992; WINTER *et al.* 2001). Interestingly another kinase, Death-associated protein kinase related (Drak), also phosphorylate Sqh, and its function is necessary when Rok activity is compromised (NEUBUESER AND HIPFNER 2010; ROBERTSON *et al.* 2012).

The regulation that Rho1 exerts on apical constriction is not restricted to the coordination of acto-myosin contraction. Another target of Rho1 is Diaphanous (Dia), the only representative of the DIA class of Formins in *Drosophila* (LIU *et al.* 2010). Formins facilitate F-actin assembly at the level of the adherens junctions, thus providing a link between the actin cytoskeleton and cell-cell junctions (WATANABE *et al.* 1997; HOMEM AND PEIFER 2008; and reviewed in LIU *et al.* 2010; KUHN AND GEYER 2014). Accordingly, concerted activity of MyoII and Dia is observed in several morphogenetic contexts including apical constriction (HOMEM AND PEIFER 2008; MULINARI *et al.* 2008; MASON *et al.* 2013) (Figure I-9C).

5. Regulation of tarsal joint development by Dysfusion

As presented above, extensive work during the past two decades unveiled to a great extent the genetic network that regulate the specification of segmental fates along the P-D axis of the *Drosophila* leg and the precise activation of the Notch pathway at the presumptive joints. Also, the morphogenetic processes that lead to the formation of prepupal folds and adult joints have been studied, albeit to a lesser degree of detail (reviewed in SUZANNE 2016; KOJIMA 2017). In this work, we use the *Drosophila* leg disc to elucidate the relationship between positional information and the cellular mechanisms that shape these appendages. Taking advantage of this preexisting knowledge, we will try to understand how the tarsal joints are uniquely specified and how morphogenesis is regulated during this developmental process. This study at the regulatory and the cellular levels could broaden our understanding of the genetic control of morphogenetic processes.

We approach this problem by searching for candidate transcription factors presenting a ring-like expression pattern in the leg, typical of Notch target genes, and which expression is restricted to the distal domain. We identified the gene *dysfusion* (*dysf*), which encodes for a bHLH-PAS containing transcription factor that is specifically expressed in the presumptive tarsal joints. *dysf* was first described for its role in tracheal migration, adhesion and fusion during embryogenesis, and was also found to be expressed in the leading edge cells during embryonic dorsal closure (JIANG AND CREWS 2003; JIANG AND CREWS 2006). *Drosophila* Dysf has a mammalian ortholog, Neuronal PAS domain protein 4 (Npas4), which has been implicated mostly in gene expression regulation in the nervous system (SIM *et al.* 2013; YOSHIHARA *et al.* 2014; SHEPARD *et al.* 2017). More recently, Npas4 has been implicated in sprouting angiogenesis, a requirement reminiscent of Dysf function in *Drosophila* tracheal development (ESSER *et al.* 2017).

In tracheal fusion cells Dysf forms hetrodimers with Tango (Tgo), another bHLH-PAS protein necessary for Dysf activity. Dysf-Tgo dimers bind specific DNA sequences to directly regulate target gene transcription (JIANG *et al.* 2010). Interestingly, the Dysf-Tgo functional relationship is maintained between their mammalian orthologs (Npas4 and Arnt, respectively), and even their DNA binding specificity is conserved (JIANG AND CREWS 2007). Tgo loss of function has already been implicated in leg phenotypes that include tarsal joint defects. Nevertheless, those phenotypes were previously assigned to the requirement of Tgo as a dimerization partner of Trachealess (Trh) in the pretarsus and Ss in the tarsal domain of the leg (EMMONS *et al.* 1999; TAJIRI *et al.* 2007). In this work, we set out to study the regulation of *dysf* expression in the leg, as well as its possible requirements for tarsal joint development.

OBJECTIVES

In the present Doctoral Thesis, we aim to unveil the genetic regulation and the morphogenetic mechanisms that direct the formation of the tarsal leg joints in *Drosophila melanogaster*.

We define the following specific objectives:

1. Analyze the genetic regulatory network that directs *dysf* expression in the leg and study its requirements in the process of tarsal joint formation.

2. Study the morphogenetic mechanisms that sculpt tarsal joints and their potential relationship with Dysf.

MATERIALS AND METHODS

1. Culturing Drosophila melanogaster

The culture of *Drosophila melanogaster* strains was carried out in a standard culture medium in incubation chambers at fixed constant temperatures (17°C, 25°C and 29°C, depending on the experimental requirements) and controlled humidity.

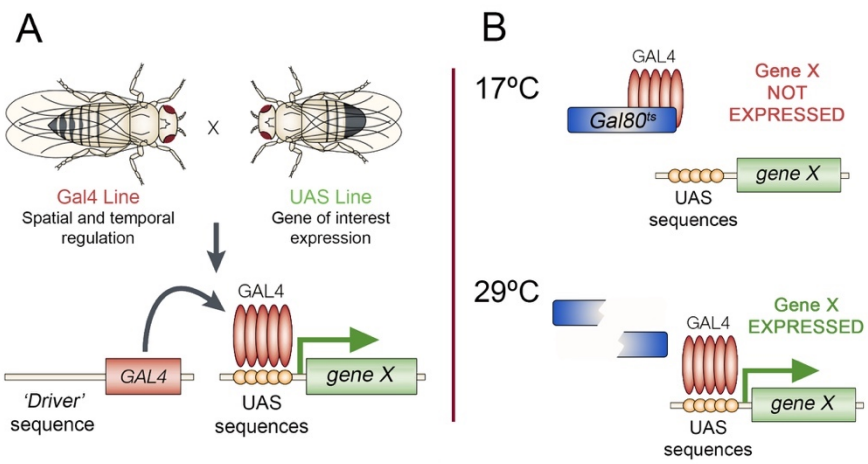

Figure M-1: Gal4/UAS system to spatially and temporally regulate ectopic gene expression. (A) The *Gal4* gene is expressed under control of a '*driver*' in a spatially and temporally localized pattern. Gal4 binds to UAS sequences to direct expression of our gene of interest (*gene X*). **(B)** The ubiquitous expression of *Gal80^{ts}* permits temporal restriction of the Gal4/UAS system. At the restrictive temperature (17°C), Gal80^{ts} blocks Gal4 binding to UAS sequences. Conversely, at the permissive temperature (29°C), Gal80^{ts} is degraded and Gal4 activate *gene X* expression (MUQIT AND FEANY 2002).

We performed most of our experiments taking advantage of the Gal4/UAS system (BRAND AND PERRIMON 1993), as a means to drive gene expression in temporally and spatially restricted domains. Briefly, the yeast transcriptional activator Gal4 is induced under the control of a regulatory region that will direct expression in a specific localization at a given developmental time, here called '*driver*' sequence. Driver sequence is usually the regulatory region of gene with a known expression pattern. When driver expression is activated, Gal4 is expressed and binds to its target UAS sequences to activate transcription of the gene cloned next to the UAS sequence. Hence, we can perform gene misexpression by simply crossing fly strains that carry a Gal4 driver with strains that bear the desired gene next to UAS sequences (Figure M-1A). Further temporal regulation of gene expression can be acquired by constitutively expressing the temperature sensitive Gal4 repressor, the protein Gal80^{ts}, under the control of *tubulin* promoter (*tubGal80^{ts}*). At the restrictive temperature (17°C) Gal80^{ts} binds Gal4, preventing its binding to UAS sequences and thus blocking target gene expression. When flies are shifted to the permissive temperature (29°C), Gal80ts is degraded, and Gal4 activate transcription of target genes (Figure M-1B). Combining these two techniques, precise spatial and temporal gene expression can be achieved.

2. Drosophila strains

Unless stated otherwise, the fly strains used are described in Flybase (http://flybase.org) and publicly available at Bloomington Drosophila Stock Center (http://www.bdsc.indiana.edu).

2.1 Gal4 Lines

We used the following Gal4 lines to drive gene expression: *GMR_13D07-* and *GMR_13B03-Gal4* and the rest of Janelia enhancer/GAL4 lines are described in the Flylight database (http://flweb.janelia.org/cgi-bin/flew.cgi) (JORY *et al.* 2012), and are publicly available at Bloomington We used the *Gal4* lines *ptc-Gal4, dpp-Gal4, Dll^{212}-Gal4, ap-Gal4, rn-Gal4, ss-Gal4, hh-Gal4, en-Gal4*, and *hhRed ci-Gal4*, to drive gene expression. A schematic representation of the expression pattern of the Gal4 lines commonly used in this work in a prepupal leg disc is shown in Figure M-2.

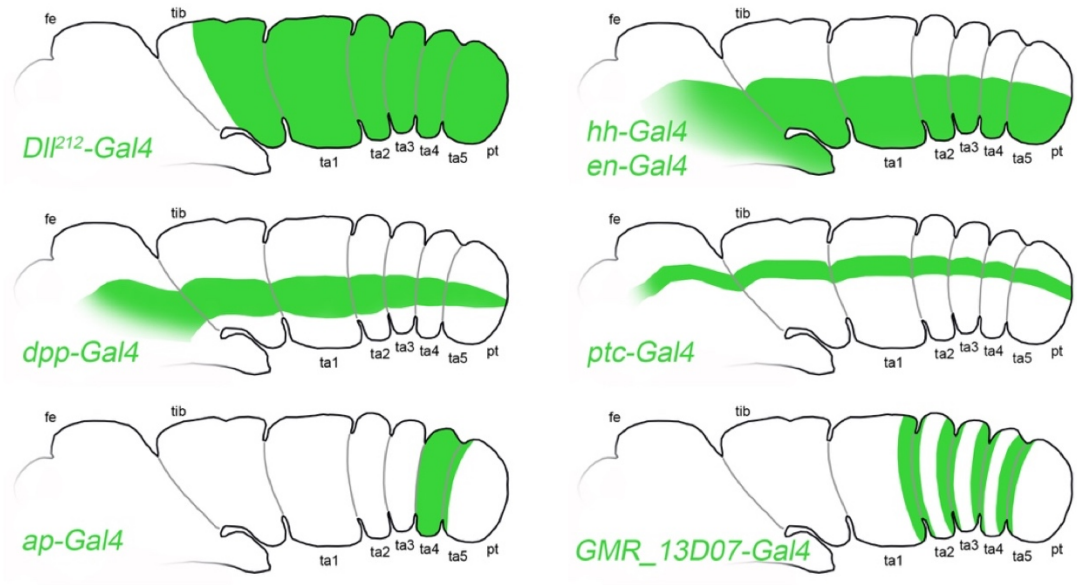

Figure M-2: Gal4 lines frequently used in the present work. The expression of Gal4 is directed by different *drivers*, which expression domains in a prepupal leg disc could be seen in green. The corresponding leg segments are indicated. Here and in the following figures Anterior is to the left and Posterior to the right.

2.2 UAS Lines

The following UAS lines were used in this work: UAS-*GFP* was used to visualize Gal4 expression and as a control, and UAS-*flp* for inducing FRT mediated recombination (see below). UAS-*Notch^{ICD}* (DE CELIS AND BRAY 1997) and UAS-*dysf* (JIANG AND CREWS 2003; BL#9592) were used to activate Notch pathway and *dysf* expression, respectively. UAS-*tkv^{QD}* was expressed to activate Dpp pathway at high levels. UAS-*miRHG* (SIEGRIST *et al.* 2010), UAS-*diap1* and UAS-*p35* (HAY *et al.* 1994; BL #5073) were used to inhibit apoptosis at different levels. We used UAS-*Rho1^{N19}* (STRUTT *et al.* 1997) to block Rho1 activity, and UAS-*Rho1.Sph* (BL #58819 (Chr. II) and #7334 (Chr. III)) to ectopically activate Rho1 pathway. UAS-*Dia^{CA}* (SOMOGYI AND RORTH 2004; BL #27616), UAS-*HA:Rok^{CAT}* (kindly provided by J.A. Zallen and described in SIMOES *et al.* 2006), UAS-*sqh^{E20E21}* (described in CORRIGALL *et al.* 2007) were used to induce F-actin nucleation, Rok activity and MyoII contractility, respectively. UAS-*rpr* was used to ectopically induce apoptosis. UAS-*deGradFP* (described in CAUSSINUS *et al.* 2011) was expressed to specifically degrade GFP-tagged Sqh protein (see below).

2.3 Interference RNA Lines

Different UAS lines driving the expression of interference RNA were used to downregulate the function of the targeted genes. UAS-*dysfRNAi* (VDRC #110381) expression to knock down Dysf function was performed in combination with UAS-*dicer* to enhance the effect of the RNAi. UAS-*tgoRNAi* (VDRC #330021), UAS-*NotchRNAi* (PRESENTE *et al.* 2002), UAS-*rnRNAi* (BL #65347), UAS-*ssRNAi* (BL #26208), UAS-*rokRNAi* (BL #28797) and UAS-*DrakRNAi* (BL #44102) were also used in the present work. VDRC stands for Vienna Drosophila Resource Center (http://stockcenter.vdrc.at).

2.4 Reporter Lines

Different constructs were utilized to monitor gene expression, protein localization or protein activity. *bib-lacZ* and *E(spl)mβ-CD2* were used to track Notch activity. To track pro-apoptotic gene expression we used the reporter lines *rpr-4kb-lacZ* (*rpr-lacZ*) (JIANG *et al.* 2000) and *hid-lacZ*^{W05014} (GRETHER *et al.* 1995), and *RhoGAP71E-* and *RhoGEF2-lacZ* to visualize the expression of Rho GTPase regulators. *bab-lacZ* (described in GODT *et al.* 1993) is used to monitor *bric-à-brac* gene expression. The biosensor UAS-*PKNG58AeGFP* (described in SIMOES *et al.* 2006), and here termed UAS-*Rho1RBD-GFP* was used to monitor Rho1 activity in the leg and wing discs. We used the GFP insertions *Rho1-GFP* (Kyoto Stock Center #110833) and *zip-GFP* (BL #51564), available in the FlyTrap collection (http://flytrap.med.yale.edu/), to monitor Rho1 and Zip localization, respectively. Sqh localization was detected with the following construction, *sqh*^{AX3}*; sqh:sqh-GFP* (ROYOU *et al.* 2004), that express a GFP tagged form of Sqh under the control of the *sqh* gene promoter in a *sqh*^{AX3} mutant background. SGMCA, a construct that express the actin-binding region of Moesin coupled to GFP in all the cells under the control of the *sqh* promoter (KIEHART *et al.* 2000), was used to monitor F-actin. UAS-*αCatRFP* (ISHIHARA AND SUGIMURA 2012) was expressed to visualize adherens junctions.

2.5 Mutant Lines

The following mutant alleles were used either to generate homozygous mutant flies or to generate clones of mutant tissue by different approaches (see below). *dysf*^{2} and *dysf*^{3} (described in JIANG AND CREWS 2006) were crossed to obtain *dysf*^{2}/*dysf*^{3} transheterozygous flies, that survived until pharate, to address leg requirements of *dysf*. The *Notch* thermosensitive mutant allele (*Notch*^{tsa}) allowed us to knockdown *Notch* activity when the flies are shifted to the restrictive temperature (29°C) (SHELLENBARGER AND MOHLER 1978). *bab*^{AR07} allele corresponds to a deletion that removes both *bab1* and *bab2* genes (BAANANNOU *et al.* 2013; BL #37298). *tgo*^{5} (BL #9589), *Drak*^{DEL} (NEUBUESER AND HIPFNER 2010), *rok*^{2} (WINTER *et al.* 2001), *rok*^{2} *Drak*^{DEL} (a gift from Franck Pichaud) and *dia*^{5} (HOMEM AND PEIFER 2008; BL #9138) mutant alleles were also used in this work. To inhibit cell death, two null mutant alleles of the initiator caspase Dronc, *dronc*^{i24} and *dronc*^{i29} (XU *et al.* 2005) were used to

generate homozygous flies that survived until pharate. We also generated large clones (see below) homozygous for the deficiency *Df(3L)H99*, that remove the pro-apoptotic *rpr*, *hid* and *grim* genes (WHITE *et al.* 1994).

2.6 Cloning and mutagenesis of *dysf640* CRM

The 640bp overlapping DNA sequence between the *GMR_13D07* and *GMR_13B03* lines as well as the different mutant conditions were cloned in the HLz attB plasmid vector, which expresses a nuclear *lacZ* reporter under the control of the cloned sequence (ESTELLA *et al.* 2008). The primers used were the following for each reporter line (restriction sites are underlined and restriction enzyme used is noted in brackets):

dysf640

Forward: 5'-cagtcctaggCCAAGCCGATGAGCCATTCCATACC-3' (AvrII)
Reverse: 5'-cagtagatctCCACTCTGGAGCAAACCACACCGAA-3' (BglII)

dysf640^{A}

Forward: 5'-cagtcctaggCCAAGCCGATGAGCCATTCCATACC-3' (AvrII)
Reverse: 5'-cagtagatctTTCTGCTGATTTTCTTCTTTAGGTT-3' (BglII)

dysf640^{B}

Forward: 5'-cagtcctaggCTCTCCATGGTTAAGCTCAGACTAA-3' (AvrII)
Reverse: 5'-cagtagatctCCACTCTGGAGCAAACCACACCGAA-3' (BglII)

Putative Su(H) binding sites were identified on the basis of a bioinformatics analysis combining data from the JASPAR CORE Insecta database (http://jaspar.genereg.net) and the Target Explorer tool (SOSINSKY *et al.* 2003). Mutagenesis of the Su(H) putative binding sites was performed using the QuikChange Site-Directed Mutagenesis Kit (Stratagene). We used the following primers:

dysf640$^{Su(H)-1}$

Forward: 5'-TCGATCCAAGAACCAAGTCcgagaccAATTTCCGTACACACACAA-3'
Reverse: 5'-TTGTGTGTGTACGGAAATTggtctcgGACTTGGTTCTTGGATCGA-3'

dysf640$^{Su(H)-2}$

Forward: 5'-GGAGGAAGAAAAAACTCAGtggagacagCAAATTAAGATAATCG-3' Reverse: 5'-CGATTATCTTAATTTGctgtctccaCTGAGTTTTTTCTTCCTCC-3'

dysf640-lacZ reporter construct was inserted both in the 2R (51D) and 3R (86Fb) chromosomal locations. To allow proper comparison, all the *dysf640-lacZ* versions (*dysf640-lacZ, dysf640^{A}-lacZ, dysf640^{B}-lacZ, dysf640$^{Su(H)-1}$-lacZ*, *dysf640$^{Su(H)-2}$-lacZ* and *dysf640$^{Su(H)-1+2}$-lacZ*) were inserted in the same location. Confocal settings were kept constant when imaging wild type and mutant versions of *dysf640-lacZ*, so *lacZ* expression levels are comparable between these conditions.

3. Clonal analyses

Clonal analyses allow the generation of groups of mutant cells in specific regions of the *Drosophila* body and therefore analyze gene function in the cases where the mutant alleles are deleterious for the fly.

To generate *tgo* mutant clones we utilized the null allele *tgo^{5}* (BL #9589) and the MARCM technique, which allowed us to simultaneously eliminate *tgo* function and express *dysf* cell autonomously. The detailed genotype is:

yw hs-flp, tub-Gal4; UAS-dysf; FRT 82B tubGal80/ FRT 82B tgo^{5}.

Mutant clones for different alleles were generated using the following genotypes:

yw hs-flp; ;babA^{R07} FRT80B/ ubiGFP FRT80B

yw hs-flp; dia^{5} FRT40/ ubiGFP M(2)z FRT40

y *rok^{2} Drak^{DEL} FRT19A/tubGal80 hsflp FRT19A; act-Gal4, UAS-CD8 GFP/UAS-miRHG*

Loss of function clones were created by heat-shocking the larvae for 1 hour at 37°C 48 to 72 hrs after egg laying.

To generate flies in which the whole leg is mutant for either *DfH99* or *rok^{2}* we used the *Minute* technique (MORATA AND RIPOLL 1975). In the case of *rok^{2}* mutants a duplication on the Y chromosome that covers the *rok* gene (*Dp(1;Y)shi+3, y+*) (BL #5270). The genotypes are as follows:

yw hs-flp; Dll^{212}-Gal4, UAS-*flp; DfH99 FRT2A/ ubiGFP M FRT2A*

yw hs-flp; Dll^{212}-Gal4, UAS-*flp; DfH99 FRT80B/ arm-lacZ M FRT80B*

yw rok^{2} FRT^{19A}/ubi-GFP M(1)osp FRT^{19A}; Dll^{212}-Gal4, UAS-*flp*

4. Electrophoretic Mobility Shift Assay (EMSA)

An incomplete form of Su(H) protein, that bears the DNA binding domain (SAN-JUAN AND BAONZA 2011) was translated *in vitro* using the TNT T7 Quick master MiX kit (Promega) and tested for binding with a series of radioactively labeled double stranded DNA probes. 50 ng of each sense oligonucleotide were labeled following standard procedures with γ-^{32}P ATP, and then hybridized with the complementary 'cold' oligonucleotide. Wild type and mutant probes, where nucleotides at consensus Su(H) binding site were mutated, were generated for the three identified Su(H) sites. The designed oligonucleotides were the following (Mutated Su(H) sites are noted with lower case letters):

Su(H)-1 WT

Forward: 5'-CCAAGTCATGGGAAAATTTCC-3'
Reverse: 5'-GGAAATTTTCCCATGACTTGG-3'

Su(H)-1 mut

Forward: 5'-CCAAGTCcgagaccAATTTCC-3'
Reverse: 5'-GGAAATTggtctcgGACTTGG-3'

Su(H)-2 WT

Forward: 5'-GGAGGAAGAAAAAACTCAGTTTCGCACGCAAATTAAGATAATCG-3'
Reverse: 5'-CGATTATCTTAATTTGCGTGCGAAACTGAGTTTTTTCTTCCTCC-3'

Su(H)-2 mut

Forward: 5'-GGAGGAAGAAAAAACTCAGtggagacagCAAATTAAGATAATCG-3'
Reverse: 5'-CGATTATCTTAATTTGctgtctccaCTGAGTTTTTTCTTCCTCC-3'

Su(H)-3 WT

Forward: 5'-ATTTCCGTACACACACAATTTG-3'

Reverse: 5'-CAAATTGTGTGTGTACGGAAAT-3'

Su(H)-3 mut

Forward: 5'-gggaatgcacacCACAATTTGG-3'

Reverse: 5'-CCAAATTGTGgtgtgcattccc-3'

5.Temperature shift experiments

In several of our analysis, the effect of UAS lines, either for performing gain or loss of function experiments required to be temporally restricted to only affect specific stages of development. The activity of the different Gal4 lines was restricted temporally using the *tubGal80^{ts}* system previously described. Briefly, embryos were collected for 24 to 48 hrs, maintained at the restrictive temperature (17°C) and then shifted to the permissive temperature (29°C) for the required time prior to dissection. For prepupal analysis of *Notch* mutants, *Notch^{tsa}* larvae were grown at 17°C, transferred to 29°C for 72 hrs prior to dissection, and the vials were kept at 29°C to recover adult legs.

When indicated, prepupae were synchronized to properly compare fold formation phenotypes. White pupae of the chosen phenotype were selected, incubated for 3 hrs at the required temperature, and then dissected and stained following standard procedures. For the gain of function experiments performed in the wing disc, the *ptc>GFP*, *tubGal80^{ts}* line was crossed with the different UAS lines and the progeny maintained at the restrictive temperature (17°C) until shifted to the permissive temperature (29°C) for periods of 24 to 48 hrs before dissection.

For the analysis of adult phenotypes in the *ptc*>UAS-*dysf* experiment, larvae were kept 11 days at 17°C and shifted to the permissive temperature (29°C) until pharate were recovered. The *ap>Rho1^{N19}* and *ap>Rho1^{N19}, miRHG* experiments were similarly performed: larvae were kept at 17°C and until wandering L3 appeared in the walls of the tube, when the vials were shifted to 29°C for 48 hrs to ensure strong Gal4 activity during fold formation (from late larva through early pupal stages) and then transferred back to 17°C until hatching.

6. Immunostaining and adult leg preparations

Standard procedures were used to fix and stain prepupal and larval leg and wing imaginal discs. Briefly, larvae and prepupae were dissected in PBS and fixed with 4% paraformaldehyde, 0,1% Deoxicholate and 0,1%

Triton X-100, in PBS for 25 minutes at room temperature. They were blocked in PBS, 1% BSA, 0,3% Triton X-100 and 0,03% Azida (Washing Buffer) for 1 hour and incubated with the primary antibody over night at 4°C. Larvae or prepupae were then washed four times in Washing Buffer, and incubated with the appropriate fluorescent secondary antibodies for 1,5 hours at room temperature in the dark. They were then washed again four times in Washing Buffer and mounted in Vectashield mounting Medium (Vector Laboratories) for later confocal analysis.

The primary antibodies used in this work are shown in the following Table:

ANTIBODY	SPECIES	DILUTION	ORIGIN
Anti-Dysf	Rabbit	1:200	Jiang and Crews, 2003
Anti-Ser	Rat	1:1000	Ken Irvine, Rutgers University (gift)
Anti-Dll	Guinea Pig	1:2000	Estella et al., 2008
Anti-Hth	Rabbit	1:2000	Estella et al., 2008
Anti-βgal	Rabbit	1:1000	Promega
Anti- βgal	Mouse	1:1000	MP Biomedics
Anti-CD2	Rat	1:200	Serotec
Anti-Dlg	Mouse	1:50	Hybridoma Bank (DSHB)
Anti-Dcp1	Rabbit	1:200	Cell Signaling Technology
Anti-Tgo	Mouse	1:100	Hybridoma Bank (DSHB)
Anti-P-Mad	Rabbit	N.A.	Ginés Morata (gift)

We used anti-Phalloidin (TRITC) and Phalloidin-Atto 647N (both from Sigma Aldrich and diluted 1:200) to stain the F-actin cytoskeleton, and TOPRO (Thermo-Fisher, 1:100) to stain nuclei. We used secondary antibodies of the required species conjugated with Alexa Fluor Dyes 555 (1:250), 647 (1:500) or 488 (1:500) (Invitrogen/Life Technologies). TUNEL analysis to detect fragmented DNA was performed using In Situ 'Cell Death Detection Kit' (TMR Red) and 'Tunel Dilution Buffer' kits, both from Roche, and following standard procedures.

Adult or pharate (in the case of flies that could not hatch) legs of the required phenotypes were collected in 96% ethanol until mounted. We used Hoyers mounting medium in a 1:1 proportion with lactic acid (90% MERCK) to preserve the cuticle of the legs (STERN AND SUCENA 2012).

7. Image acquisition and treatment

All confocal images were obtained using a Leica LSM510 vertical confocal microscope. Multiple focal of the same specimen were obtained when needed, specifically for the analysis of ectopic fold formation in the wing disc, in order to obtain the transversal section of the wing pouch.

For Scanning Electron Microscopy, wild type, *dysf*^{2}/*dysf*^{3} mutant and *ptc*>UAS-*dysf* adult flies were collected and their legs and heads dissected without any fixation and avoiding moisture prior to preparation for SEM. The preparation of the samples and Scanning Electron Microscopy was performed at the Microscopy Unit at Universidad Autónoma de Madrid.

Optical adult leg imaging was performed using a 'Spot' digital camera coupled to a Zeiss AxioplanTM Optical microscope. Multiple focal planes of each adult leg were acquired and then combined using the Helicon Focus program (http://www.heliconsoft.com) to create a fully focused image of the legs. For the analysis of the joint defects in adult legs, we categorized the phenotypes of the different genetic combinations attending to their severity by counting the number of tarsal joints that were affected in each leg. These categories were: no defects, 1 to 2 joints affected, 3 to 4 joints affected and leg truncation.

Image treatment and analysis was performed using Fiji (https://fiji.sc) and Photoshop (http://adobe.com/photoshop) software. To determine the levels of cell death in *E(spl)mβ* and 'fold' domains, we have performed Z-stack imaging of wild type and *dysf*^{2}/*dysf*^{3} mutants and manually counted the number of Dcp1 positive cells on each domain. We selected for this analysis the joints between tarsal segments t2-t3 and t3-t4. Quantification of cell death was performed manually in the *hh*>UAS-*miRHG,* UAS-*GFP* experiment to properly distinguish between positive Dcp1 stained cells that belonged to A or P compartments. To measure Dcp1 levels in *dronc*^{i24} homo- or heterozygous mutants we used Fiji to automatize the counting of Z projections of all the cell death present in each leg disc.

Statistical analyses were performed using Graph Pad Prism software (https://www.graphpad.com). The specific test used in each experiment is noted in the corresponding Figure.

RESULTS

REQUIREMENTS AND GENETIC REGULATION OF *dysf* IN TARSAL JOINT FORMATION

1. *dysf* EXPRESSION AND REQUIREMENTS

Notch activity is completely required for the formation of all leg joints, however not all are equal: adult joints are classified into proximal or 'true' joints and distal or 'tarsal' joints, based upon morphological and functional differences and their distinct evolutionary origin (SNODGRASS 1935; DE CELIS *et al.* 1998; BISHOP *et al.* 1999; RAUSKOLB *et al.* 1999; CASARES AND MANN 2001; MIRTH AND AKAM 2002; TAJIRI *et al.* 2010). Importantly, the genetic mechanisms that regulate their development are specific for each joint type (HAO *et al.* 2003; MANJON *et al.* 2007). Therefore, we set out to identify Notch effectors that could mediate the distinction between proximal and distal joints.

1.1 *dysf* is expressed specifically at the tarsal joints

To find candidate regulators specific for proximal or distal joint development, we searched the FlyLight database (JORY *et al.* 2012) for *cis*-regulatory modules (CRMs) that were active in a ring-like pattern specifically at the proximal or the distal domain of the leg disc. We found two lines, *GMR_13D07* and *GMR_13B03*, that drive the expression of the green fluorescent protein gene (*GFP*) in concentric rings restricted to the distal domain of the leg and antenna third instar imaginal disc (from now on, *imaginal discs* would be referred to simply as 'discs') (Figure 1B and C). To better visualize the activity of *GMR_13D07* we dissected prepupal leg discs and stained for *big brain* (*bib-lacZ)*, a target of Notch that is expressed in all presumptive joints. The activity of this line was observed in four bands that encompass the presumptive tarsal joints (ta 1-4), but was not active in the 'true' joints (arrows in Figure 1D). These two lines map between exons 2 and 3 of the *dysfusion (dysf)* gene (Figure 1A). To confirm that *dysf* is expressed in the presumptive tarsal joints, we used an antibody against Dysf (JIANG AND CREWS 2003). We observed Dysf staining in the distal-most region of tarsal segments t1 to t4, and in an incomplete ring in the distal tibia, that was not reproduced by the CRMs previously identified (Figure 2A). We also observed Dysf in several rings in the antenna disc (data not shown).

To explore whether *dysf* expression could be regulated by Notch in the tarsal region, we stained for Dysf and the Notch ligand Ser and the Notch targets *bib* and *Enhancer of split mβ* (*E(spl)mβ*). *Ser* is expressed in concentric rings in the distal region of each presumptive leg segment, immediately proximal and adjacent to the band of cells that activate the Notch pathway. We observed that Dysf co-localizes with *bib-lacZ* and *E(spl)mβ-CD2* reporters (Figure 2A-C), and is located distally and adjacent to the band of Ser labeled cells (Figure 2D, E). We conclude that *dysf* expression is restricted to the Notch-activating cells at the presumptive tarsal joints, which makes *dysf* a good candidate for regulating tarsal joint formation in response to Notch.

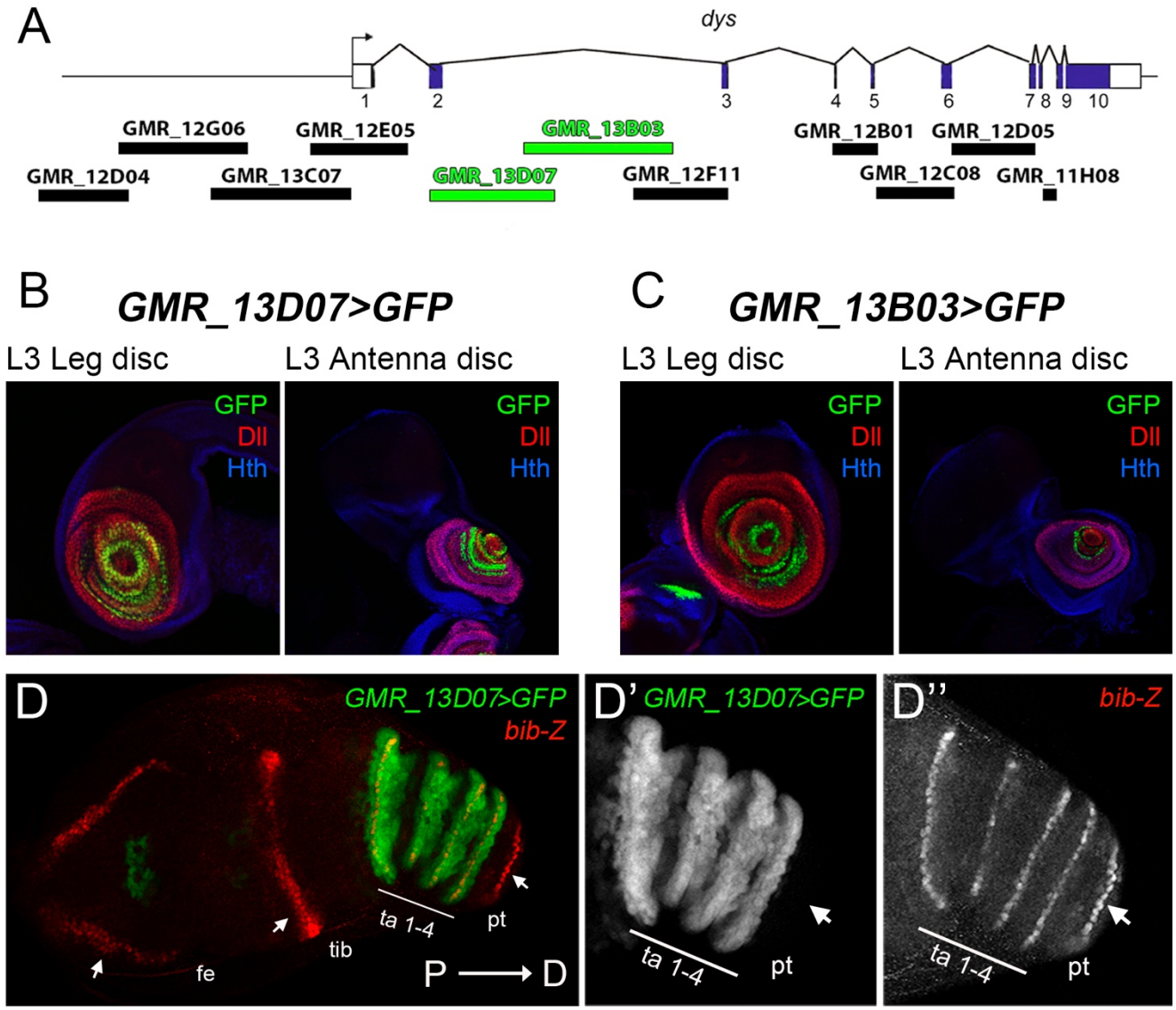

Figure 1. Two putative enhancer sequences at dysf genomic locus drive reporter expression around the presumptive tarsal joints. (A) Schematic representation of the *dysf* genomic locus (modified from (JIANG *et al.* 2010), showing the DNA elements available in the Janelia FlyLight database tested for GFP expression in imaginal discs (black horizontal bars). Of these, two lines (GMR_13D07 and GMR_13B03, green bars) drive GFP expression in the tarsal segments of the leg and in the antenna L3 imaginal discs **(B and C)**. GFP is in green, Dll in red and Hth in blue. Images extracted from the FlyLight database. **(D)** Prepupal leg disc showing GFP expression (green and separate channel in **D'**) under the control of the GMR_13D07 DNA fragment. *bib-Z* expression (in red and separate channel in **D''**) is used to mark all presumptive joints. Note that GFP expression is restricted to the four presumptive tarsal joints (ta 1-4) and is absent from true joints (arrows). In this figure and onwards, Proximal is to the left and Distal to the right. fe: femur, tib: tibia, ta 1-4: tarsus 1 to 4, pt: pretarsus.

1.2 *dysf* is required for tarsal joint formation

To address the contribution of Dysf to tarsal joint morphogenesis we used two strategies to knock down its function. First, we used a combination of *dysf* null alleles, $dysf^{2}$ and $dysf^{3}$, that produce truncated forms of the Dysf protein (JIANG AND CREWS 2006). Each allele is lethal in homozygosis and adult flies are not recovered. Nevertheless, when $dysf^{2}/dysf^{3}$ flies are generated, a very low proportion of escapers could be found and analyzed. The second approach was the expression of interference RNA against *dysf* (UAS-*dysfRNAi*) in the distal domain of the leg using the Dll^{212}-*Gal4* driver. The *dysfRNAi* construct efficiently eliminates Dysf protein from

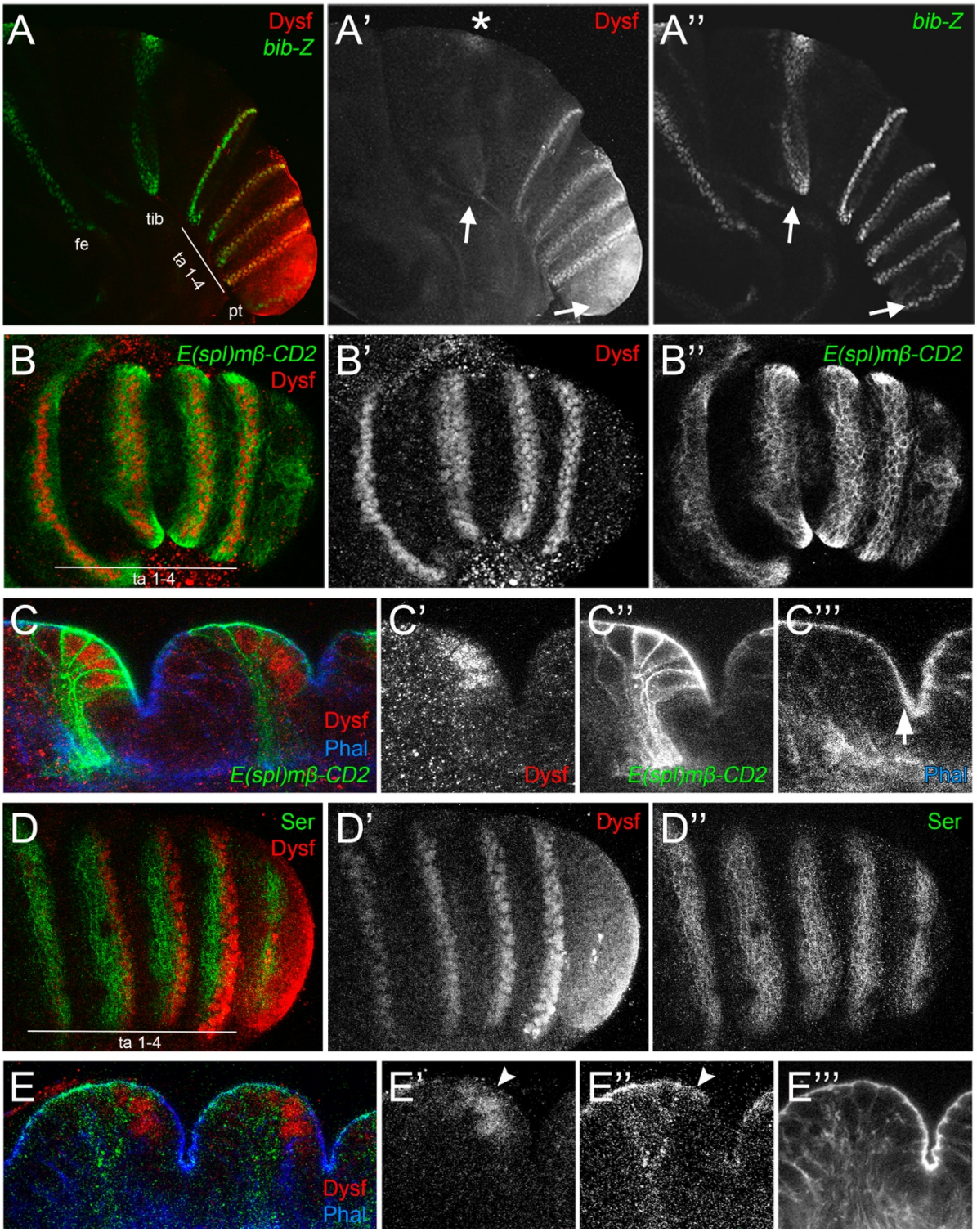

Figure 2. dysf expression at the presumptive tarsal joints is compatible with regulation by Notch. (A) Prepupal leg disc stained for Dysf (red and separate channel in **A'**) and *bib-Z* (green and separate channel in **A''**). Note that Dysf is present in a ring of cells in all four tarsal segments, and is absent from true joints (arrows) except for an incomplete ring observed in the tibial presumptive joint (asterisk). **(B and C)** Dysf (red and separate channel in **B'** and **C'**) co-localizes with the direct target of Notch *E(spl)mβ-CD2* (green and separate channel in **B''** and **C''**) in the tarsal region of a prepupal leg disc. Apical view is shown in **(B)** and a sagittal view is shown in **(C)**. Dysf and *E(spl)mβ-CD2* are positioned just proximal to the epithelial fold (arrow in **C'''**). Phalloidin (Phal, blue in **C** and separate channel in **C'''**) is used to stain F-actin to visualize cell shape. **(D and E)** The Notch ligand Ser (green and separate channel in **D''** and **E''**) is located proximal to *dysf*-expressing cells (red and separate channel in **D'** and **E'**), although some overlapping of their expression domains could be observed (arrowheads in **E'** and **E''** marks the distal-most end of Ser staining). Cell shape is visualized with Phal (blue in **E** and separate channel in **E'''**).

the leg disc (Figure 3J). The loss of Dysf activity in the distal domain of the leg causes the complete absence of the four tarsal joints, which is accompanied by a slight reduction in the length of the tarsal region (compare Figure 3A and D with Figure 3B, C and E). Nevertheless, the 'true' joints, including the tib-ta or the ta5-pt, remained unaffected (arrows in Figure 3A-E). In the antenna the loss of the joint between the a5 segment and the arista was also detected (Figure 3K). As Notch activity is required to form the joints (DE CELIS *et al.* 1998; BISHOP *et al.* 1999; RAUSKOLB AND IRVINE 1999), we compared *dysf* knockdown phenotypes with those of a temperature-inducible mutant of *Notch* (*Notch^{tsa}*) hemizygous mutant fly (SHELLENBARGER AND MOHLER 1978; and see Materials and Methods). *Notch^{tsa}* mutants shifted to the restrictive temperature (29°C) at third instar larva fail to form all tarsal joints and the ta5-pt joint, consistent with the requirement of Notch to form tarsal joints and 'true' joints alike (Figure 3F).

The formation of adult joints is prefigured during prepupal stages by the formation of deep folds in the leg disc epithelium that will maturate during pupation to give rise to the adult structure (MIRTH AND AKAM 2002; TAJIRI *et al.* 2010; MONIER *et al.* 2015). Therefore, loss of prepupal folds correlate with adult joint defects. Consequently, both *Dll^{212}>dysfRNAi* and *Notch^{tsa}* prepupal leg discs do not form tarsal epithelial folds in the prepupal stage (Compare Figure 3H and I with G). These results demonstrate that Dysf activity is completely required for prepupal fold and adult joint formation in the tarsal region of the leg.

1.3 Dysf activity is sufficient to form ectopic folds

After assessing the requirement of *dysf* for tarsal joint formation, we tested whether *dysf* misexpression would be sufficient to form ectopic joint-like structures. We used the *patched* (*ptc*)-*Gal4* driver to ectopically express *dysf* in a row of cells along the P-D axis of the leg. As the expression of *ptc*>UAS-*dysf* during the whole development cause severe deformations in the legs, we decided to restrict *dysf* expression using the *tubGal80^{ts}* technique (see Materials and Methods). Using this method we were able to recover adult legs that presented a sharp cleft in the cuticle along the P-D axis, perpendicular to the tarsal joints (arrows in Figure 4A). Although it is more evident in the tarsal segments, *dysf* also form ectopic folds in more proximal segments such as the tibia (arrows in Figure 4B). These phenotypes are reminiscent of a Notch ectopic activation in the leg (DE CELIS *et al.* 1998; BISHOP *et al.* 1999; RAUSKOLB AND IRVINE 1999).

The ability of Dysf to form ectopic folds was also tested in third instar larva leg discs, where misexpression of *dysf* in the *ptc* domain induce folding of the epithelium (more visible in the distal tip of the leg; see Figure 4D). Interestingly, Notch activation is dispensable for this function, as *dysf* ectopic expression form folds in a *Notch^{tsa}* mutant background (Figure 4E). These data confirm the ability of Dysf to form ectopic folds both in imaginal discs and adult cuticle, which resembles the processes that occur during normal joint development. Nevertheless, we cannot conclude that ectopic *dysf* expression generates a complete ectopic

tarsal joint, which would require the formation of the complex ball and socket architecture that we have not observed.

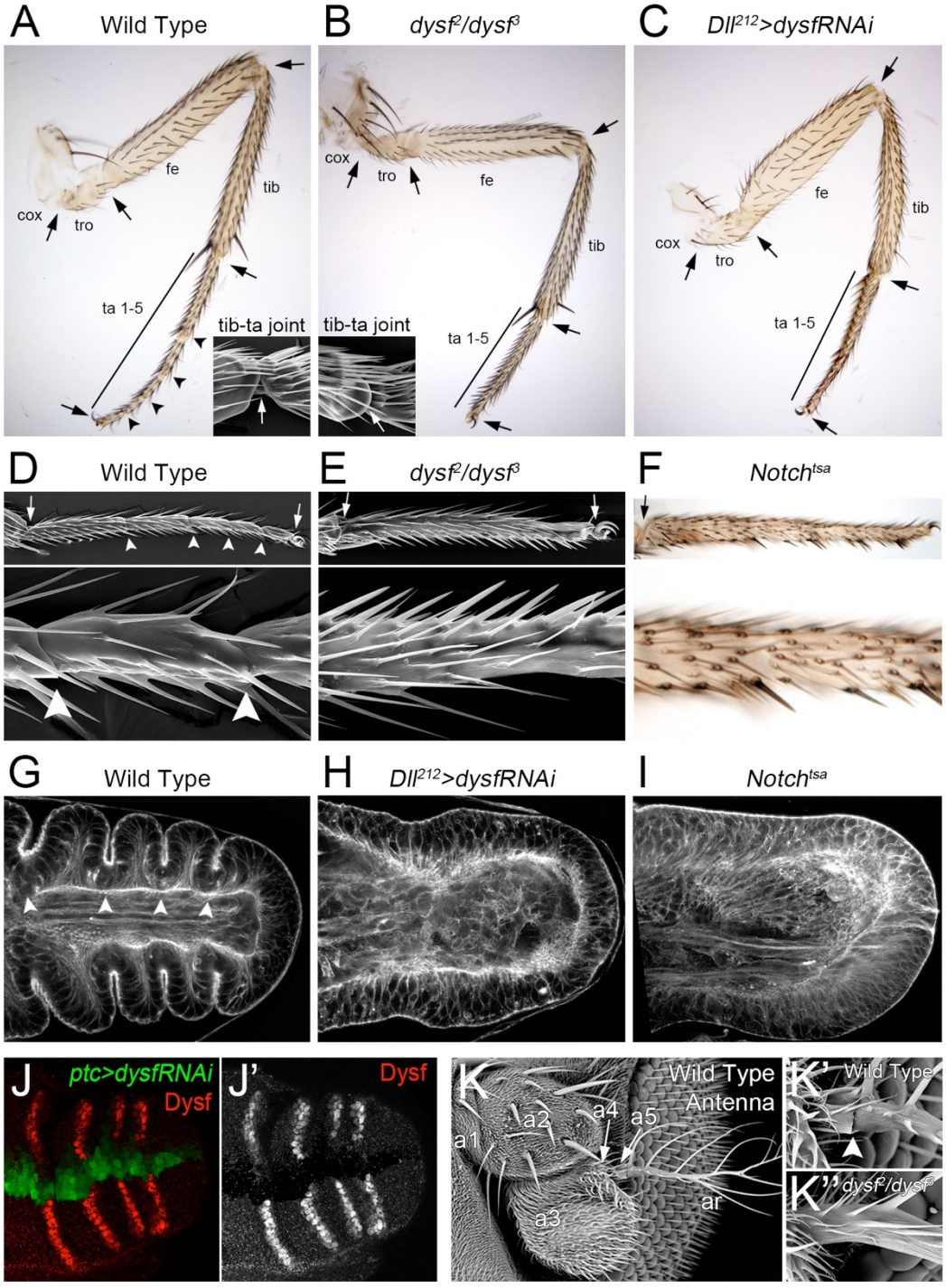

Figure 3. Dysf is required for tarsal fold and joint formation and resembles Notch phenotypes. (A-E) Phenotype of a wild type **(A)** and a *dysf²/dysf³* mutant **(B)** adult leg. Note that *dysf²/dysf³* mutants lose all tarsal joints and present a shortened tarsal region, while 'true' joints remain unaffected. Insets in **A** and **B** are Scanning Electron Microscopy (SEM) images of the tibia-tarsal (tib-ta) joint of the corresponding genotype. **(C)** *Dll²¹²*>UAS-*dysfRNAi* adult leg phenotype is almost identical to *dysf²/dysf³* mutants. **(D and E)** SEM imaging of the tarsal region of a wild type and a *dysf²/dysf³* leg, respectively. **(F)** *Notch^tsa* leg phenotype also exhibits lack of tarsal joint formation. Lower panels in **D-F** present a magnification of the tarsal region. In all previous panels, arrows point to 'true' joints, while arrowheads indicate normal tarsal joint formation. cox: coxa, tro: trochanter, fe: femur, tib: tibia, ta 1-5: tarsus 1 to 5. **(G-I)** Sagittal view of the tarsal region of wild type **(G)**, *Dll²¹²*>UAS-*dysfRNAi* **(H)** and *Notch^tsa* **(I)** prepupal leg discs. The folds that prefigure the adult tarsal joints are visible in **G** (arrowheads) and absent in **H** and **I**. Cell shape is visualized with Phal. **(J)** *ptc*>UAS-*dysfRNAi* expression eliminates Dysf protein (red and separate channel in **J'**) from prepupal leg discs. *ptc* is marked with GFP. **(K)** Wild type antenna, with the antennal segments 1 to 5 (a1-5) and the arista (ar) indicated. The joint between a5-ar (arrowhead in **K'**) is lost in *dysf²/dysf³* mutants **(K'')**.

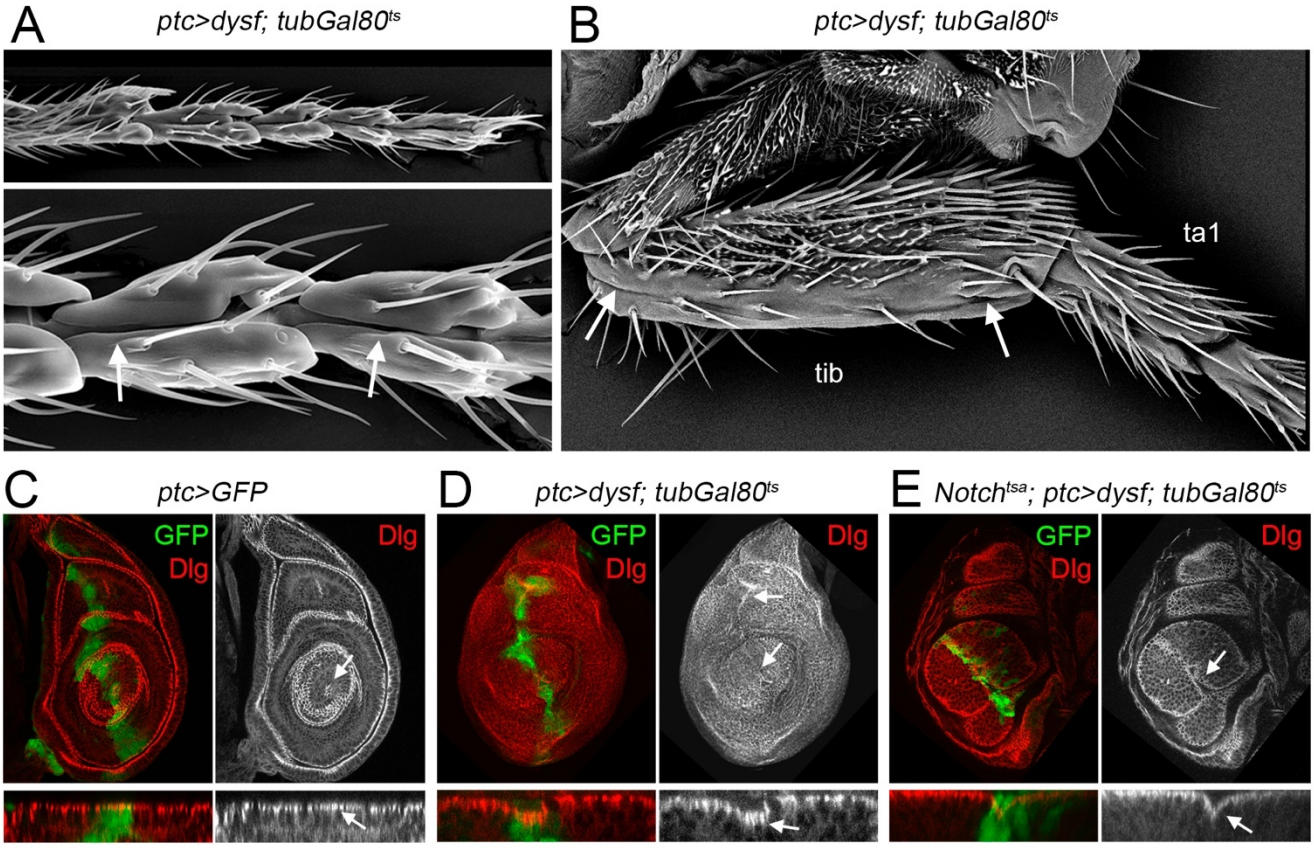

Figure 4. Dysf induces ectopic fold formation in adult legs and imaginal discs. (A and B) Adult leg of a *ptc*>UAS-*dysf; tubGal80ts* fly, switched to 29°C after 11 days at 17°C. *dysf* misexpression cause an ectopic fold along the P-D axis in the tarsal region (arrows in **A**) and in more proximal regions (arrows in **B**). **(C-E)** Third instar leg discs stained with Discs-large (Dlg, red and separate channels to the right) of the following genotypes: *ptc*>UAS-*GFP* **(C)**, *ptc*>UAS-*dysf*; *tubGal80*^{ts} **(E)** and *Notch*^{tsa}; *ptc*>UAS-*GFP*; UAS-*dysf*; *tubGal80*^{ts} **(E)**. *ptc* domain is visualized by GFP expression (green). A Z-section of the distal-most tip of the leg discs is shown in the panels below. Arrows indicate the presence of ectopic folds in the epithelium. Note that Dysf can induce ectopic folds in a *Notch*^{tsa} mutant background.

2. TRANSCRIPTIONAL REGULATION OF *dysf* EXPRESSION

We have shown that Dysf is localized in the cells that activate the Notch pathway in the tarsal region, and that its function is required for tarsal joint formation. This made *dysf* a good candidate to be a Notch target in this developmental context. In this section, we explore the regulatory relationship between *Notch* and *dysf*.

2.1 *dysf* expression depends on Notch activity

To elucidate whether *dysf* expression is regulated by Notch, we either knocked down or ectopically activated the Notch pathway in the *ptc* domain using UAS-*NotchRNAi* and UAS-*Notch*^{ICD} (the intracellular domain of the Notch receptor), respectively, in prepupal leg discs. We observed that Dysf is depleted when Notch activation is impaired, whereas *dysf* expression is induced upon ectopic Notch activation (Figure 5A and B, respectively). Interestingly, although Notch is ectopically activated along the P-D axis of the leg in *ptc*>UAS-*Notch*^{ICD}, ectopic *dysf* expression is restricted to the tarsal region (asterisk in Figure 5B').

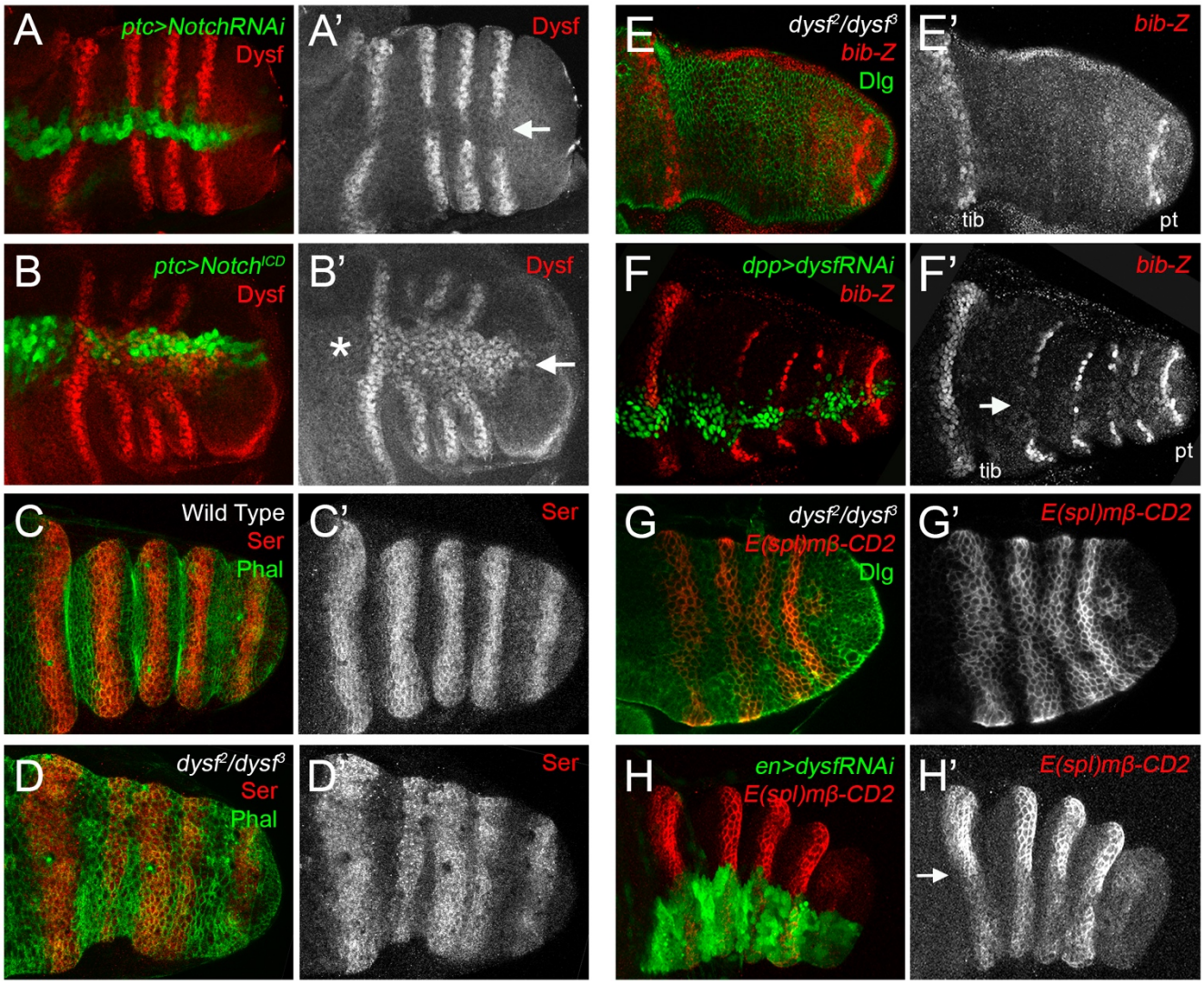

Figure 5. *dysf* expression depends on Notch. (A) Notch knockdown by RNA interference in the *ptc* domain in a prepupal leg disc (*ptc*>UAS-*NotchRNAi*) cause the loss of Dysf staining (arrow). **(B)** Ectopic activation of Notch in the *ptc* domain in a prepupal leg disc (*ptc*>UAS-*Notch^{ICD}*) induces ectopic Dysf in the tarsal region (arrow) but not in more proximal segments (asterisk). *ptc* domain is marked by GFP expression (green in **A** and **B**) and Dysf staining is in red in **A** and **B** and separate channel in **A'** and **B'**. **(C and D)** Ser staining (red and separate channel in **C'** and **D'**) is maintained in a *dysf^2/dysf^3* mutant prepupal leg disc. Phal is in green. **(E and F)** *dysf* loss of function causes the loss *bib-Z* expression (red and separate channel in **E'** and **F'**) in a *dysf^2/dysf^3* mutant prepupal leg disc **(E)** or expressing UAS-*dysfRNAi* **(F)** in the *dpp* domain (marked by GFP expression, green). Note that *bib-Z* expression is only affected in the tarsal region (arrow), while its expression is maintained in the presumptive 'true' joints (tib and pt). **(G and H)** *dysf* loss of function does not eliminate *E(spl)mβ-CD2* expression (red and separate channel in **G'** and **H'**) in a *dysf^2/dysf^3* mutant prepupal leg disc **(G)** or expressing UAS-*dysfRNAi* **(H)** in the *en* domain (marked by GFP expression, green), indicating that Notch activity is still present. Nevertheless, in *en*>UAS-*dysfRNAi* leg discs *E(spl)mβ-CD2* expression appears to be slightly downregulated in the absence of Dysf **(H')**.

To further study the relationship between *dysf* and the Notch pathway, we analyzed the presence of the Notch ligand Ser in *dysf^2/dysf^3* mutant leg discs. Despite fold formation is abrogated, the localization of Ser is not compromised (compare Figure 5C and D). Next, we tested if *dysf* is necessary for the expression of two known Notch targets, *bib* and *E(spl)mβ*. Either in *dysf^2/dysf^3* mutants or in *dpp>dysfRNAi* prepupal legs, *bib-lacZ* expression was eliminated only from the tarsal region (Figure 5E and F). Conversely, *E(spl)mβ-CD2* remains expressed and correctly positioned in *dysf^2/dysf^3* mutant legs, indicating a normal Notch activation in *dysf* loss of function. Nevertheless, *dysfRNAi* expression in the posterior compartment using the *en-Gal4* driver reveals a

slight downregulation of *E(spl)mβ-CD2* expression levels (Figure 5G and H). These results indicate that *dysf* regulates some, but not all, Notch targets in the presumptive tarsal joints. Importantly, our experiments show that the phenotypes caused by *dysf* loss of function in the legs are not due to defects in leg segmentation nor Notch pathway activation.

Up to now, our results suggest that *dysf* is a downstream target of Notch, however the functional relationship between both genes to form the tarsal joints is unknown. To clarify this, we first studied independently the ability of *dysf* and UAS-*Notch^{lCD}* to form ectopic folds in the adult leg when expressed under control of the *ptc-Gal4* driver. We temporarily restricted *dysf* and *Notch^{lCD}* misexpression using the *tubGal80^{ts}* system (see Materials and Methods). As we previously described, ectopic *dysf* expression form a joint-like fold along the P-D axis of the leg (Figure 6D with Figure 4A). Analogously, ectopic activation of Notch also forms a joint-like fold in the leg (Figure 6E). Next, we expressed *dysf* in a *Notch^{tsa}* background and observed that, while endogenous tarsal joints are absent, we can observe a fold along the P-D axis of the leg (compare Figure 6F with the control in B). This result places *dysf* epistatic to Notch activity in the formation of ectopic joint-like folds in the leg. Surprisingly, expression of *Notch^{lCD}* in a *dysf^{2}/dysf^{3}* mutant background also generates a cuticular fold (compare Figure 6G with the control in C). This suggests that forced Notch activation may regulate other genetic programs in order to form joint-like structures in the tarsal region in the absence of *dysf.* Consistently, ectopic expression of *odd* and *sob*, genes normally expressed in the proximal joints, also cause ectopic folds in the tarsal region (HAO *et al.* 2003).

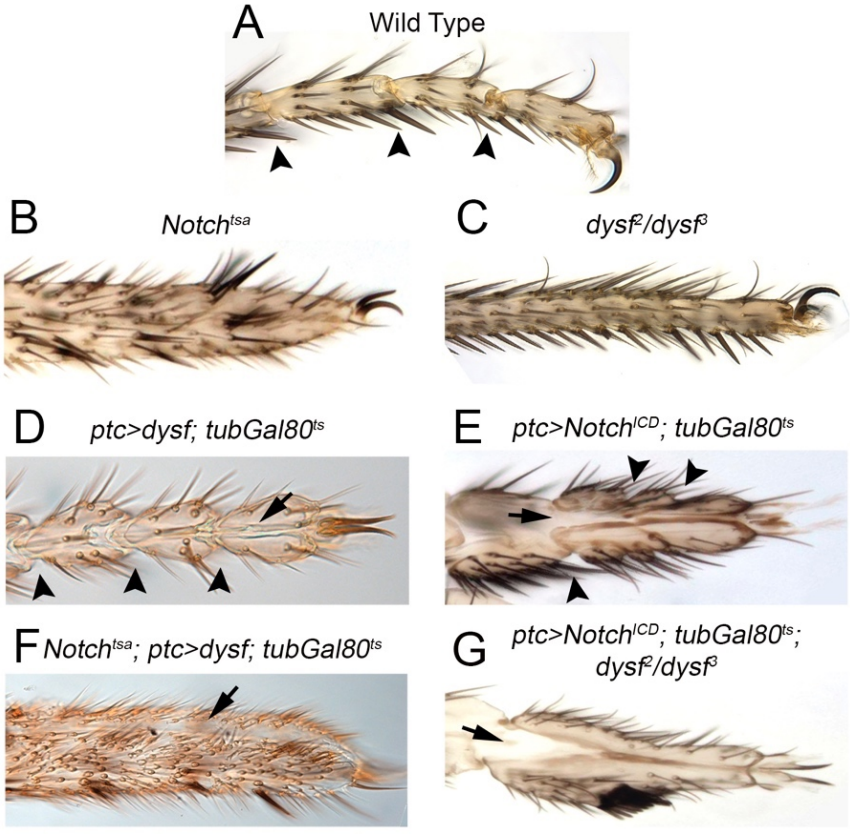

Figure 6. Epistatic relationship between Notch and dysf. Tarsal region of adult legs corresponding to the following genotypes: wild type **(A)**, *Notch^{tsa}* **(B)**, *dysf^{2}/dysf^{3}* **(C)**, *ptc*>UAS-*dysf*; *tubGal80^{ts}* **(D)**, *ptc*>UAS-*Notch^{lCD}*; *tubGal80^{ts}* **(E)**, *Notch^{tsa}*; *ptc*>UAS-*dyfs*; *tubGal80^{ts}* **(F)** and *ptc*>UAS-*Notch^{lCD}*; *tubGal80^{ts}; dysf^{2}/dysf^{3}* **(G)**. Normal joint formation is pointed out with arrowheads while ectopic folds along the PD axis are marked with arrows. Note the absence of tarsal joints in *dysf^{2}/dysf^{3}* **(C)** and *Notch^{tsa}* **(E)** legs, and the ectopic folds induced by *dysf* **(D)** or *Notch^{lCD}* **(E)** misexpression either in a wild type background or in a *Notch^{tsa}* **(F)** or *dysf^{2}/dysf^{3}* **(G)** mutant background, respectively.

2.2 *dysf640* CRM reproduces *dysf* expression pattern and is regulated by *Notch*

In order to understand how the Notch pathway exerts its regulation over *dysf*, we searched for CRMs that could direct *dysf* expression in the tarsal region of the leg. We surveyed 11 DNA fragments from the FlyLight database that span the *dysf* genomic locus, including the 5' region adjacent to the *dysf* gene and its intronic regions. Of those, only two overlapping DNA fragments drive expression of *GFP* in rings in the tarsal region of the leg (see Figure 1). We cloned the 640bp-long overlapping sequence into a nuclear *lacZ* reporter vector to test its activity *in vivo* (see Materials and Methods). This sequence, henceforth named *dysf640*, contains all the necessary information to reproduce *dysf* expression in the tarsal region (Figure 7A and B). In an attempt to further define the minimal region that directs *dysf* expression, we divided *dysf640* into two halves (*dysf640*^{A} and

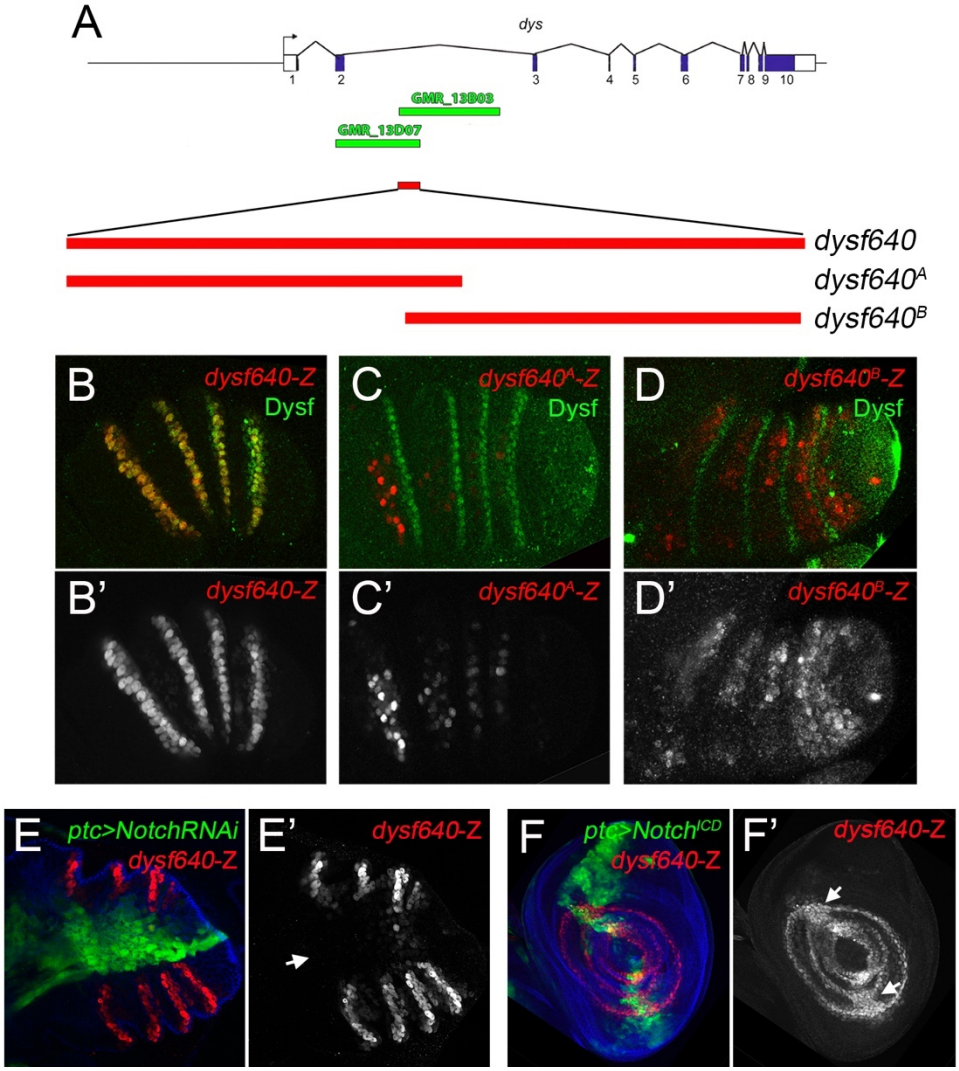

Figure 7. The dysf640 CRM reproduces dysf expression and is regulated by Notch. (A) Schematic representation of the genomic locus of *dysf* showing the two Janelia database sequences that drive GFP exression in the tarsal region (see **Figure 1**). The 640 bp overlapping fragment between GMR_13D07 and GMR_13B03, dubbed here *dysf640*, and smaller fragments of it (*dysf640A* and *dysf640B*) are represented below (red bars). *dysf640* **(B)**, *dysf640A* **(C)** and *dysf640B* **(D)** were cloned to drive *lacZ* reporter expression. *lacZ* expression (red in **B-D** and separate channels in **B'-D'**) is compared with Dysf antibody staining (green in **B-D**). *dysf640-Z* recapitulates Dysf expression while *dysf640A-Z* and *dysf640B-Z* does not. **(E)** UAS-*NotchRNAi* expression in the *ptc* domain in a prepupal leg disc. Notch loss of function downregulates *dysf640-Z* expression (arrow). **(F)** Expression of UAS-*Notch*^{ICD} in the *ptc* domain of a third instar larva leg disc. Notch pathway activation induces *dysf640-Z* expression in the tarsal region (arrows), but not in more proximal regions of the leg. *ptc* domain is marked by GFP expression (green in **E** and **F**), and *dysf640-Z* expression is in red in **E** and **F** and separate channels in **E'** and **F'**.

dysf640^{B}). None of these smaller fragments was able to reproduce the complete *dysf640* CRM expression: *dysf640*^{A}*-lacZ* is expressed in small and disperse patches, while *dysf640*^{B}*-lacZ* is weakly expressed in the interjoint domains throughout the tarsal region (Figure 7C and D).

Next, we confirmed that Notch regulation of *dysf* was exerted through the *dysf640* CRM. Knockdown of Notch (*ptc>NotchRNAi*) resulted in the loss of *dysf640-lacZ* expression, while forced activation of the Notch pathway (*ptc>Notch*^{ICD}) caused ectopic *dyfs640-lacZ* expression that was restricted to the tarsal region of the leg disc (Figure 7E and F, respectively). These results were identical to those observed when using Dysf antibody, what led us to conclude that the *dysf640* CRM is regulated by Notch in the same manner that the endogenous *dysf* gene.

2.3 *dysf* is directly regulated by Notch through a dedicated Su(H) binding sites

Having shown that *dysf* expression is likely regulated by Notch through the *dyfs640* CRM, we asked whether this regulation is direct. Notch transcriptional regulation requires Supressor of Hairles (Su(H)), a binding partner of Notch that recognizes and binds to the regulatory region of Notch target genes (BRAY AND FURRIOLS 2001; LAI 2002; and see Figure I-4B). A bioinformatic survey identified three highly conserved Su(H) putative sites within the *dysf640* CRM. Next, we tested the ability of Su(H) protein to bind these putative sites by an electrophoretic mobility shift assay (EMSA) (see Materials and Methods). We observed that the migration of the Su(H)-1 and Su(H)-2 probes in a gel was shifted upwards when in the presence of the Su(H) protein, indicating that Su(H) bind these sites and forms protein-DNA complexes with reduced mobility in the gel (Figure 8C). This shift was not observed for the Su(H)-3 probe. When Su(H)-1 and Su(H)-2 binding sites were mutated, the binding and consequent shift is not observed, a proof of specific protein-DNA interactions. This experiment indicates that Su(H) can directly and specifically bind *dysf640* CRM through at least two binding sites, allowing the direct regulation of *dysf* expression by Notch.

To test *in vivo* the contribution of each Su(H) binding sites to *dysf640-lacZ* expression, we cloned mutated versions of each site, and the combination of both (termed *dysf640*$^{Su(H)-1}$, *dysf640*$^{Su(H)-2}$ and *dysf640*$^{Su(H)-1+2}$, respectively), in the same *lacZ* reporter vector. All constructs were inserted at the same chromosomal location as the control wild type version, to allow proper comparison of *lacZ* expression levels. As previously described, *dysf640-lacZ* is expressed at high levels in Dysf positive cells (Figure 8D and schematic representation in H). Mutation of either site alone caused a clear reduction, but not complete inhibition, of *lacZ* expression. Interestingly, we observed a slight derepression of *lacZ* expression in the interjoint regions that is stronger in the fourth tarsal segment (Figure 8E and F and schematic representation in I). When both sites were mutated

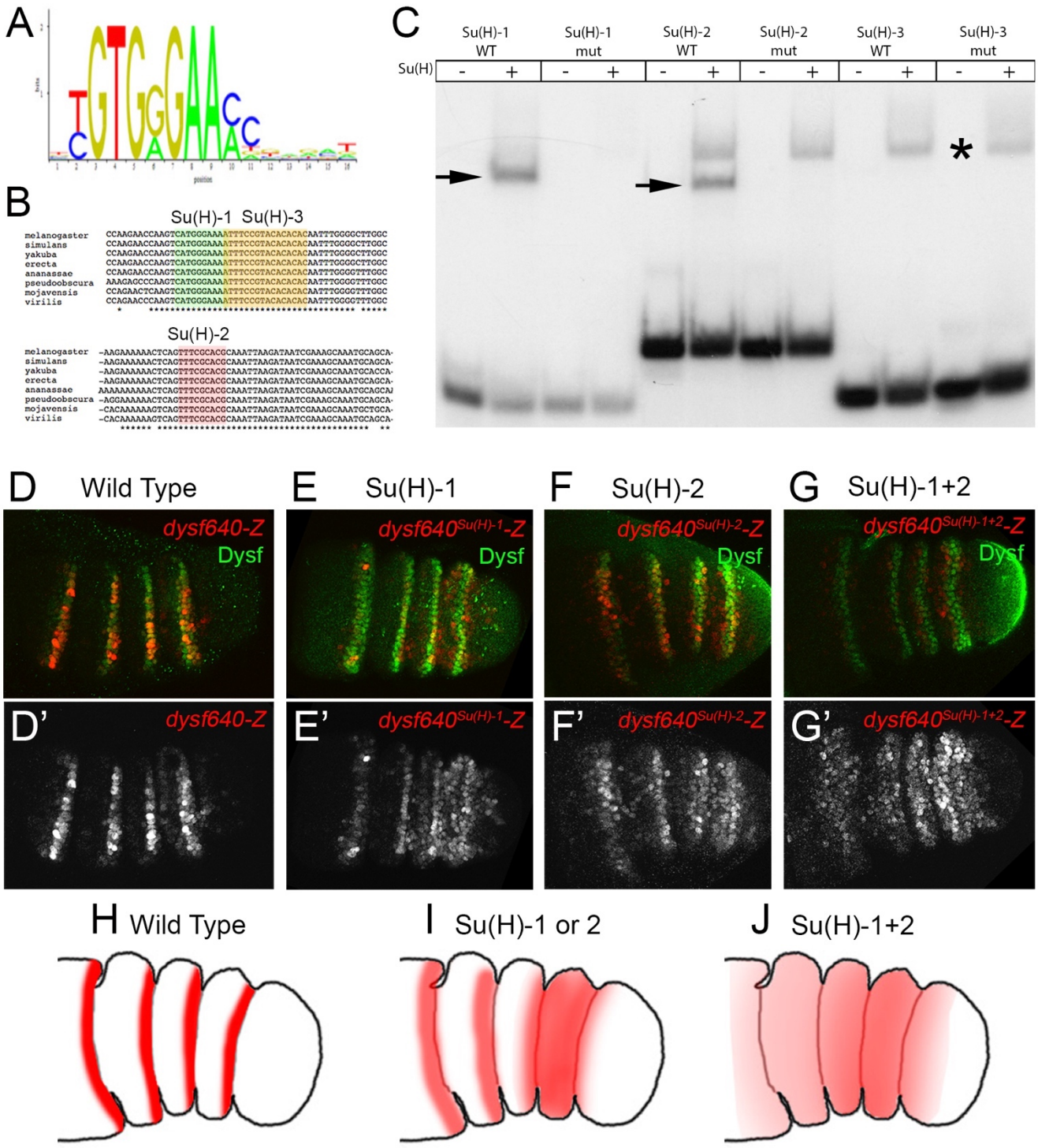

Figure 8. dysf is directly regulated by Notch through Su(H) binding sites. (A) Signature for predicted Su(H) binding sites obtained from the Jaspar Database. **(B)** Fragments of the *dysf640* CRM sequence showing three predicted Su(H) binding sites, marked by different colors, and the conservation of these predicted sites among *drosophilids*. **(C)** Electrophoretic Mobility Shift Assay (EMSA) to assess binding of Su(H) protein to DNA probes containing the predicted Su(H) binding sites (WT) or probes where the putative binding sites were mutated (mut). DNA probes were radioactively labeled (see Materials and Methods for sequences). Su(H) protein directly binds Su(H)-1 and Su(H)-2 DNA probes, causing the formation of protein-DNA complexes that are evident by the delay in electrophoretic mobility (arrows). Asterisk indicate an nonspecific band present in both wild type and mutant probes in Su(H)-2 and Su(H)-3. **(D-G)** Prepupal leg discs stained for Dysf (green) and for *dysf640-Z* **(D)**, *dysf640*$^{Su(H)-1}$*-Z* **(E)**, *dysf640*$^{Su(H)-2}$*-Z* **(F)** and *dysf640*$^{Su(H)-1+2}$*-Z* **(G)** expression (red and separate channel in **D'-G'**). All constructs have been inserted in the same genomic location, and images were obtained keeping the confocal settings constant in the merged image **(D-G)**. Separate channels are displayed below, and for *dysf640*$^{Su(H)-1+2}$*-Z* **(G')** the gain has been increased for visualization purposes. **(H-J)** Schematic representation of *lacZ* reporter expression in *dysf640* wild type **(H)**, mutated Su(H)-1 or Su(H)-2 sites **(I)** and both binding sites mutated **(J)**.

simultaneously, the overall *lacZ* expression is strongly reduced, while a clear derepression in the interjoint regions could be observed throughout the tarsal region of the leg disc (Figure 8G and schematic representation in J). In the light of these results, we propose a double role of Su(H), repressing *dysf* expression in the interjoint domains while allowing *dysf* activation by Notch in the presumptive joint cells.

2.4 Tarsal-specific TFs may restrict *dysf* expression

Although Notch is activated in rings in every joint along the leg P-D axis, *dysf* expression is restricted to the tarsal region. Moreover, when Su(H) activity is removed by mutation of its binding sites, *dysf640-lacZ* is derepressed exclusively in the tarsal region. Taken together, these two observations led us to postulate the requirement of another element that restrict *dysf* expression to the tarsal region. The fate of the leg segments is determined by the establishment of a transcription factor code along the P-D axis; thus, we reasoned that one or several of these TFs might be responsible for *dysf* restricted expression in the tarsus. To test this hypothesis, we selected three TFs which expression encompasses the tarsal region, *rotund* (*rn*), *bric à brac* (*bab*) and *spineless* (*ss*), to perform loss of function experiments and visualize *dysf640-lacZ* expression. *rn* expression (*rn>GFP*), covers all the tarsal folds except it only partially overlaps with Dysf cells in the t4-t5 joint (Figure 9A). Interference RNA against *rn* does not modify *dysf640-lacZ* expression (Figure 9D). In *Drosophila*, there are two partially redundant *bab* genes, *bab1* and *bab2* (COUDERC *et al.* 2002). *bab1* expression covers all the presumptive tarsal joints, as seen with an *lacZ* enhancer trap reporter. To knock down its activity, we generated clones of a deficiency that eliminates both *bab* genes (bab^{AR07}). Nevertheless, loss of *bab* does not alter *dysf640-lacZ* expression nor Dysf protein (Figure 9E). The third candidate TF, Ss, is required for the correct development of the tarsal domain. However, *ss* is only transiently expressed in the tarsal region during early to mid-third instar larval stages (DUNCAN *et al.* 1998; NATORI *et al.* 2012) (Figure I-3C). We used an *ss-Gal4* line that keeps active in the leg until prepupa to drive expression of GFP, and observed that *ss* domain spans all the presumptive tarsal joints (Figure 9C). Knockdown of *ss* function via RNAi expression in the *ptc* domain cause the downregulation of *dysf640-lacZ* signal (Figure 9F). These experiments points to a requirement for *ss*, but not for *rn* and *bab* in the regulation of *dysf* expression in the tarsal region.

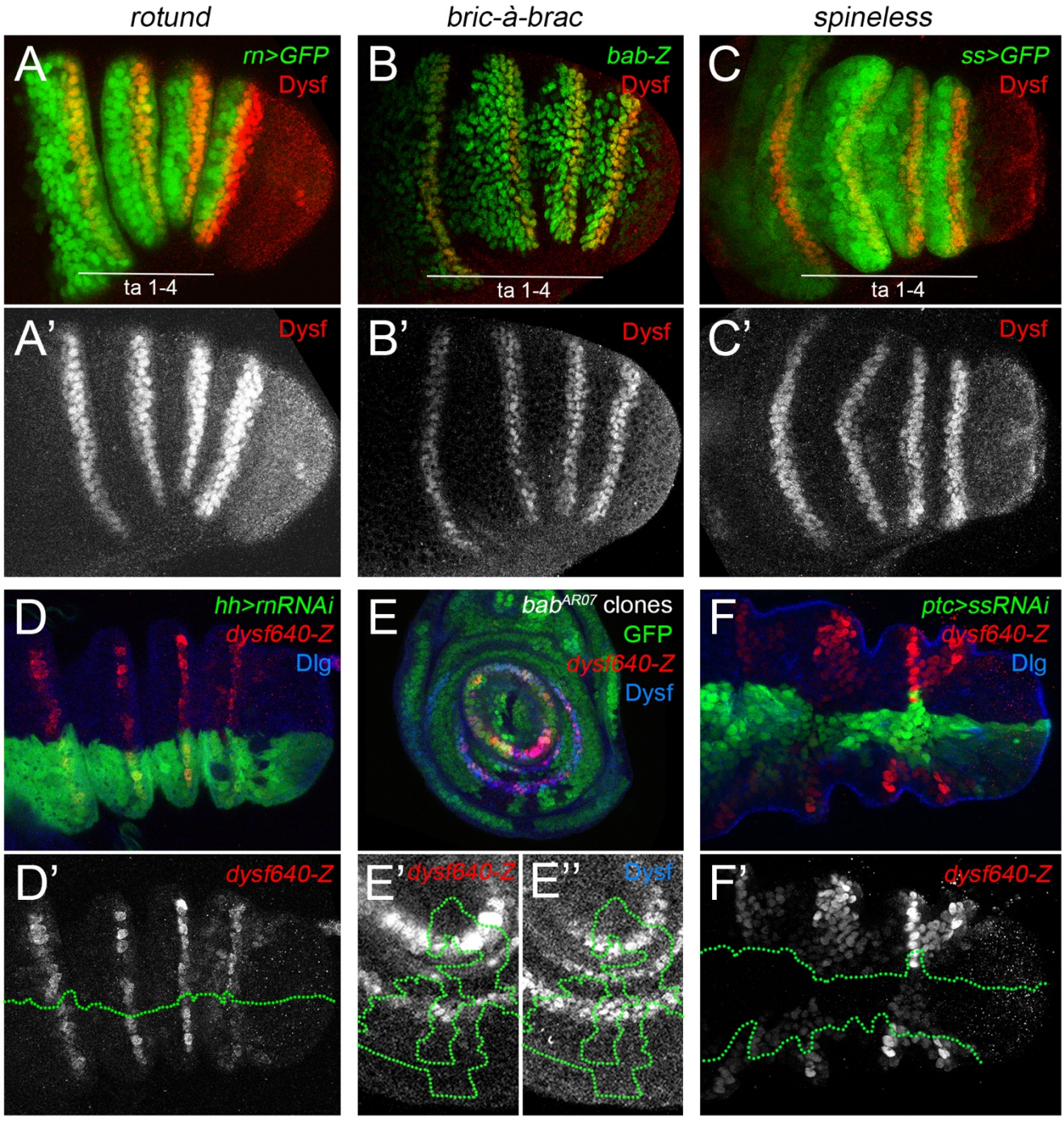

Figure 9. dysf expression requires Spineless (Ss). (A and B) Expression of *rn*>UAS-*GFP* and *bab-Z* (green in **A** and **B**, respectively) and Dysf antibody (red and separate channel in **A'** and **B'**) in prepupal leg discs. **(C)** Expression of *ss* detected by in situ hybridization in early and late third instar larva leg imaginal discs (modified from (DUNCAN *et al.* 1998). **(D)** Schematic representation of *ss* expression compared with the tarsal region of an adult leg (orange bar, modified from (NATORI *et al.* 2012). Note that *ss* expression disappears in late third instar larva (asterisk). **(E)** Expression of RNAi against *rn* in the posterior compartment (marked by GFP expression, green and dotted line in **E'**) does not affect *dysf640-Z* expression (red and separate channel in **E'**) in a prepupal leg disc. **(F)** *bab*^{AR07} clones (marked by the absence of GFP expression, green and dotted line in **F'** and **F''**) in a third instar larva leg disc does not abolish *dysf640-Z* or *dysf* expression (red and blue, and separate channels in **F'** and **F''**, respectively). **(G)** Expression of RNAi against *ss* in the *ptc* domain (marked by GFP expression, green and dotted line in **G'**) cause the loss of *dysf640-Z* expression (red and separate channel in **G'**). Dlg, in blue in **E** and **G**, is used to mark leg disc contours.

dysf REGULATION OF TARSAL JOINT FORMATION

3. Dysf REGULATES GENES IMPLICATED IN TARSAL JOINT MORPHOGENESIS

We have demonstrated that Dysf activity is completely necessary to form epithelial folds and adult joints in the tarsal region. Two morphogenetic processes have been described to play important functions during tarsal joint formation, namely local regulation of Rho GTPases activity (GREENBERG AND HATINI 2011) and programmed cell death (MANJON *et al.* 2007; MONIER *et al.* 2015). In this section, we study the possible relationship between these two processes and Dysf activity, which could possibly explain how this TF can impact tarsal joint morphogenesis.

3.1 Dysf transcriptionally controls the expression of Rho GTPase regulators and pro-apoptotic genes

Several Rho GAPs and GEFs are expressed and required in tarsal joint development. Theregore, we examined the potential relationship between Dysf and two Rho GTPase activity regulators, RhoGAP71E and RhoGEF2 which expression, monitored with *lacZ* reporters, is restricted to the tarsal region (GREENBERG AND HATINI 2011). Both genes are specifically expressed in the cells that form the folds (Figure 10A-D). *RhoGAP71E-lacZ* and *RhoGEF2-lacZ* expressions are partially overlapping with Dysf, and extend their expression one or two

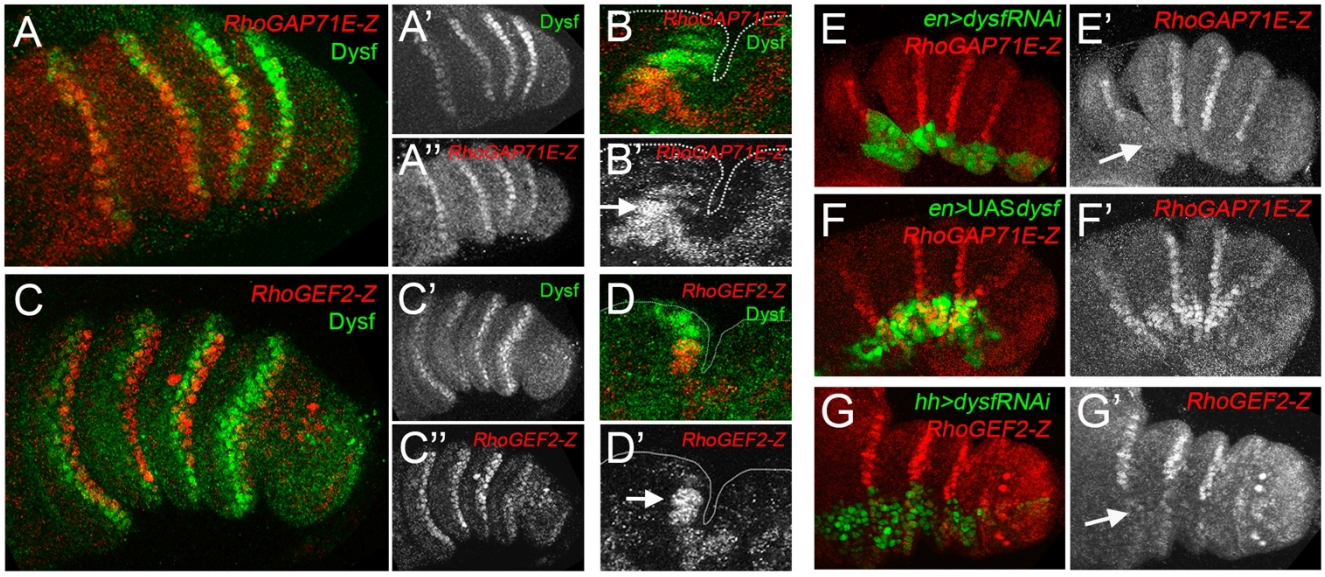

Figure 10. Dysf regulates the expression of Rho GTPase regulators. (A and C) Prepupal leg discs stained for Dysf antibody (green and separate channels in **A'** and **C'**) and *lacZ* reporters of *RhoGAP71E* (red and separate channel in **A''**) and *RhoGEF2* (red and separate channel in **C''**) expression. **B** and **D** correspond to a sagittal section of an epithelial tarsal fold form **A** and **C**, respectively. Apical contour of the epithelium is outlined by a dotted line. Note that *RhoGAP71E-Z* and *RhoGEF2-Z* expression coincides partially with the distal rows of Dysf positive cells (arrows in **B'** and **D'**) and extends distally to a couple rows of cells towards the fold. **(E and G)** UAS-*dysfRNAi* expression in the *en* and *hh* domain, respectively (marked by GFP expression, green), blocks the expression of *RhoGAP71E-Z* and *RhoGEF2-Z* (arrows) (red in **E** and **G** and separate channels in **E'** and **G'**, respectively). **(F)** UAS-*dysf* expression in the *en* domain (marked by GFP expression, green) causes the ectopic expression of *RhoGAP71E-Z* (red and separate channel in **F'**) in the tarsal region of the prepupal leg disc (arrow).

rows of cells distally towards the fold (Figure 10B and D). Importantly, *dysf* RNAi-mediated knock down in the posterior compartment using *en-* or *hh-Gal4* drivers, reduced expression of both reporters (Figure 10E and G), whereas *dysf* misexpression for 24 hrs cause *RhoGAP71E-lacZ* ectopic expression in the *en* domain (Figure 10F).

Next, we studied the relationship between Dysf and the pro-apoptotic genes *rpr* and *hid*, which have been described to take part in the morphogenesis of the tarsal joints (MANJON *et al.* 2007; MONIER *et al.* 2015). *lacZ* reporters of *rpr* and *hid* are expressed in four bands in the tarsal region, that only partially overlap with *dysf* expressing cells (Figure 11A-D). Note that *rpr-lacZ* and *hid-lacZ* expression patterns are virtually identical to those of *RhoGAP71E-lacZ* and *RhoGEF2-lacZ*. Downregulation of Dysf levels by RNAi in the *dpp* or the *en* domain cause the loss of *rpr-lacZ* and *hid-lacZ* expression, respectively, while forced expression of *dysf* for 24 hrs in the posterior compartment results in the cell-autonomous gain of these reporters in the tarsal region (Figure 11E-H). This transcriptional activation of *rpr* and *hid* upon *dysf* misexpression is accompanied by increased levels of cell death, visualized by the presence of cleaved (active) executioner caspase Dcp1, either in third instar larva and prepupal leg discs (Figure 12A and B). As previously observed, Dysf is epistatic to Notch to form ectopic cuticular folds in the adult leg (Figure 6). Therefore, we tested if Dysf ability to control target genes in the tarsal

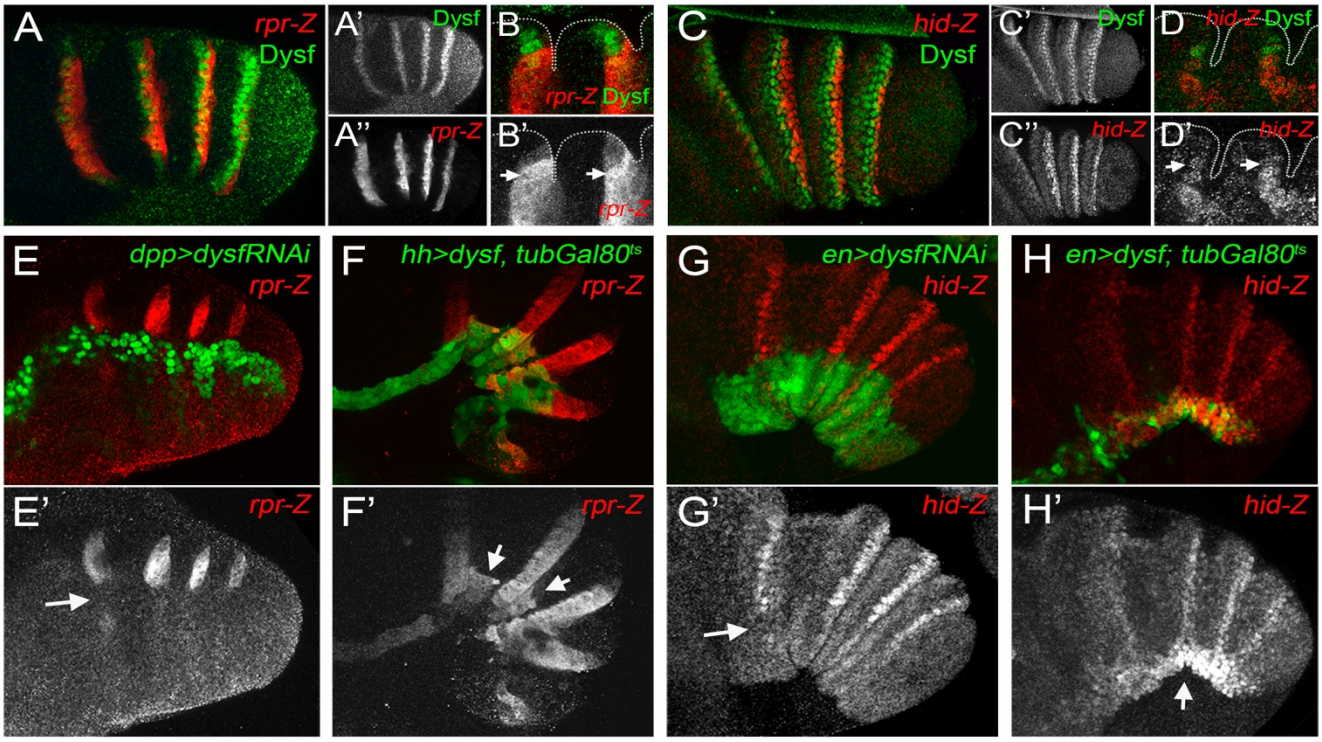

Figure 11. Dysf regulates the expression of pro-apoptotic genes. (A and C) Prepupal leg imaginal discs stained for Dysf antibody (green and separate channels in **A'** and **C'**) and *lacZ* reporters of *rpr* and *hid* (red and separate channels in **A''** and **C''**) expression. **B** and **D** correspond to a transversal section of an epithelial tarsal fold from **A** and **C**, respectively. Apical contour of the epithelium is outlined by a dotted line. Note that *rpr-Z* and *hid-Z* expression coincides partially with *dysf*-expressing cells (arrows in **B'** and **D'**) and extends distally to the fold. **(E and G)** UAS-*dysfRNAi* expression in the *dpp* and *en* domain, respectively (marked by GFP expe, green) eliminates *rpr-Z* and *hid-Z* (red and separate channels in **E'** and **G'**, respectively) expression (arrows). **(F and H)** Expression of UAS-*dysf* in the *hh* and *en* domain, respectively (marked by GFP expression, green), ectopically activates *rpr-Z* and *hid-Z* (red and separate channel in **F'** and **H'**, respectively) expression in the tarsal region of the prepupal leg disc (arrows).

region was also independent of Notch. *Notch*^{tsa} leg discs shifted to 29°C for 24 to 48 hrs prior to dissection showed no *rpr-lacZ* expression (see Materials and Methods). Interestingly, ectopic expression of *dysf* in the *apterous* (*ap*) domain triggers *rpr-lacZ* expression in a *Notch*^{tsa} mutant background (Figure 12C-E).

These experiments demonstrate that Dysf transcriptionally regulates the expression of Rho GTPase regulators and pro-apoptotic genes in the tarsal region in a cell autonomous manner, despite the divergence in the expression domains of *dysf* and its putative targets. This regulation provides a possible morphogenetic mechanism through which the TF Dysf may control fold and joint formation.

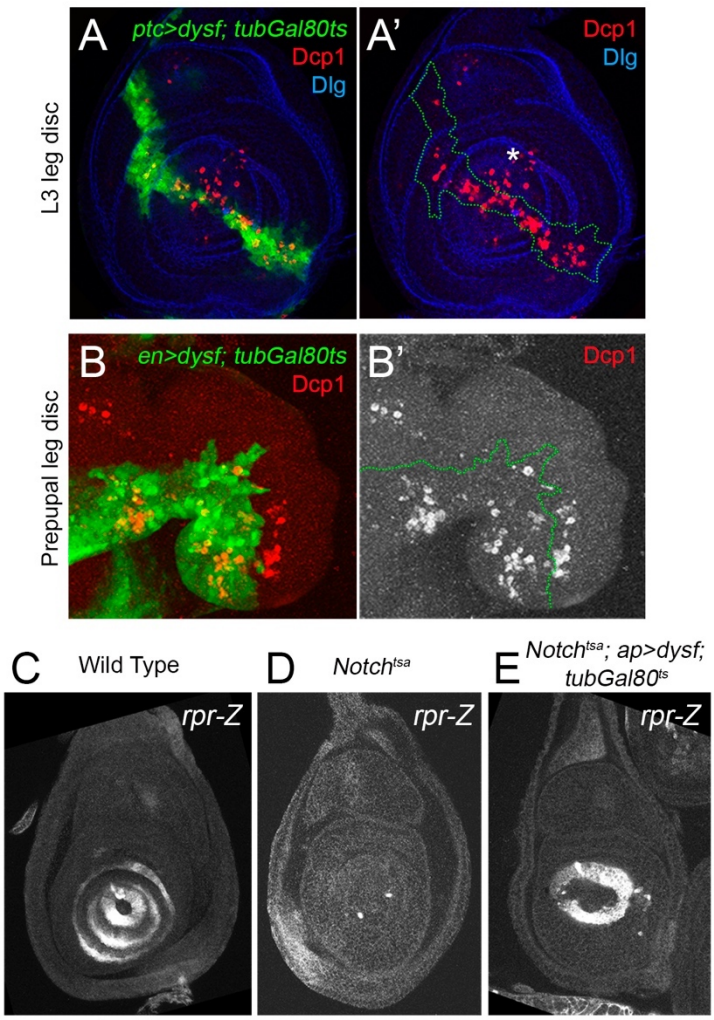

Figure 12. dysf ectopic expression induce cell death independently of Notch. (A) *ptc*>UAS-*dysf; tubGal80*^{ts} third instar larva leg disc. Ectopic *dysf* expression for 24 hrs increases cell death (detected by Dcp1 staining, red in **A** and **A'**) within the *ptc* domain (marked by GFP expression, green in **A** and dotted line in **A'**). Asterisk indicates endogenous cell death typically found in the distal tip of the leg disc. Dlg (blue) is used to visualize the shape of the leg disc. **(B)** *en*>UAS-*dysf; tubGal80*^{ts} prepupal leg disc. *dysf* misexpression for 24 hrs induces caspase activity (Dcp1, red and separate channel in **B'**) in the posterior compartment (marked by GFP expression, green in **B** and dotted line in **B'**). **(C-D)** *rpr-Z* expression in wild type **(C)**, *Notch*^{tsa} **(D)** and *Notch*^{tsa}; *ap*>UAS-*dysf*; *tubGal80*^{ts} **(E)** third instar larva leg disc. *Notch*^{tsa} larvae were shifted to 29°C for 24-48 hrs prior to dissection to generate Notch mutant legs **(D and E)** and to simultaneously activate UAS-*dysf* expression in **E**. Note that the ring-like expression of *rpr-Z* observed in the wild type is lost in *Notch*^{tsa} leg discs, but is rescued by dysf expression in the *ap* domain.

3.2 Dysf loss of function alters Dpp activity borders at the presumptive tarsal joints

It has been proposed that the formation of the tarsal folds and the expression of the pro-apoptotic gene *rpr* are regulated by the presence of sharp borders of Dpp activity in the presumptive tarsal joints (MANJON *et al.* 2007). Therefore, we compared the activity of Dpp (using P-Mad antibody staining as a readout of Dpp pathway activation) with the expression of *bib-lacZ*, as a marker of *dysf* expressing cells. In prepupal leg discs Dpp is expressed in bands that are more visible in the dorsal region (MANJON *et al.* 2007), and the highest levels of P-Mad are coincident with the cells that express *bib-lacZ* (Figure 13A). Downregulation of Dysf activity in the *ptc* domain strongly reduces the levels of P-Mad (Figure 13B). It was previously reported that flip-out clones expressing a constitutively active form of the Dpp receptor Thickveins (UAS-*tkv*^{QD}) cause the activation of *E(spl)mβ* in the leg disc (MANJON *et al.* 2007). We decided to test if the

expression of *dysf*, a direct target of Notch, is also affected by Dpp activity. The expression of UAS-*tkv*^{QD} in the *ap* domain aborts t4-t5 fold formation, cause ectopic *dysf* activation in the proximal part of the t4 segment and disrupts *dysf* endogenous expression at the presumptive t4-t5 joint (Figure 13C). These results indicate that Dpp activity in the leg discs could impact tarsal joint formation possibly through regulation of Notch and subsequent *dysf* expression.

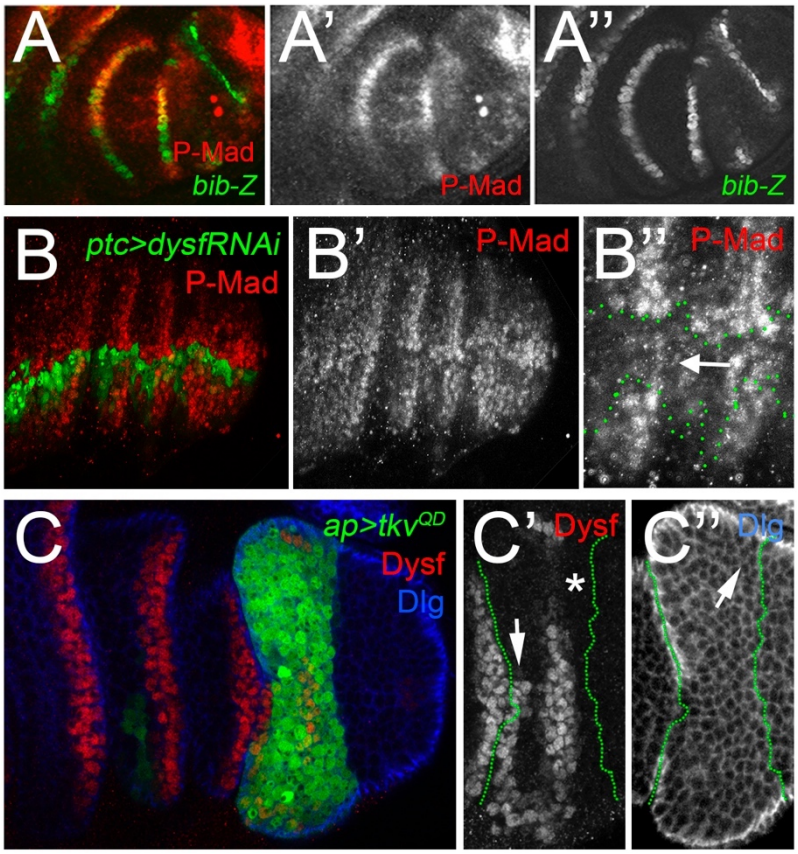

Figure 13. dysf loss of function alters Dpp activity. (A) P-Mad antibody (red and separate channel in **A'**), is accumulated in *bib-Z* (green and separate channel in **A'**) expressing cells in a prepupal leg disc. **(B)** P-Mad levels (red and separate channel in **B'** and **B''**) are downregulated (arrow in **B''**) by UAS-*dysfRNAi* expression in the *ptc* domain (marked by GFP expression, green in **B** and dotted line in **B''**). A close-up of the P-Mad channel is shown in **B''**. **(C)** Expression in the *ap* domain (marked by GFP expression, green and dotted line in **C'** and **C''**) of UAS-*tkv*^{QD}. Dpp inhibition does not affect Dysf (red and separate channel in **C'**) or fold formation (arrow in **C''**). Dlg, in blue and separate channel in **C''**, is used to visualize fold formation.

3.3 *dysf* mutants display altered cell death localization

To our surprise, despite Dysf being required for the expression of the pro-apoptotic genes *rpr* and *hid*, *dysf* mutants still show elevated levels of cell death (Figure 14B). To make sure that the Dcp1 positive cells were indeed apoptotic, we co-stained with TUNEL to detect the DNA fragmentation characteristic of apoptotic cells (GAVRIELI *et al.* 1992). In wild type and *dysf*^{2}/*dysf*^{3} mutant prepupal leg discs, the cells stained for Dcp1 corresponded with TUNEL signal, indicating that in both cases cell death was actually taking place (Figure 14A and B).

A model in which cell death provides the initial force that drives the formation of the tarsal folds has been recently proposed (MONIER *et al.* 2015). According to this model, the presence of a number of dying cells in the presumptive fold region would generate a mechanical force that cause transient invaginations of the neighboring tissue. In the light of this hypothesis, correct localization of cell death is essential to form the folds,

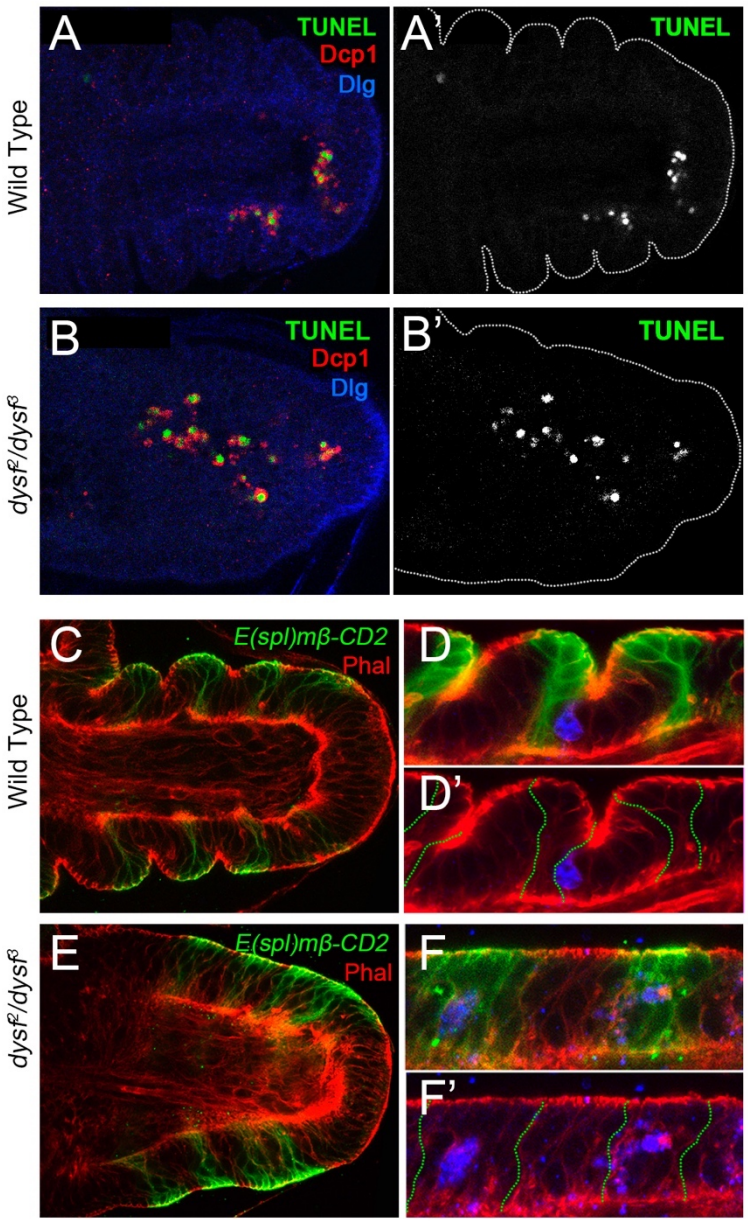

Figure 14. Cell death distribution is altered in dysf mutants. (A and B) Cell death detection by TUNEL staining (green and separate channel in **A'** and **B'**) in wild type **(A)** and *dysf²/dysf³* mutant **(B)** prepupal leg discs. Note that TUNEL signal is coincident with Dcp1 staining (red in **A** and **B**). Dlg (blue and dotted line in **A'** and **B'**) is used to evidence epithelial morphology. **(C-F)** To analyze the distribution of cell death (Dcp1 staining, blue in **D**, **D'** and **F**, **F'**), *E(spl)mβ-CD2* (green in **C-F** and dotted lines in **D'** and **F'**) was used to accurately distinguish between 'Fold' and 'E(spl)mβ' domains in the tarsal region of wild type **(C and D)** and *dysf²/dysf³* mutant leg discs **(E and F)**. Phal staining (red in **C-F**) is used to visualize epithelial shape. **(G)** Quantification of the number of Dcp1 positive cells in 'Fold' and 'E(spl)mβ' domains, and total cell death, in wild type (n=16 joints) and *dysf²/dysf³* (n=20 joints). Only the joints between t2-t3 and t3-t4 were selected for counting. **p<0.01, with *Student's t* test, indicates a significant difference from control. ns, non-significant. Error bars represent SEM.

and mislocalization of dying cells is predicted to abolish their formation. Therefore, we decided to study whether the loss of tarsal folds observed in *dysf* mutants could be explained by incorrect localization of apoptotic cells rather than by a lack of apoptosis. We took advantage of the fact that the Notch target *E(spl)mβ* remains correctly patterned in *dysf²/dysf³* mutants in order to have accurate positional information to compare cell death distribution between wild type and *dysf* mutant leg discs (Figure 14C and E). We counted the number of Dcp1 cells present in the *E(spl)mβ* domains and in the regions between them (here termed *fold* domains) in wild type and *dysf²/dysf³* prepupal leg discs (Figure 14D and F). In wild type legs, apoptotic cells are localized preferentially towards the *fold* domain, in most cases just distally to the *E(spl)mβ* cells (Figure 14D and quantified in G). This pattern of apoptosis is lost in *dysf* mutants, where dying cells are equally distributed across *fold* and *E(spl)mβ* domains (Figure 14F and quantified in G). Remarkably, the total numbers of Dcp1 positive cells are almost equal in wild type and *dysf* mutant legs (Figure 14G). In summary, we observed an altered distribution of cell death in

dysf loss of function, which might explain the loss of epithelial folds and subsequent loss of tarsal joints, according to the model proposed by Monier and colleagues.

3.4 Dysf requires Tgo to regulate tarsal joint formation

The transcription factor Dysf belongs to the Tango (Tgo) dimerization partners of the bHLH-PAS family of TFs, along with other bHLH-PAS proteins that play different roles during development (*i.e.* Spineless (Ss) and Trachealess (Trh)). All of them share the requirement of Tgo to form DNA-binding heterodimers in order to exert their genetic regulation (CREWS 2003). Tgo is present in the cytoplasm and translocates into the nucleus as a heterodimer when one of its dimerization partners is present (WARD *et al.* 1998). During embryonic tracheal development, Dysf requires the presence of Tgo to regulate the expression of its target genes (JIANG AND CREWS 2007). Therefore, we examined if this dependency is also present in the context of tarsal joint formation and the regulation of the Dysf target genes in the leg. We observed that Tgo is accumulated in the nucleus in Dysf expressing cells (Figure 15A), and that *dysf* ectopic expression for 24 hrs in the *ptc* domain is sufficient to promote nuclear localization of Tgo (Figure 15B). Conversely, depletion of Dysf in the posterior compartment (*en>dysfRNAi*) prevents the nuclear accumulation of Tgo in the presumptive joint cells (Figure 15C). These results are in accordance with the described behavior of Tgo, which only translocates to the nucleus if forming heterodimers with its bHLH-PAS partners, in this case with Dysf.

tgo mutants display a variety of tarsal phenotypes, ranging from loss of tarsal segments to defects in tarsal joint formation, depending on the severity of the allele (EMMONS *et al.* 1999). Until now, these phenotypes were ascribed to defects in Ss and Trh function, that cause similar tarsal phenotypes (DUNCAN *et al.* 1998; EMMONS *et al.* 1999; TAJIRI *et al.* 2007). To avoid possible defects related with Ss or Trh function, we knocked down Tgo specifically in the presumptive tarsal joints using *GMR_13D07-Gal4* as a driver (see Figure 1D) to express an UAS-*tgoRNAi* construct. Downregulation of Tgo only at the tarsal joints abrogates joint formation without affecting P-D patterning or leg size. (Figure 15E). To test the efficiency of Tgo knockdown, we stained prepupal leg discs of the same phenotype for Tgo and Dysf, and observed that, while Dysf is still present in the nuclei, Tgo levels are indeed reduced (Figure 15F). Then, we decided to test if Dysf requires Tgo for the regulation of its target genes in the leg. Tgo downregulation in the *dpp* domain (*dpp>tgoRNAi*) suppressed the expression of *bib-lacZ* and *rpr-lacZ* from the putative tarsal joints in a similar manner as *dysfRNAi* does (Figure 15G and H). Next we tested whether Dysf requires Tgo for its transcriptional activity regulating the expression of *rpr* (Figure11E). As expected, *dysf* gain of function clones that are at the same time mutant for *tgo* cannot activate *rpr-lacZ* expression in larval leg discs (Figure 15I and see Materials and Methods).

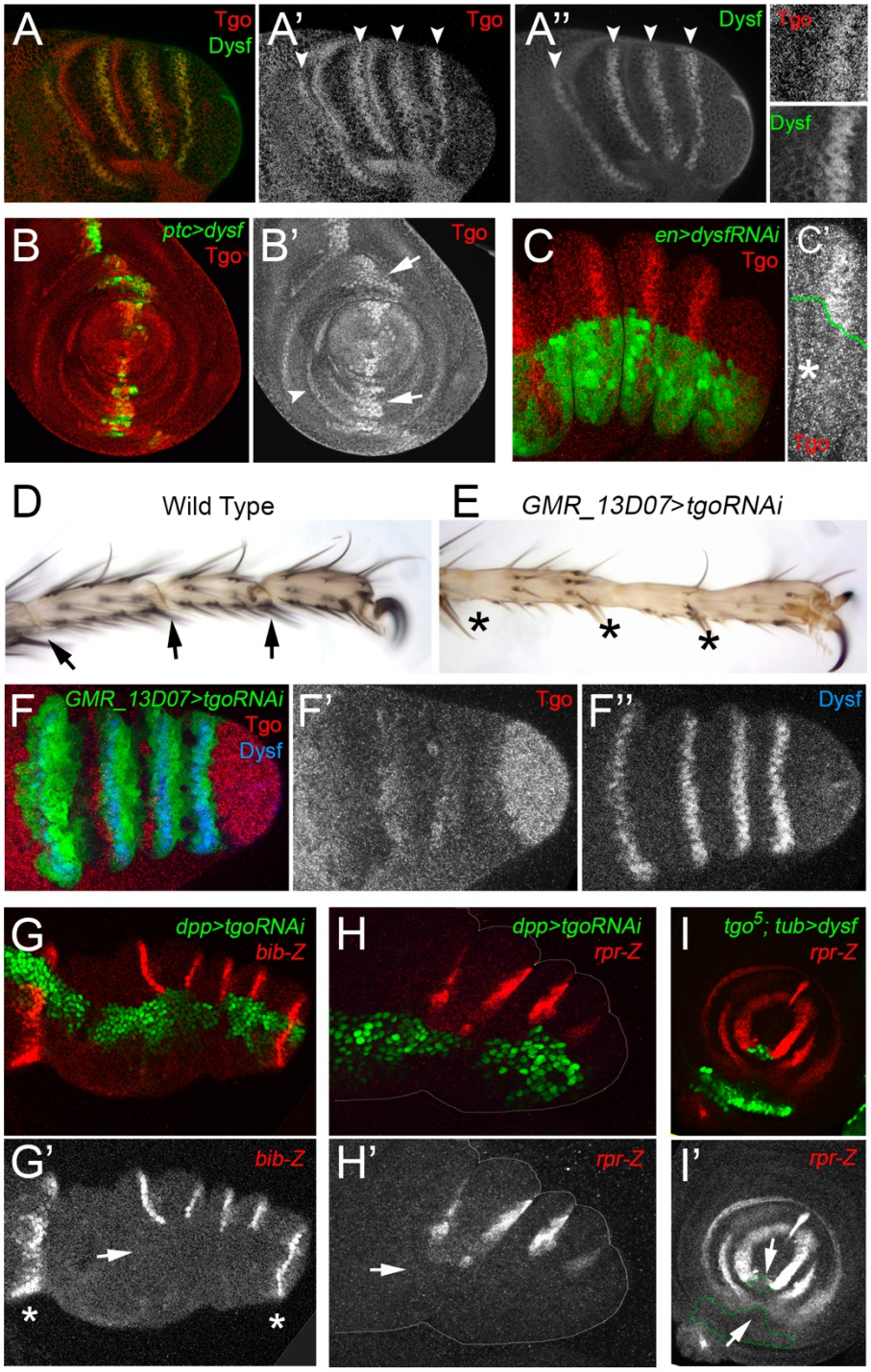

Figure 15. Tgo is a necessary dimerization partner of Dysf during tarsal joint development. (A) Prepupal leg disc double-stained with Tgo (red and separate channel in **A'**) and Dysf (green and separate channel in **A''**) antibodies. Both proteins co-localize in four rings that correspond with the presumptive tarsal joints (arrowheads). Detail of the nuclear co-localization of Tgo and Dysf in a single presumptive joint is shown in insets to the right. **(B)** *ptc*>UAS-*dysf* third instar larva leg disc. Dysf misexpression (marked by GFP expression, green) cause nuclear localization of Tgo (red and separate channel in **B'**) in the *ptc* domain (arrows). Note that the endogenous ring-like Tgo staining in the presumptive joints is maintained (arrowhead). **(C)** *en*>UAS-*dysfRNAi* prepupal leg disc. *dysf* knockdown in the posterior domain (marked by GFP expression, green and dotted line in **C'**) results in the loss of nuclear localization of Tgo (red and separate channel in **C'**). A single presumptive joint is shown in **C'**. **(D and E)**. Tarsal region of an adult leg of wild type **(D)** and *GMR_13D07*>UAS-*tgoRNAi* **(E)**. *GMR13D07-Gal4* directs the knockdown of Tgo specifically at the tarsal joints inhibiting its formation. **(F)** Prepupal leg disc of the same genotype in **E**. UAS-*tgoRNAi* expression is marked by GFP expression (green), Tgo antibody is in red and separate channel in **F'**, and Dysf is in blue and separate channel in **F''**. Note that Tgo is depleted from the presumptive joints while Dysf remains localized. **(G and H)** UAS-*tgoRNAi* expression in the *dpp* domain (marked by GFP expression, green) in prepupal leg discs result in the downregulation of the Dysf targets *bib-Z* (red in **G** and separate channel in **G'**) and *rpr-Z* (red in **H** and separate channel in **H'**). Arrows indicate loss of *lacZ* expression, and asterisks points to *bib-Z* expression at the presumptive 'true' joints, which remains unaffected. **(I)** UAS-*dysf* *'flip-out'* clones (marked by GFP expression, green and dotted outline in **I'**) also mutant for *tgo* (*tgo*^{5}) lose *rpr-Z* expression (arrow) (red and separate channel in **I'**).

4. STUDY OF THE MORPHOGENETIC MECHANISMS THAT SCULPT TARSAL JOINTS

We have shown that Dysf regulates both the expression of the Rho GTPase activity regulators, *RhoGEF2* and *RhoGAP71E* and of the pro-apoptotic genes *rpr* and *hid*. However, the specific role of Rho GTPases, specifically Rho1, during fold and joint formation, and the functional relationship between Rho1 and cell death in this process is unknown. In this section, we are going to study in depth how the implementation of these pathways coordinate the cellular mechanisms that lead to the formation of folds in the prepupal epithelium. In this context, the *dysf* loss of function phenotype provides a valuable model in which folds are completely eliminated to study the process of fold formation.

4.1 Apical constriction is impaired in *dysf* loss of function

During prepupal development, adult joint formation is prefigured by the formation of four deep folds in the epithelium that physically delimitates the future five tarsal segments (Figure 16A). To form these folds, four bands of cells coordinately undergo apical constriction, characterized by the accumulation of F-actin in their apical region and a prominent shortening in their apico-basal axis (Figure 16D and 17). In a time course of t4-t5 fold formation, we could observed the accumulation of F-actin as fold cells begin to apically constrict (mid-fold stage), and accumulate increasing levels of F-actin as their apical surface shrinks and their apico-basal length shortens (late fold stage) (Figure 17A and C). It is remarkable to note that fold cells reduce their apical surface preferentially along the P-D axis of the leg (Figure 16A and analyzed in MONIER *et al.* 2015). Interestingly, and in stark contrast with other models of apical constriction such as ventral furrow formation during embryogenesis (LEPTIN AND GRUNEWALD 1990; MARTIN AND GOLDSTEIN 2014) and see Figure I-9), the basal membrane remains almost completely flat in the prepupal leg disc epithelium, and apically constricted cells do not invaginate. Another interesting feature is that during leg fold formation the epithelium changes from pseudostratified to simple, as indicated by the alignment of cell nuclei in a single row (Figure 16D''' and described in DE MADRID *et al.* 2015).

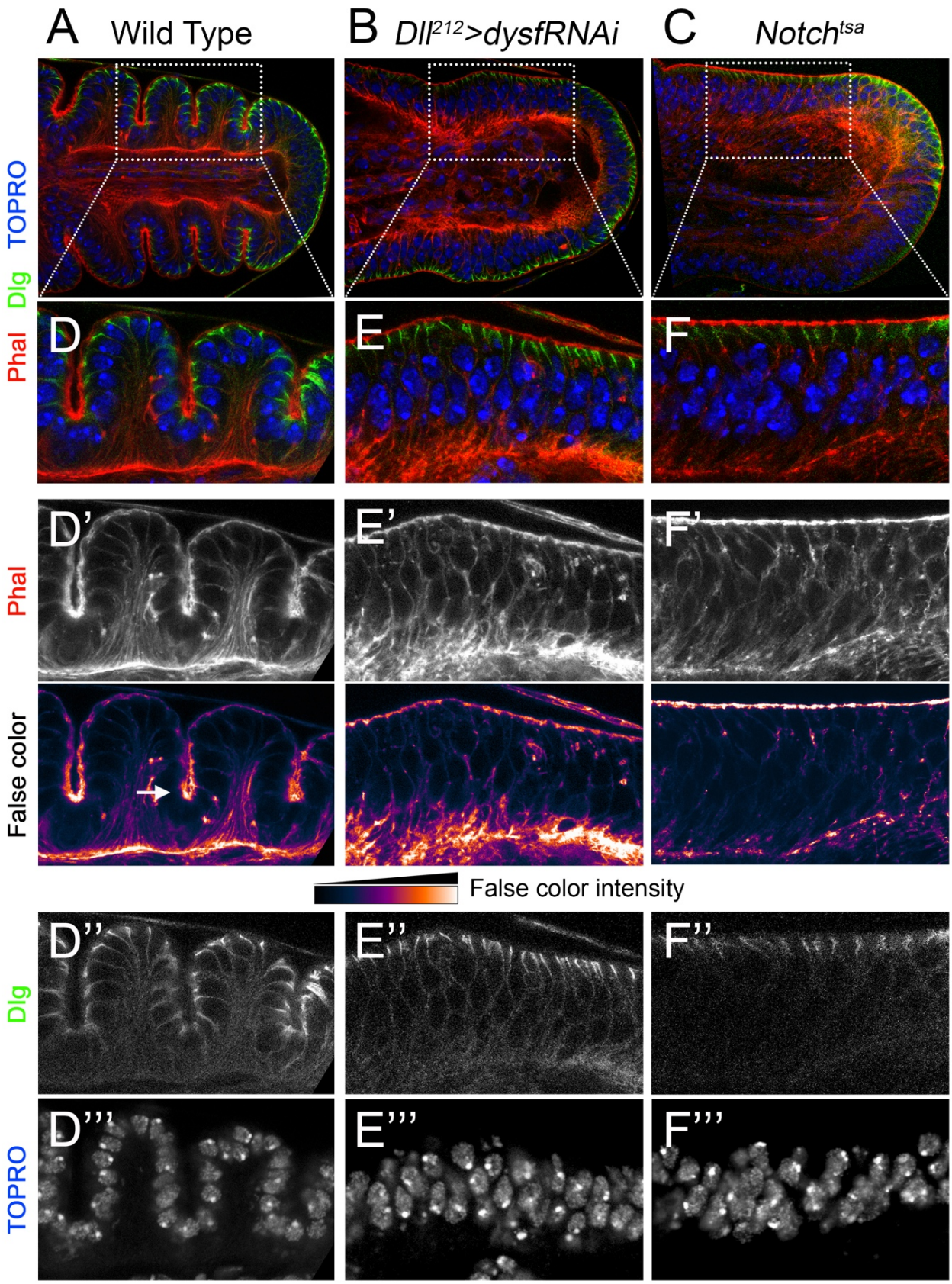

Figure 16. Fold formation is impaired in *dysf* loss of function. (A-C) Tarsal region of wild type **(A)**, *Dll*^{212}*>dysfRNAi* **(B)** and *Notch*^{tsa} **(C)** prepupal leg discs (sagittal view). **(D-F)** Magnification of the leg disc epithelium from the genotypes above (dotted squares). Phal staining is in red in **A-F** and separate channels in **D'-F'**, and false color is used to enhance contrast (lower panels). F-actin is intensely accumulated in the folds (arrow in **D'**). Compare **D'** with **E'** and **F'**, where no folds are formed and the intensity of apical F-actin remains homogeneous throughout the epithelium. The baso-lateral protein Dlg (green in **A-F** and separate channels in **D''-F''**) is used to mark subapical cell-cell contacts. Nuclei are marked with TOPRO (blue in **A-F** and separate channels in **D'''-F'''**). Note that nuclei are aligned in the wild type epithelium while it remains pseudostratified in *Dll*^{212}*>dysfRNAi* and *Notch*^{tsa} prepupal leg discs.

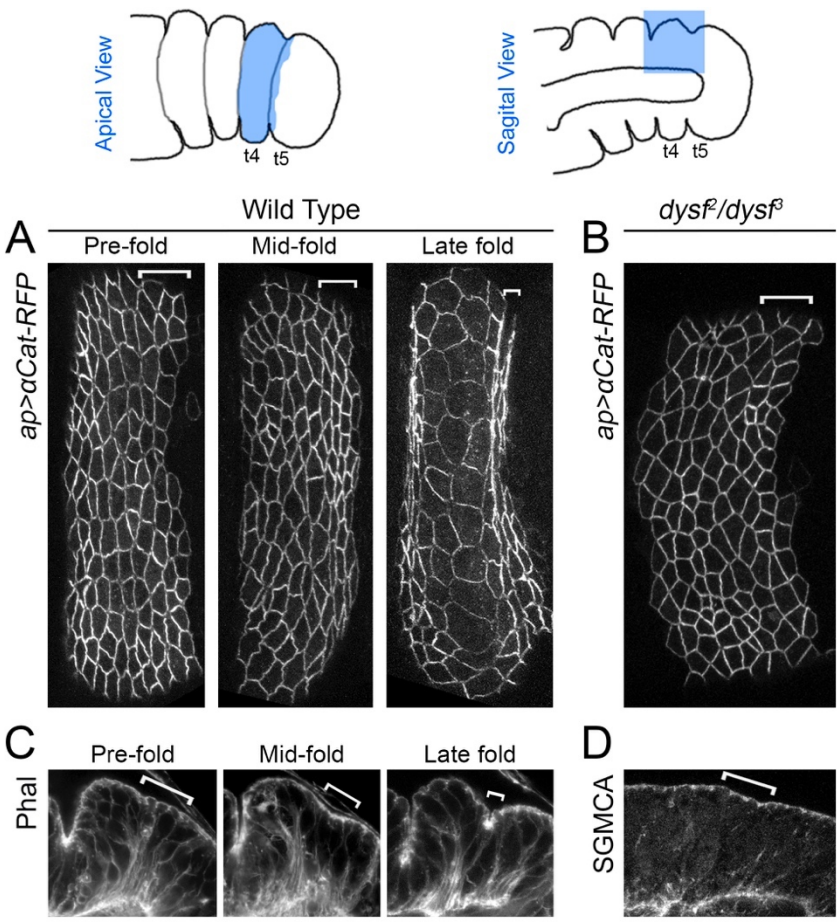

Figure 17. Time course of tarsal fold formation. (A) Apical view of the *ap* domain that encompasses the entire fourth tarsal segment and the cells that would form the fold between t4 and t5. Expression of UAS-*αCatenin-RFP* under the control of the *ap-Gal4* driver is used to visualize cell contacts at the level of the adherens junctions in different time points of fold formation: Pre-fold stage, Mid-fold stage and Late fold stage. **(B)** UAS-*αCatenin-RFP* expressed in the *ap* domain of a $dysf^{2}/dysf^{3}$ mutant. Note that presumptive fold-forming cells do not undergo apical constriction. **(C)** Transversal section of the t4-t5 region of a wild type prepupal leg disc during Pre-fold stage, Mid-fold stage and Late fold stage. Phal is used to visualize F-actin cytoskeleton. Note that the accumulation of F-actin starts at Mid-fold and coincides with the formation of a fold. **(D)** Sagital view of the t4-t5 region (marked with Ap antibody, not shown) of a $dysf^{2}/dysf^{3}$ mutant prepupal leg disc. F-actin is visualized by SGMCA. No F-actin accumulation or folding is observed in these discs. Brackets indicate the rows of cells that would form the t4-t5 fold, and that remain unconstricted and unfolded in *dysf* mutants.

Next, we studied the effects of *dysf* loss of function on tarsal fold formation. To properly compare phenotypes, wild type and *dysf* knockdown prepupae were synchronized and dissected 3 hrs after puparium formation (APF) (see Materials and Methods). In Dll^{212}>*dysfRNAi* prepupal leg discs, apical constriction and subsequent fold formation are impaired, and the epithelium remains flat (Figure 16B). In contrast with the control, apical F-actin is homogeneously distributed through the tarsal epithelium (Figure 16E). It is important to emphasize that the P-D patterning of the tarsal region, and therefore the presumptive joint domains are maintained in *dysf* loss of function (see Figure 5). Consequently, putative fold forming cells, identified as the distal-most rows of cells within the *ap* domain, do not accumulate F-actin and remain unconstricted in mutant $dysf^{2}/dysf^{3}$ prepupal leg discs (Figure 17B and D). We confirmed that the difference in apical F-actin accumulation between wild type and Dll^{212}>*dysfRNAi* is not caused by apico-basal polarity defects of the putative fold forming cells, as the baso-lateral marker Discs large (Dlg) is correctly located in the absence of Dysf (compare 16E'' and D''). Additionally, when fold formation is inhibited, the epithelium remains pseudostratified and nuclei are not aligned (compare Figure 16E''' with D'''), a phenotype previously described for RhoGAP68F knockdown, which also causes defects in fold formation (MONIER *et al.* 2015). Homogeneous apical F-actin distribution, normal Dlg positioning and retention of the pseudostratified state of the epithelium are phenotypes also observed in $Notch^{tsa}$ mutant leg discs (Figure 16F and see Materials and Methods).

Contractile force for apical constriction results from the mobilization of actin filaments by the Rho1-dependent activation of the non-muscle myosin type II (MyoII) (MARTIN AND GOLDSTEIN 2014). MyoII heavy chain is encoded in *Drosophila* by the gene *zipper* (*zip*). Using GFP-tagged forms, we monitored the localization of Rho1 and Zip during the process of fold formation. Zip-GFP is located subapically at the level of cell-cell contacts, possibly adherens junctions, across the leg disc epithelium and no changes in localization are observed in fold-forming cells (Figure 18A-C). Instead, Rho1-GFP is specifically enriched in the apical domain of fold cells as folding progresses, and co-localizes with the accumulation of F-actin (Figure 18D-F). Then, we decided to analyze whether the localization of Rho1, Zip, or MyoII regulatory light chain, *spaghetti squash* (*sqh*, visualized using a GFP-based reporter, Sqh-GFP) is altered in *dysf* knockdown epithelia. To that end, we expressed UAS-*dysfRNAi* in the anterior compartment using the *cubitus interruptus* (*ci*) *-Gal4* driver to inhibit fold formation, and used the posterior compartment of the same disc as a control (Figure 19A, C and E). As a validation of this experimental procedure, *ci>dysfRNAi* adult legs fail to form tarsal joints in the anterior compartment (Figure 19G). In the control domain, both Zip-GFP and Sqh-GFP are localized sub-apically at the level of the adherens junctions. This subcellular localization is maintained in the *dysf* defective domain (compare Figure 19B-B' and D-D'). On the contrary, the apical accumulation of Rho1-GFP in the fold cells of the control compartment is lost

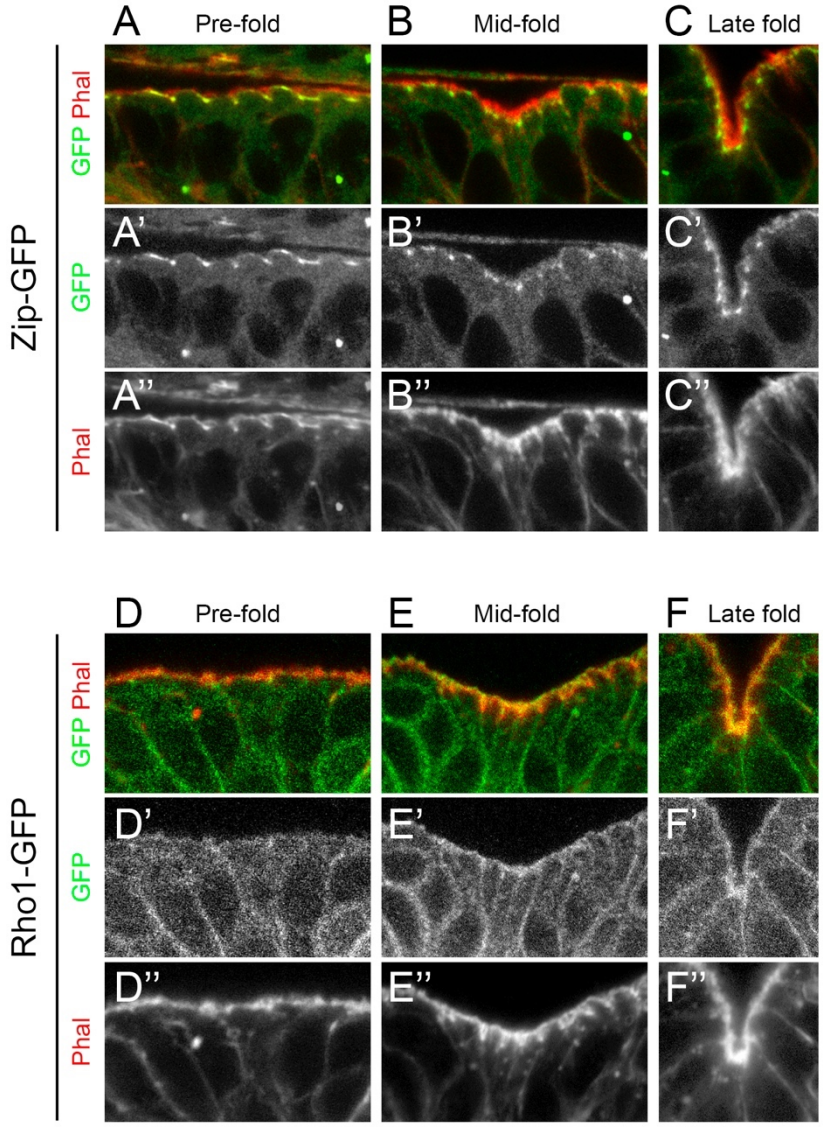

Figure 18. Time course of MyoII and Rho1 localization during tarsal fold formation. (A-C) Time course imaging of the apical region (sagittal view) of the t4-t5 tarsal fold at the Pre-fold stage **(A)**, Mid-fold stage **(B)** and Late fold stage **(C)**, of Zip-GFP expressing prepupal leg discs. Zip-GFP is in green and separate channels in **A'-C'**, and Phal is in red and separate channel in **A''-C''**. **(D-F)** Same imaging procedure for Rho1-GFP expressing prepupal leg discs. Rho1-GFP is in green and separate channels in **D'-F'**, and Phal is in red and separate channels in **D''-F''**. Note that Zip-GFP remains localized at subapical puncta as the fold formation proceeds, while Rho1-GFP is accumulated in the apical region from Mid-fold onwards, resembling the accumulation of F-actin.

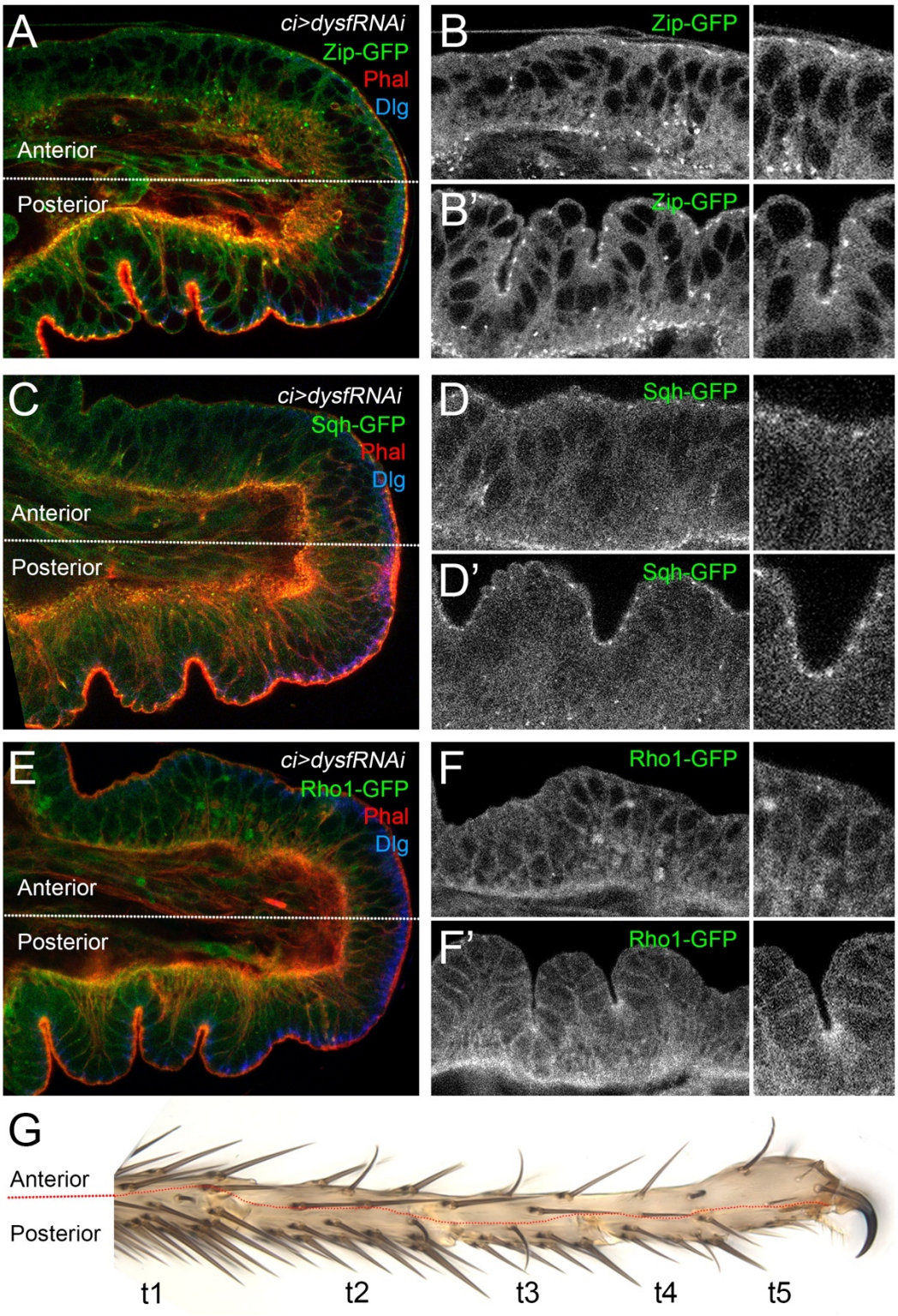

Figure 19. Rho1 localization, but not MyoII, is altered in *dysf* loss of function. (A, C and E) *ci>dysfRNAi* prepupal leg discs stained with Phal (red) and Dlg (blue) to observe F-actin cytoskeleton and subapical cell contacts, respectively. GFP fused forms of the MyoII heavy chain, Zip **(A)**, light chain, Sqh **(C)** and Rho1 **(E)** are shown in green. Anterior compartments of **A**, **C** and **E**, where *dysf* is knocked down, are magnified in **B**, **D** and **F** and posterior compartments in **B'**, **D'** and **F'**, respectively. A close zoom of a single tarsal joint is at the right of each panel. Zip-GFP and Sqh-GFP are localized at the level of adherens junctions in wild type (posterior) and UAS-*dysfRNAi* expressing (anterior) compartment. Meanwhile, Rho1 is apically accumulated in folds, along with Phal, in the posterior compartment, and this accumulation is lost upon *dysf* knockdown. **(G)** Adult *ci>dysfRNAi* leg, showing the lack of tarsal joints in the anterior compartment. Dotted red line divides the anterior and posterior compartments.

when *dysf* is downregulated (compare Figure 19F and F'). These results indicate that, while the MyoII motor protein is correctly localized, Rho1 fails to accumulate at the apices of the presumptive fold-forming cells in the absence of Dysf. Therefore, the lack of apical F-actin accumulation in *dysf* loss of function is probably due to impaired MyoII activation by Rho1, rather than caused by MyoII localization defects.

4.2 Rho1 activity in the tarsal folds depends on *dysf*

As Rho1 localization is altered in the absence of Dysf, we decided to evaluate whether changes in Rho1 activity could also be observed in *dysf* loss of function. To do so, we used a GFP-based biosensor that can be expressed *in vivo* (using the Gal4/UAS system, see Figure M-1) and that binds specifically to the active, GTP-bound form of Rho1. When this construct, here termed UAS-*Rho1RBD-GFP* (Rho1 Rho Binding Domain-GFP), is expressed, GFP accumulates preferentially in the regions where Rho1 is active (SIMOES *et al.* 2006). We used the *Dll^{212}-Gal4* driver to express UAS-*Rho1RBD-GFP* in the distal region of control, *Dll^{212}>dysfRNAi* and *Notch^{tsa}* prepupal leg discs. In control *Dll^{212}>Rho1RBD-GFP* prepupal leg discs (dissected 3 hrs APF), GFP is detected in stripes that encompasses the four tarsal folds (Figure 20A). Separating each bands we can observe regions of low GFP signal, that correspond with the interjoint regions of the tarsal segments (Figure 20E and I). Interestingly, the highest levels of GFP are found in the apical region of the cells that accumulate F-actin and constrict to form the fold, indicating a concentration of active Rho1 in that subcellular domain (Figure 20I and M). This result is consistent with the accumulation of Rho1 protein previously described in fold forming cells (Figure 18D-F). Accordingly, Rho1RBD-GFP is progressively accumulated at the apices of fold-forming cells as the fold progresses (Figure 21). We also find high levels of GFP in small clusters that may correspond with unidentified trafficking vesicles (Figure 20I).

Fold formation is impaired when Dysf is knocked down in *Dll^{212}>Rho1RBD-GFP; dysfRNAi* prepupal leg discs (3 hrs APF). In this case we observe that, in contrast to wild type discs, the levels of GFP are homogeneously distributed throughout the distal region of the leg (Figure 20B, F and J), and apical F-actin remains evenly distributed in the epithelium (Figure 20N). In this case, no clear bands of activated Rho1 can be detected, and consequently the characteristic apical GFP accumulation observed in control discs is no longer present (Figure 20J). Meanwhile, the presence of small clusters of GFP is still observed. To better analyze Rho1RBD-GFP and apical F-actin distribution, we quantified the relative enrichment of GFP signal and F-actin staining in fold-forming cells compared to proximal interfold cells (identified by Ser staining, see Figure 22). In control legs, the fold/interfold signal ratio for GFP and F-actin is close to 1,5 and 2, respectively, indicating an enrichment of both signals in the fold with respect to the interfold domain (Figure 22A and quantified in D and E, respectively). These ratios drop to almost 1 in *Dll^{212}>dysfRNAi* legs, indicating that there is no significant enrichment of either GFP or F-actin staining in presumptive fold-forming cells (Figure 22C and quantified in D and E, respectively).

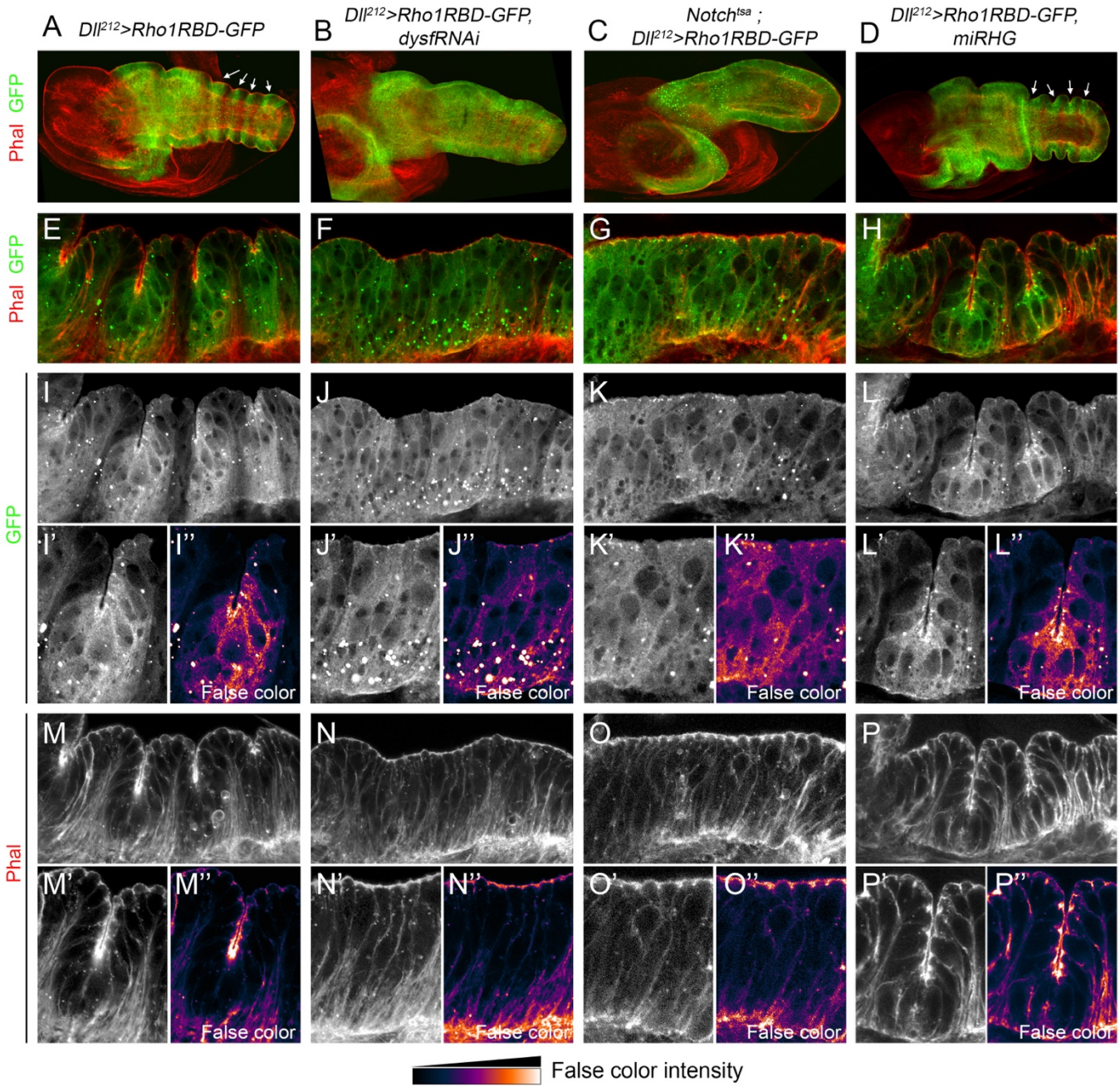

Figure 20. Rho1 activity pattern is altered in *dysf* and *Notch* loss of function. (A-D) Prepupal leg discs of the following genotypes: *Dll*^{212}>UAS-*Rho1RBD-GFP* **(A)**, *Dll*^{212}>UAS-*Rho1RBD-GFP*, UAS-*dysfRNAi* **(B)**, *Ntsa*; *Dll*^{212}>UAS-*Rho1RBD-GFP* **(C)** and *Dll*^{212}>UAS-*Rho1RBD-GFP*, UAS-*miRHG* **(D)**. Note the striped pattern of Rho1 activity in **A** and **D** (arrows) that is lost in **B** and **C**. Phal is in red and Rho1RBD-GFP expression in green. **(E-H)** Close up views of the tarsal leg epithelium (sagittal view) of the above genotypes. Regions of enhanced GFP levels are seen around the folds in **E** and **H** that are separated by regions of lower GFP levels in the interfold regions. This pattern is lost in **F** and **G**, where GFP levels remain homogeneous throughout the epithelium. **(I-P)** Magnification of a fold or putative fold region of the genotypes above could be seen in **I'-L'** for Rho1RBD-GFP, and in **M'-P'** for Phal. GFP and F-actin are accumulated apically in **I', L'** and **M', P'** in the cells that form the fold, while in **J', K'** and **N', O'** are evenly distributed across the cells. Rho1RBD-GFP expression is in green and in separate channels in **I-L**. Phal is in red and in separate channels in **M-P**. False color is displayed in **I''-L''** and **M''-P''** to enhance contrast.

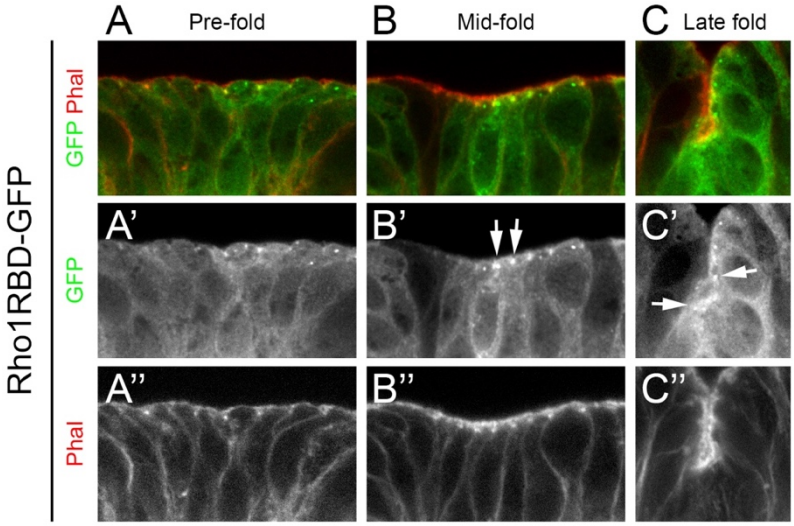

Figure 21. Time course of Rho1 activity localization during tarsal fold formation. (A-C) Time course imaging of the apical region (sagittal view) of the t4-t5 tarsal fold at the Pre-fold stage **(A)**, Mid-fold stage **(B)** and Late fold stage **(C)**, of *Dll*^{212}>UAS-*Rho1RBD-GFP* prepupal leg discs. Rho1RBD-GFP expression is in green in A-C and separate channels in **A'-C'**, and Phal is in red and separate channels in **A''-C''**. Active Rho1 is progressively accumulated, along with F-actin, in the apical region of the fold-forming cells, forming clusters at the level of adherens junctions (arrows in **B'** and **C'**).

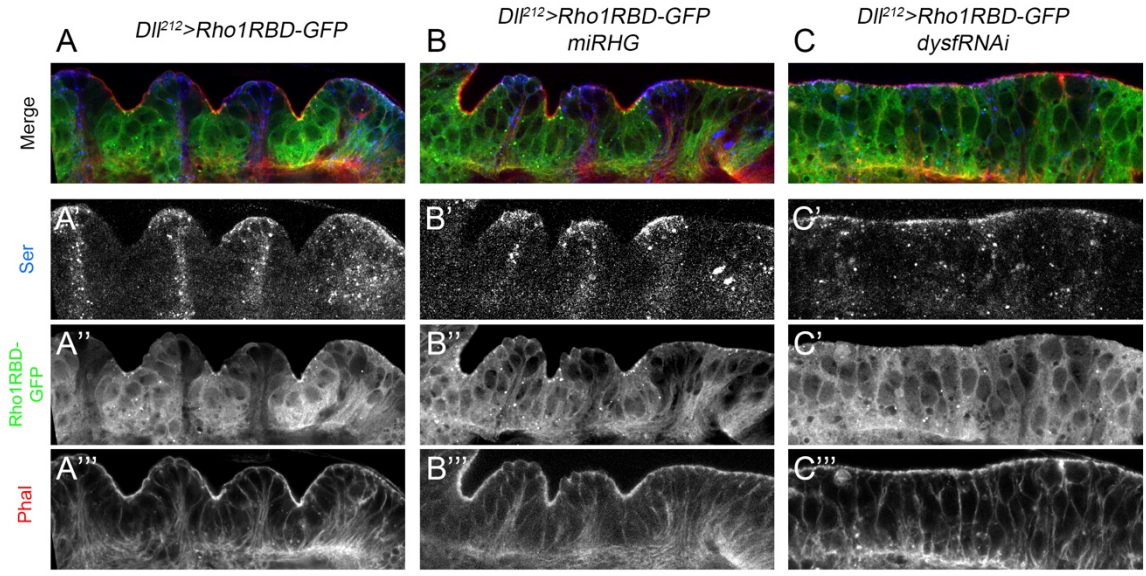

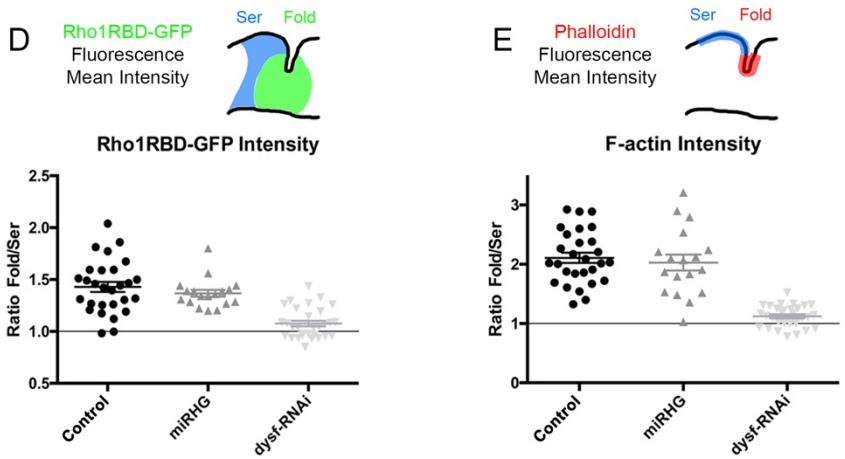

Figure 22. Quantitative analysis of Rho1 activity and F-actin distribution in the tarsal folds. (A-C) Prepupal leg discs of the following genotypes: *Dll*^{212}>*Rho1RBD-GFP* **(A)**, *Dll*^{212}>*Rho1RBD-GFP, dysfRNAi* **(B)** and *Dll*^{212}>*Rho1RBD-GFP, miRHG* **(C)** stained with Ser antibody to delimitate interfold regions (blue and separate channel in **A'-C'**). Rho1RBD-GFP is in green and separate channel in **A''-C''** and Phal is used to visualize F-actin (red and separate channel in **A'''-C'''**). **(D)** Ratio of fluorescence levels of Rho1RBD-GFP (mean intensity) within 'Fold' domain and 'Ser' domain for the previous genotypes. **(E)** Ratio of fluorescence levels of apical Phal (mean intensity) within 'Fold' domain and 'Ser' domain for the previous genotypes. In both cases, a ratio of 1 would imply the same levels in Fold and Ser domains, while any increment over 1 means higher levels in the Fold vs. Ser domain. In **D** and **E**, the Fold/Ser ratio is close to 1 when *dysf* is knocked down, while is significantly higher in wild type and upon UAS-*miRHG* expression. Only t2-t3 and t3-t4 folds were used for quantification (wild type n=28 joints; miRHG n=30 joints and dysf-RNAi n=18 joints for both measurements). ****p<0.0001, with *Student's t* test, indicates a significant difference from control. ns, non-significant. Error bars represent SEM.

Similar phenotypes were found in *Notch^{tsa}; Dll^{212}>Rho1RBD-GFP* prepupal leg discs shifted to 29°C 72 hrs prior to dissection. No bands of increased Rho1 activity were found (Figure 20K), and apical actin was also evenly distributed throughout the epithelium (Figure 20O). These results indicate that there is a correlation between activated Rho1, apical F-actin accumulation and fold formation in wild type prepupal leg discs. Accordingly, when Dysf is knocked down or Notch activity is downregulated, patterned Rho1 activity, apical F-actin accumulation and fold formation are lost. Therefore, we propose a model where Dysf regulates Rho1 activation at the developing tarsal folds, and Rho1 in turn activate the cytoskeleton dynamics (*i.e.* regulating MyoII activity) that lead to apical constriction and fold formation.

It has been proposed that apoptosis regulates fold formation through the activation of MyoII (MONIER *et al.* 2015). So far in this work, we have demonstrated that *dysf* regulates *hid* and *rpr* expression and the preferential localization of apoptotic cells at the joint domain. In addition, we have shown that *dysf* is required for patterned Rho1 activity at the developing tarsal folds. Therefore, we reasoned that *dysf*-dependent cell death could regulate Rho1 activity to promote MyoII activity and apical constriction. We used a miRNA-based construct that simultaneously inhibits the pro-apoptotic genes *rpr*, *hid* and *grim* (UAS-*miRHG*) to efficiently block cell death (SIEGRIST *et al.* 2010) and see Figure 23). We co-expressed UAS-*miRHG* and UAS-*Rho1RBD-GFP* under the control of *Dll^{212}-Gal4* to test the role of apoptosis in Rho1 activity and fold formation. Surprisingly, when cell death is inhibited the pattern of Rho1 activity, the accumulation of apical F-actin and the formation of folds are indistinguishable from the control (Figure 20D, H, L and P). Quantification of Rho1RBD-GFP and apical F-actin distribution in apoptosis-defective prepupal leg discs yielded identical results to those measured for the control (Figure 22B, D and E). Importantly, the adult tarsal joints are also correctly formed in *Dll^{212}>miRHG* legs (Figure 26C).

4.3 Cell death is not required to form tarsal folds and joints

Our results indicate that cell death inhibition does not affect the formation of tarsal folds or adult joints, and differs from previous findings where a fundamental role for cell death directing joint development has been proposed (MANJON *et al.* 2007; MONIER *et al.* 2015). In this section, we will try to solve these discrepancies using a wide range of genetic tools to inhibit apoptosis at different levels of the apoptotic pathway and observe its effects in prepupal fold and adult joint formation (Figure I-8).

We started blocking the apoptotic pathway at the level of the pro-apoptotic genes, *rpr*, *hid* and *grim*, using two different approaches. First, we inhibited cell death expressing UAS-*miRHG* under the control of the *hh-Gal4* driver in third instar larva leg discs. In *hh>miRHG* leg discs, Dcp1 positive cells are almost absent in the posterior compartment as compared with the anterior compartment or with the posterior compartment of control *hh>GFP* leg discs (Figure 23A, B and quantified in F). Moreover, prepupal leg discs of the same genotype

display the equal reduction of cell death while fold formation is still observed in the posterior compartment (Figure 23C). To ensure that cell death was actually being inhibited, we stained for TUNEL, an unambiguous marker of apoptosis, and observed almost identical results, as cell death is nearly completely abolished from the posterior compartment in larval and prepupal *hh>miRHG* leg discs (Figure 23D, E and quantified in G). Adult *hh>miRHG* legs have normal tarsal joints, and their only visible phenotype is a slight thickening of the tarsal segments (Figure 23H).

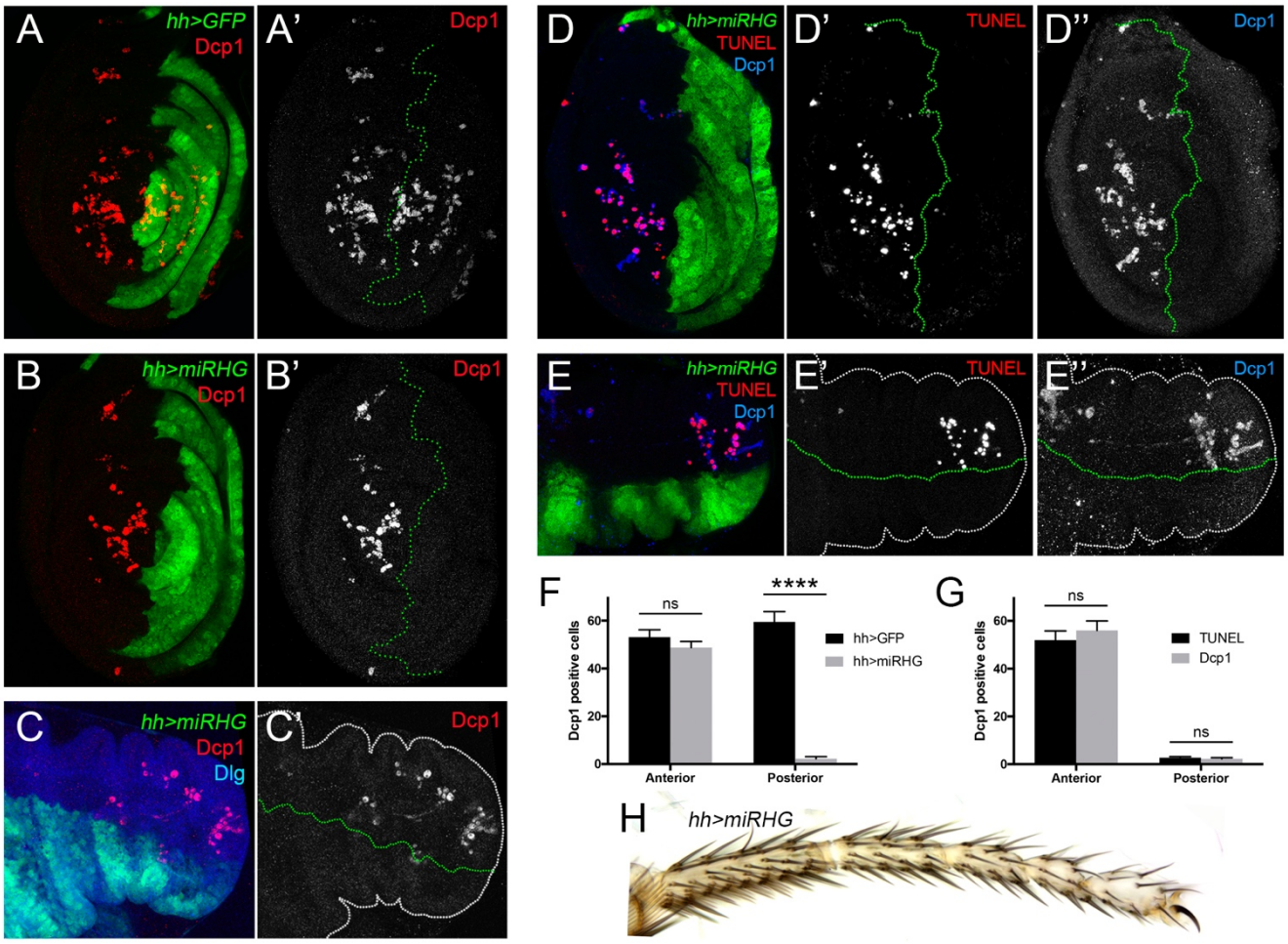

Figure 23. miRHG expression inhibits cell death but does not affect tarsal fold and joint formation. (A and B) Third instar larva leg disc of *hh*>UAS-*GFP* **(A)** and *hh*>UAS-*miRHG* **(B)**. *hh* domain is marked by GFP expression (green and dotted line in **A'** and **B'**) and cell death is assessed by Dcp1 staining (red and separate channels in **A'** and **B'**). Cell death is almost completely absent from the posterior compartment when UAS-*miRHG* is expressed. **(D)** Third instar larva *hh*>UAS-*miRHG* leg disc. TUNEL (red and separate channel in **D'**) is used to address DNA damage associated with apoptosis, and is compared with Dcp1 staining (blue and separate channel in **D''**). Dcp1 and TUNEL stainings are coincident, and both are lost in the *hh* domain (green and dotted line in **D'** and **D''**). **(C and E)** Prepupal leg disc of the same genotypes shown in **B** and **D**. Dlg is in blue in **C**. White dotted lines are drawn in **C'**, **E'** and **E''** to visualize epithelial shape. Note that tarsal folds are still present despite cell death inhibition. **(F)** Quantification of Dcp1 positive cells in the A and P compartments of control (*hh>GFP*, n=9) and *hh*>UAS-*miRHG* (n=12) third instar leg discs. **(G)** Quantification of TUNEL and Dcp1 positive cells in the A and P compartments of *hh*>UAS-*miRHG* third instar leg discs (n=13). ****p<0.0001, with *Student's t* test, indicating a significant difference from control P compartment. ns, non-significant. Error bars represent SEM. **(H)** Tarsal region of an *hh*>UAS-*miRHG* adult leg. Note that tarsal joint formation is maintained, despite a slight thickening of the tarsi respect to wild type (see Figure 3).

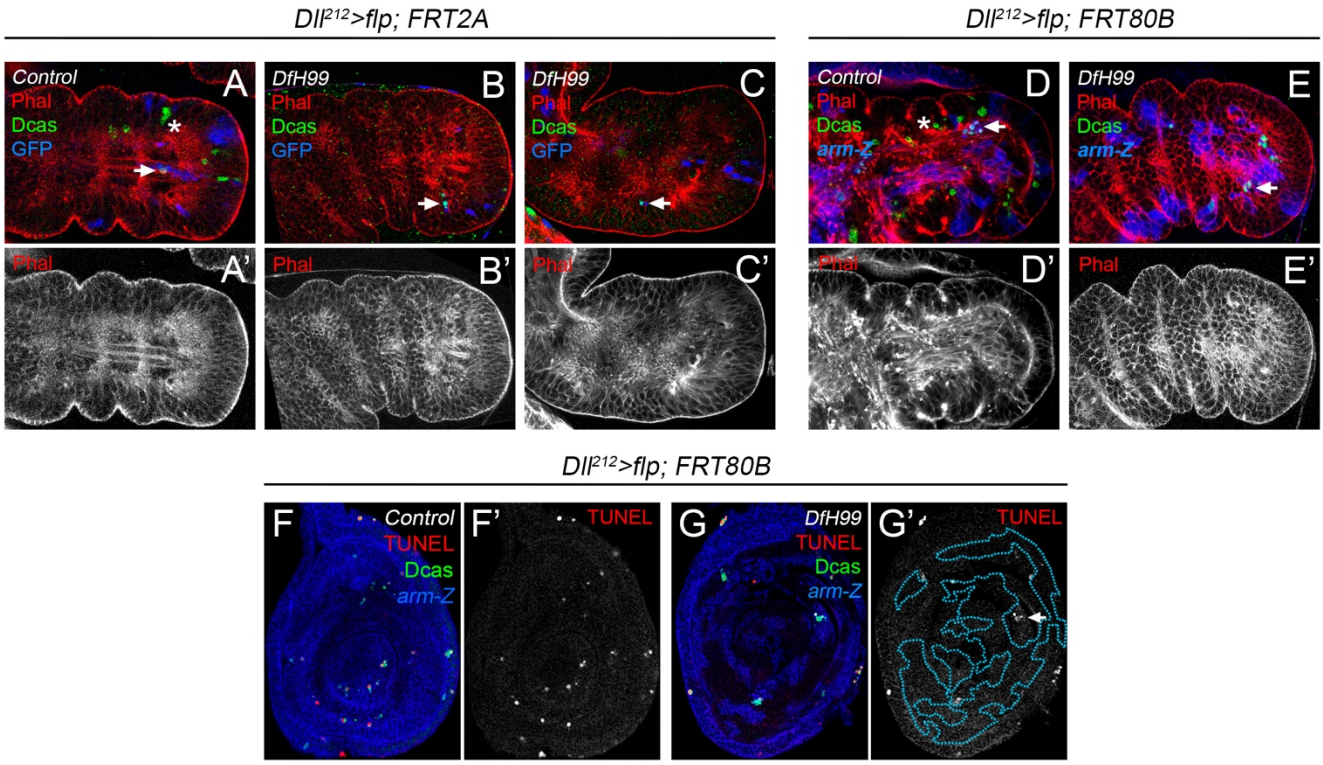

Figure 24. *DfH99* inhibits cell death but does not affect tarsal fold formation. (A-E) Control and *DfH99* clones (marked by the absence of GFP expression, blue) were generated in the distal region of prepupal leg discs by *Dll*^{212}>UAS-*flp* expression, using either the *FRT2A* **(A-C)** or the *FRT80B* **(D and E)** chromosomes. The *Minute* technique was used to maximize the size of mutant clones (see Materials and Methods). The genotypes are as follow: *Dll*^{212}>UAS-*flp, Control, FRT2A* **(A)**; *Dll*^{212}>UAS-*flp, DfH99, FRT2A* **(B and C)**; *Dll*^{212}>UAS-*flp, Control, FRT80B* **(D)** and *Dll*^{212}>UAS-*flp, DfH99, FRT80B* **(E)**. Phal staining (red and separate channels in **A'-E'**) is used to visualize leg disc shape, and cell death is visualize by Dcp1 staining (green). In control discs **(A and D)** cell death is observed both within (arrows) and outside (asterisks) of GFP expressing cells. In *DfH99* discs **(B, C and E)**, cell death is always observed within wild type cells (arrows), demonstrating efficient cell death inhibition in *DfH99* cells. Fold defects are observed in a fraction of *DfH99, FRT2A* leg discs (compare **B** and **C**), but never in *DfH99, FRT80B* **(E)**. **(F and G)** TUNEL (red and separate channels in **F'** and **G'**) and Dcp1 (green in **F** and **G**) staining of *Dll*^{212}>UAS-*flp, Control, FRT80B* **(F)** and *Dll*^{212}>UAS-*flp, DfH99, FRT80B* **(G)** third instar larva leg discs. Mutant cells are marked by lack of GFP expression (blue and dotted lines in **F'** and **G'**). In **G** cell death is only observed within wild type (blue) cells and never in the *DfH99* territory.

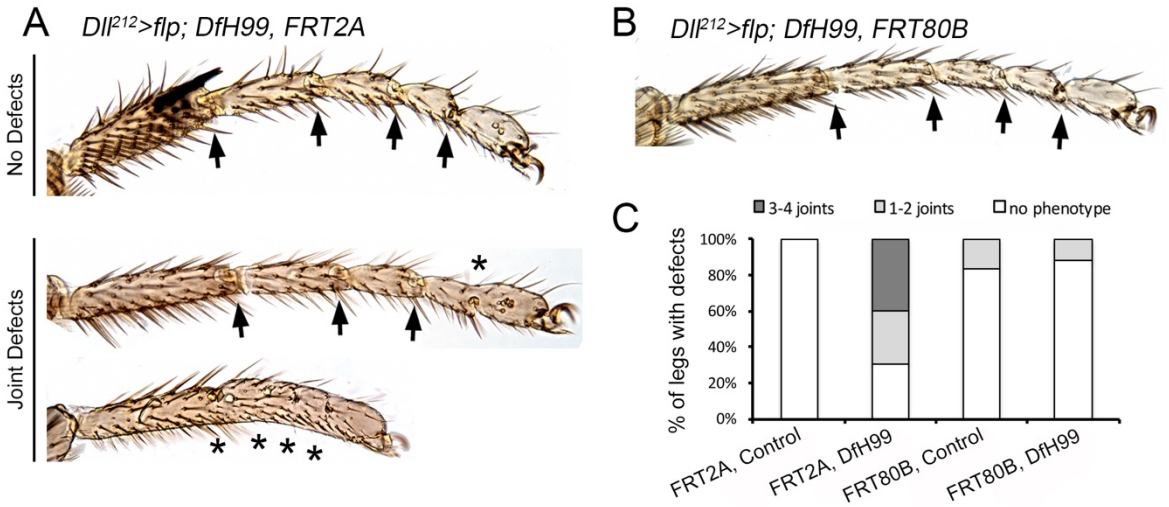

Figure 25. Adult tarsal joint defects are related with *FRT2A* chromosome. (A and B) Adult legs of *Dll*^{212}>UAS-*flp, DfH99, FRT2A* **(A)**, showing different grades of joint defects, and *Dll*^{212}>UAS-*flp, DfH99, FRT80B* **(B)**, in which no joint defects are observed. Arrows indicate normal joint formation, and asterisks point to loss of joints. **(C)** Quantification of the leg joint phenotypes of the genotypes in **A** (n=73) and **B** (n=59), and using the empty *FRT2A* (n=70) and *FRT80B* (n=90) as controls. Individual legs were grouped according to severity of joint defects: *no phenotype*, *1-2 joints* and *3-4 joints*. *DfH99* legs generated using the *FRT2A* chromosome presented much increased joint defects than controls or *DfH99, FRT80B* legs.

Second, we took advantage of a deletion (*DfH99*) that removes *rpr*, *hid* and *grim* to eliminate apoptosis from imaginal leg discs (WHITE *et al.* 1994). We generated *DfH99* clones in the distal region of the leg using the *Dll^{212}-Gal4* driver. To maximize the size of the mutant tissue we used the *Minute* technique (MORATA AND RIPOLL 1975) and see Materials and Methods), which allowed us to generate legs almost entirely mutant for *rpr*, *hid* and *grim*. In this technique, the mutant tissue is identified by the absence of markers in the leg discs (GFP or LacZ) or in the adult legs (*yellow^{+}*). We used two available *DfH99* mutant chromosomes associated with two different frequent recombination targets (*FRT2A* and *FRT80B*). Control and *DfH99* clones using either FRT were generated that span much of the leg. In *DfH99* mutant tissue, cell death is completely absent compared to control clones carrying a control FRT chromosome (Figure 24A-C and D-E). Unexpectedly, severe discrepancies arise when using *FRT2A* or *FRT80B, DfH99* chromosomes. Only when using the *FRT2A* we observe, in some cases, clear defects in tarsal fold formation (compare Figure 24B and C). These defects were also observed in adult legs, and range from severe (three or four tarsal joints affected per leg in ∼40% of the legs), to milder defects (affecting one or two joints in ∼30%) and to normal formation of all tarsal joints (∼30% of adult legs) (Figure 25A and quantified in C). In contrast, *Dll^{212}>flp; FRT80B, DfH99* prepupal leg discs present normal fold formation (Figure 24B). Most of the adult legs do not have any joint defect (88% of the legs), while only 12% presented mild defects affecting just one tarsal joint (Figure 25C). To make sure that cell death was effectively eliminated in *Dll^{212}>flp; DfH99, FRT80B* leg discs, we conducted TUNEL staining and observed that cell death was only present in the control tissue, and never within *DfH99* mutant clones (Figure 24F-G).

Pro-apoptotic genes function through the degradation of Diap1 (Drosophila Inhibitor of Apoptosis 1) protein. Therefore, we overexpressed *Diap1* in the *hh* domain of third instar larva leg discs to attempt to inhibit cell death. Based on previous experiments, we decided to express two copies of UAS-*Diap1* to cause a stronger reduction of apoptosis. We observed a significant decrease in Dcp1 positive cells in the posterior compartment of *hh*>UAS-*Diap1; Diap1* leg discs, as compared with the P compartment of control *hh*>UAS-*GFP* discs (Figure26A and B, and quantified in D). Nevertheless, this reduction of apoptosis does not cause any defects in fold formation in prepupal leg discs or in adult tarsal joint development (Figure 26C and E, respectively).

Next, we analyzed fold and joint formation using a mutant allele of the initiator caspase Dronc, *dronc^{i24}*, which produce truncated forms of the protein and is unable to trigger normal levels of apoptosis (XU *et al.* 2005). Homozygous *dronc^{i24}* mutants present a strong reduction of cell death levels, detected both with Dcp1 and TUNEL staining, compared with their corresponding heterozygous *dronc^{i24}/+* mutants (Figure 27A and B and quantified in F). In these mutants, the formation of tarsal folds is indistinguishable from their corresponding control prepupal legs (Figure 27C and D). Accordingly, adult *dronc^{i24}* homozygous mutant legs display correct joint formation, despite certain thickening of the tarsal segments could be observed (Figure 27E).

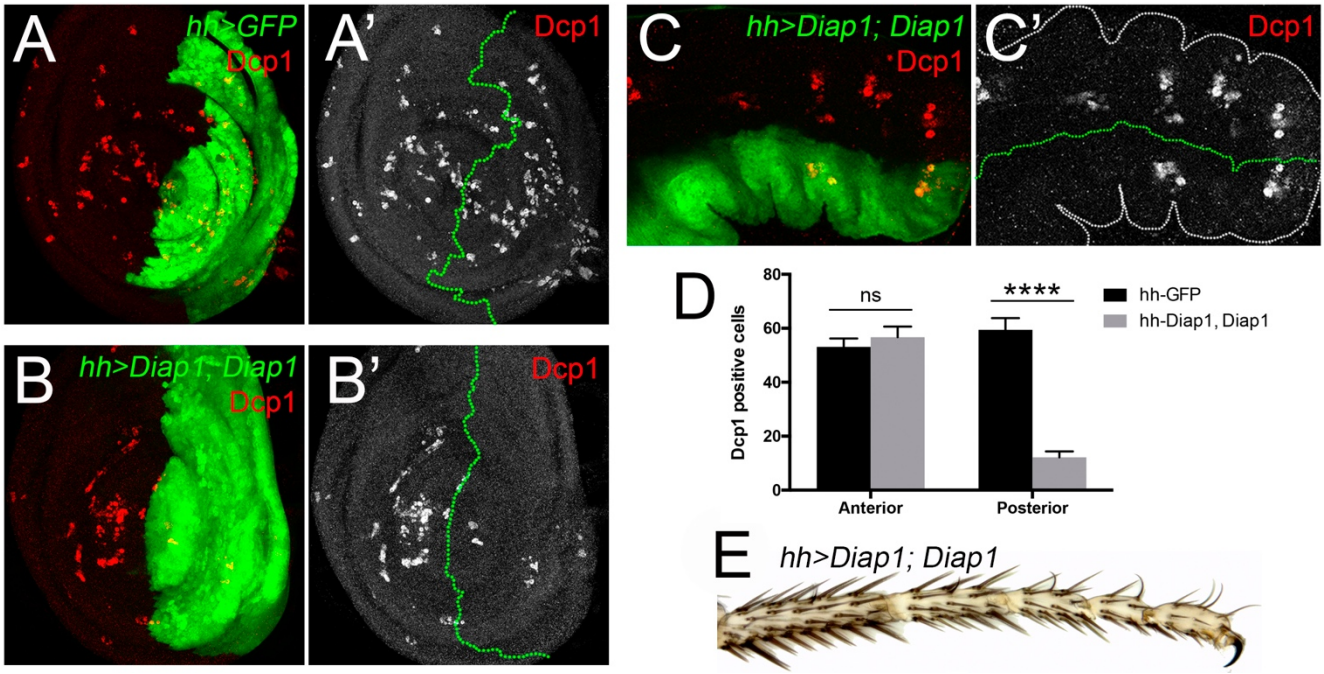

Figure 26. Overexpression of Diap1 inhibits apoptosis and does not affect joint development. (A and B) Third instar leg discs of control *hh*>UAS-*GFP* **(A)** and *hh*>UAS-*Diap1;* UAS-*Diap1* **(B)**. Two copies of Diap1 are expressed to enhance cell death inhibition. **(C)** prepupal leg disc of the same genotype presented in **(B)**. The outline of the disc is indicated by a dotted white line. Leg discs are stained for Dcp1 to visualize apoptosis (red and separate channel in **A'-C'**). In all the confocal images, a Z-stack of all planes of the Dcp1 channel is presented to show the total cell death present in each disc. GFP is used to delimitate the Posterior compartment (in green in **A-C**, and delimitated by a dotted green line in **A'-C'**). Note that cell death levels are severely reduced by Diap1 overexpression, while fold formation is maintained. **(D)** Quantification of Dcp1 positive cells in the A and P compartments of control *hh*>UAS-*GFP* (n=9) and *hh*>UAS-*Diap1;* UAS-*Diap1* (n=12) third instar leg discs. ****p<0.0001, with *Student's t* test, indicating a significant difference from control P compartment. ns, non-significant. Error bars represent SEM. **(E)** Tarsal region of an *hh*>UAS-*Diap1;* UAS-*Diap1* adult leg, showing no defects in joint formation.

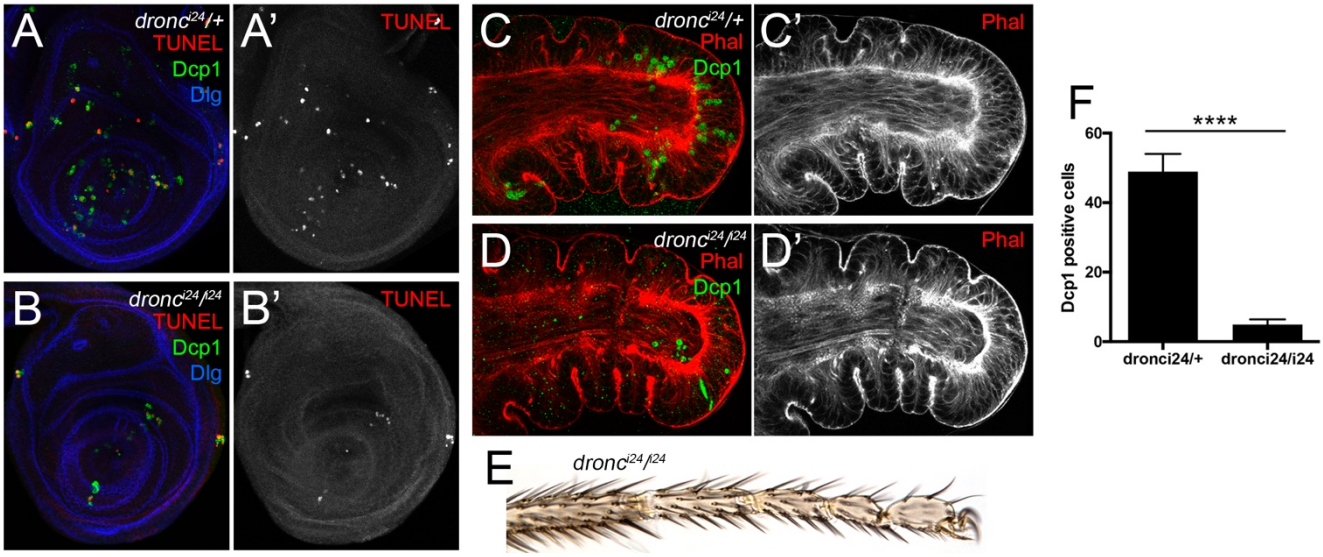

Figure 27. *dronc*^{i24} mutants present reduced cell death but no tarsal fold or joint defects. (A and B) Third instar leg discs of control *dronc*$^{i24/+}$ **(A)** and *dronc*$^{i24/i24}$ **(B)** mutant flies, stained for Dcp1 (green) and TUNEL (red and separate channels in **A'** and **B'**). Dlg is in blue in **A** and **B**. *dronc*^{i24} mutants present highly reduced cell death levels, as could be observed both with TUNEL and Dcp1. **(C and D)** Distal region of prepupal leg discs of the same genotypes shown in **A** and **B**, respectively, stained for Dcp1 (green) and Phal (red and separate channels in **C'** and **D'**) to assess fold formation. In *dronc*^{i24} mutants cell death is nearly absent while fold formation still occurs. In all the confocal images, a Z-stack of all planes of the Dcp1 and TUNEL channels is presented to show the total cell death present in each disc. **(E)** Tarsal region of an adult *dronc*^{i24} homozygous mutant, that display normal joint formation and a slight thickening of the tarsi (compare with Figure 3). **(F)** Quantification of Dcp1 positive cells in third instar leg imaginal discs of the *dronc*^{i24} mutants and their correspondent controls (*dronc*$^{i24/+}$ n=10; *dronc*$^{i24/i24}$ n=11). The levels of cell death are significantly reduced in *dronc*^{i24} homozygous mutants as compared with the heterozygous controls. ****p<0.0001, with *Student's t* test, indicating a significant difference from control discs.

Another approach to inhibit cell death consists on the ectopic expression of the baculovirus protein p35, which blocks the function of executioner caspases (*i.e.* Dcp1 and Ice), preventing the last stages of the apoptotic process (HAY *et al.* 1994; FUCHS AND STELLER 2015). We expressed an UAS-*p35* construction in the *Dll* domain of prepupal leg discs and observed no defects in fold formation (Figure 28A). Interestingly, Dcp1 staining is observed within the epithelium, which is expected as p35 blocks the function of Dcp1, but does not inhibit its cleavage. Nevertheless, no apoptotic features were observed in Dcp1 positive cells, supporting the efficiency of p35 inhibiting apoptosis. Control *Dll^{212}-Gal4* adult legs already present a minimal joint phenotype consistent on the incomplete formation of one tarsal joint in ~5% of the legs. This phenotype is slightly enhanced in *Dll^{212}*>UAS-*p35* adult legs, that display incomplete formation of 1 or 2 tarsal joints in ~25% of the legs (Figure 28B, and quantified in C). Nevertheless, is possible that these phenotypes are caused by epithelial defects caused by the presence of undead cells at the presumptive joints.

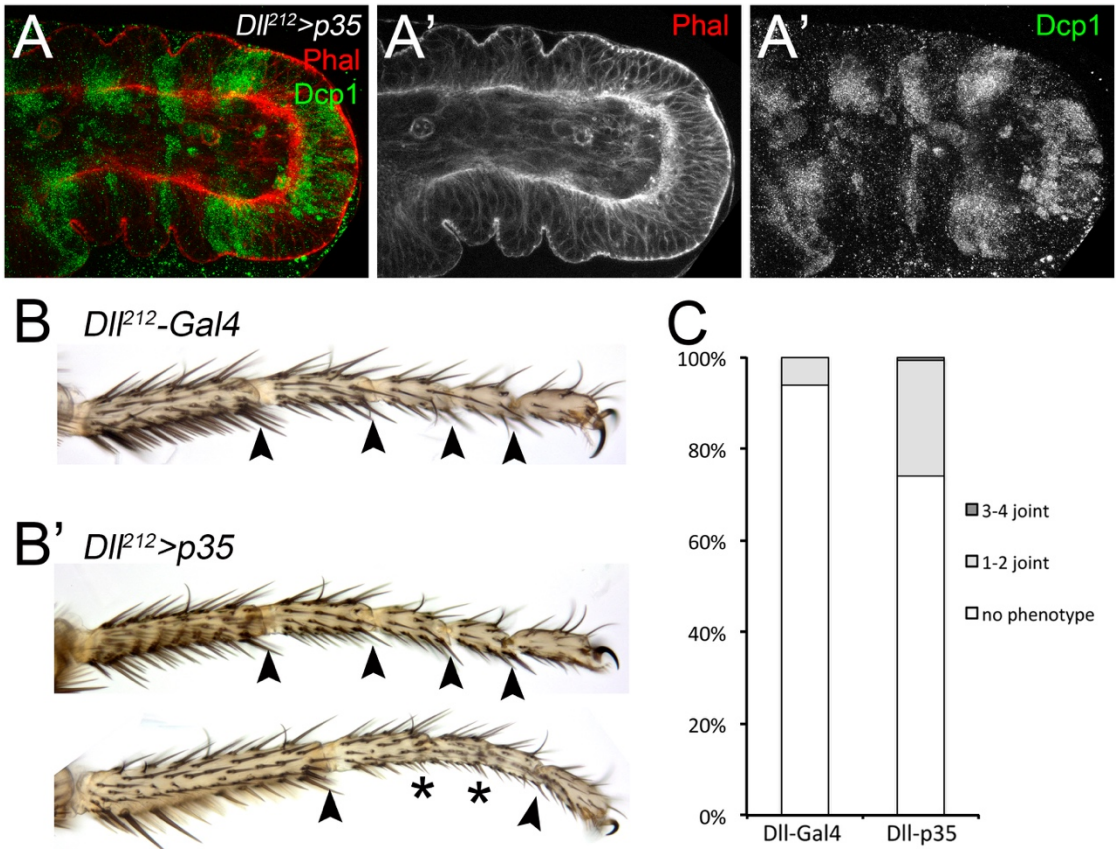

Figure 28. Inhibition of Diap1 activity cause minimal joint defects. (A) Tarsal domain of prepupal legs of Dll^{212}>UAS-*p35*, stained for Phal (red and separate channel in **A'**) and Dcp1 (green and separate channel in **A''**) Note that Dcp1 staining is present in the epithelium, but the cells do not show the rounded and fragmented morphology typical of apoptosis, while folds are still correctly formed. **(B)** Adult legs (tarsal domain) of control Dll212-Gal4 **(B)** and Dll212>UAS-p35 **(B')** flies. Arrowheads mark correct joint formation and asterisk indicate incomplete joint formation. **(C)** Quantification of joint defects of the genotypes in **(B)** (Dll-Gal4, n=99; Dll-p35, n=127). Note that control legs already present subtle defects in the formation of one tarsal joint in ~5% of the legs. This phenotype is slightly enhanced by the expression of UAS-*p35*, which causes defects in the formation of 1 or 2 joints in ~25% of the legs.

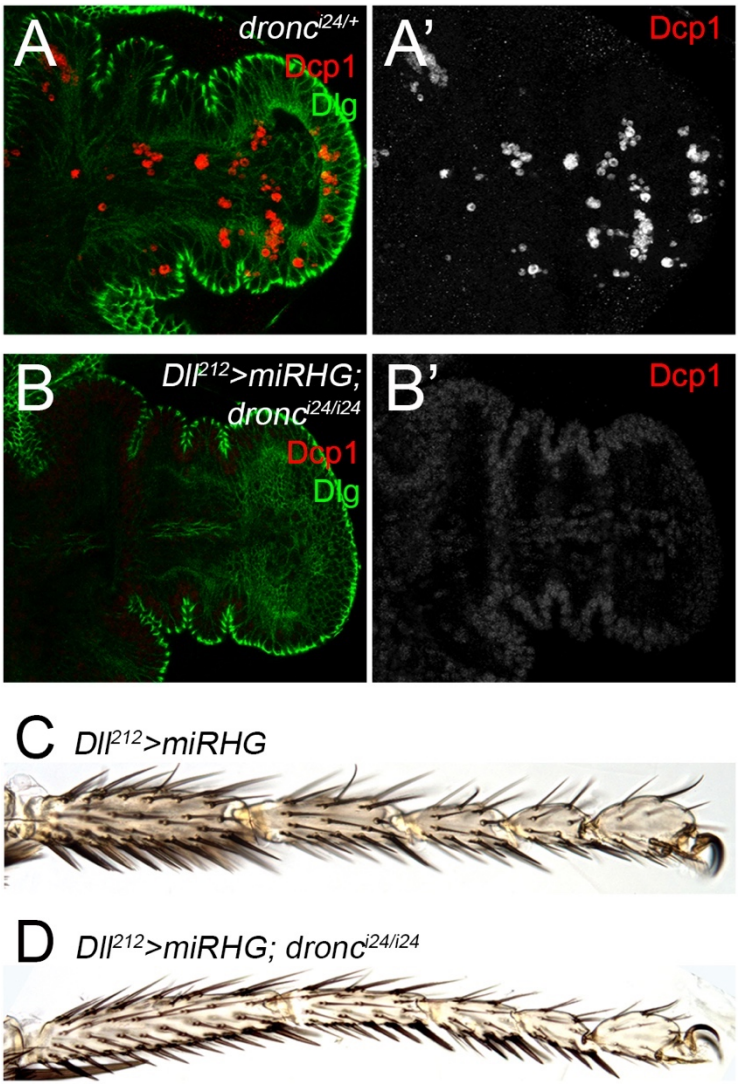

Figure 29. Complete inhibition of apoptosis does not affect fold and joint formation. (A and B) Distal region of a *dronc*$^{i24/+}$ heterozygous **(A)** and a *Dll*^{212}>UAS-*miRHG; dronc*$^{i24/i24}$ mutant **(B)** prepupal leg discs. Dlg is in green and a Z-stack of Dcp1 staining is shown in red and separate channels in A' and B'. No apoptosis could be observed in B, while fold formation occurs normally. **(C and D)** Tarsal region of *Dll*^{212}>UAS-*miRHG* **(C)** and *Dll*^{212}>UAS-*miRHG*; *dronc*$^{i24/i24}$ mutant **(D)** adult legs. The only observable

Finally, we expressed the UAS-*miRHG* in the distal domain of *dronc*^{i24} homozygous mutant legs. This caused the complete elimination of Dcp1 signal from leg discs, while the formation of tarsal folds was unaffected (Figure 29B). Also, normal joint formation was observed in *Dll*^{212}*>miRHG; dronc*^{i24}*/dronc*^{i24} adult legs (Figure 29D).

This exhaustive analysis of the cell death requirements during leg development precludes the role of apoptosis as the main driver for tarsal joint morphogenesis. Unfortunately, the strong joint phenotypes observed in *Dll*^{212}*>flp; DfH99, FRT2A* seem to be caused by an undetermined mutation associated to the *FRT2A* chromosome. The same experiment performed with FRT80B yields legs with normal joint formation and inhibition of apoptosis, a result that is in accordance with the rest of conditions of cell death downregulation.

4.4 Rho1 activity is required for epithelial folding and tarsal joint formation

Up until now, we have shown that Rho1 is accumulated and activated around developing folds in the prepupal leg disc epithelium. Nevertheless, the requirement of Rho1 in the process of fold and tarsal joint formation has not been directly assessed. To this end we blocked Rho1 activity by expressing a dominant negative form, UAS-*Rho1*^{N19} (STRUTT *et al.* 1997), in the *ap* domain that encompasses the t4-t5 joint. To properly compare phenotypes, we dissected prepupal leg discs dated 3 hrs APF. In control *ap>GFP* flies, the t4-t5 fold is already formed at this time point. F-actin is accumulated apically in the fold forming cells, and Dcp1 positive cells are observed near the fold (Figure 30A). As continuous *Rho1*^{N19} expression resulted lethal, we restricted its activity for 24 hrs prior to dissection using the *tubGal80*^{ts} technique, and observed that fold formation was inhibited within the *ap* domain. Nevertheless, the epithelium was severely disorganized with a number of GFP

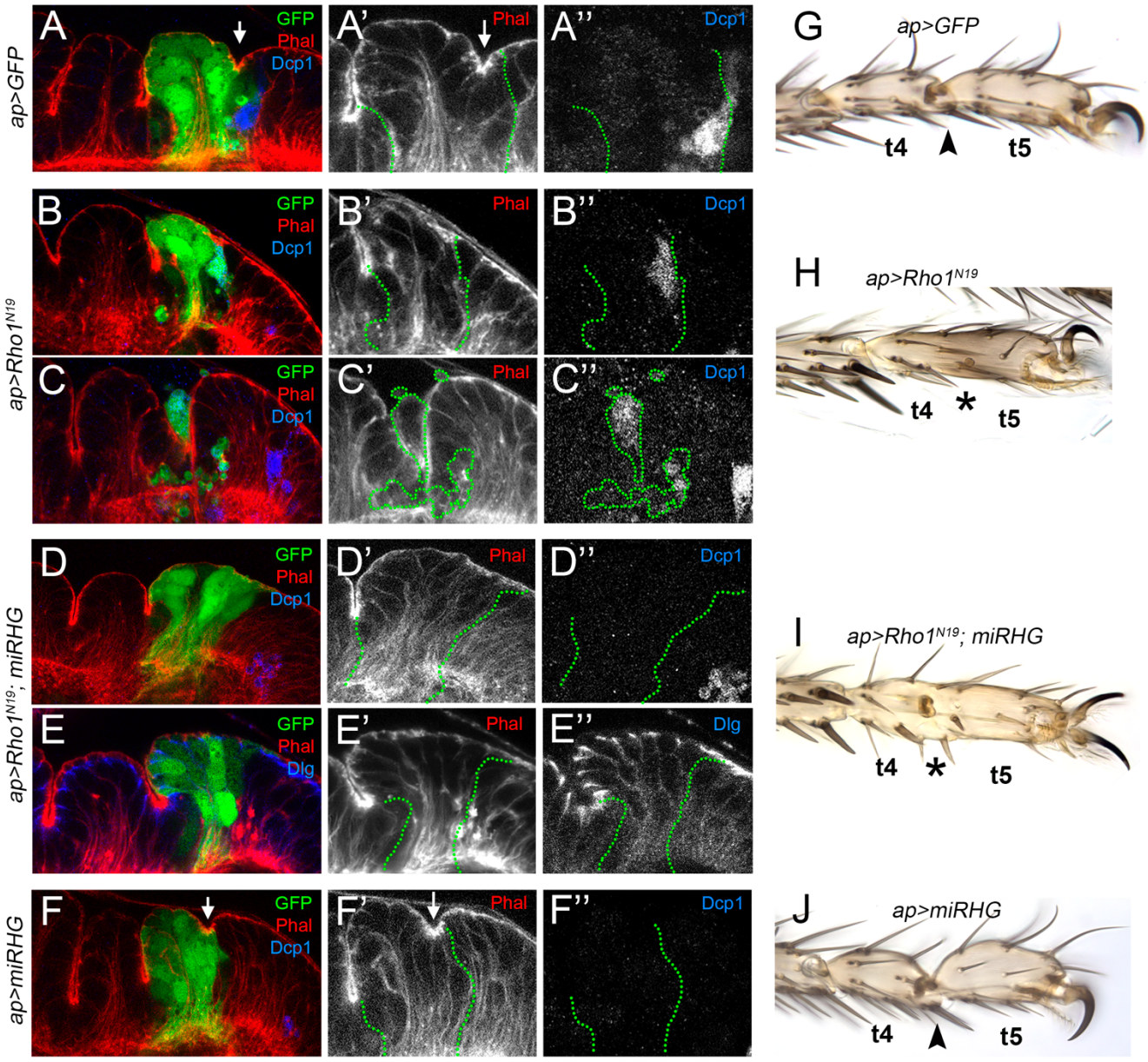

Figure 30. Rho1 activity is necessary for fold and joint formation. (A-F) Distal region of prepupal leg discs dissected 3 hrs APF. The *ap* domain, that encompasses the fold between the fourth and fifth tarsal segments, is marked by GFP expression (green and dotted lines in **A'-F'** and **A''-F''**). Right panels show a detail of the t4-t5 fold (arrows indicate normal fold formation). In **A-F** Phal is in red and separate channel in **A'-F'** and Dcp1 is in blue in **A-F** and separate channel in **A''-F''**. Dlg is in blue in **E** and separate channel in **E''**. The activity of the *ap-Gal4* driver was restricted to 24 hrs before dissection using the *tubulin-Gal80^{ts}* system, except in **A** and **F** where it was continuously active (see Material and Methods). **(A)** *ap*>UAS-*GFP* control. **(B-C)** *ap*>UAS-*Rho1^{N19}*; **B** and **C** correspond to opposite sides of the same leg disc. The t4-t5 fold is lost in **B**, while the epithelial integrity is severely altered in **C**. **(D-E)** *ap*>UAS-*Rho1^{N19}*, UAS-*miRHG*; the t4-t5 fold is lost while the epithelial integrity is not compromised, as visualized by Dlg staining. **(F)** *ap*>UAS-*miRHG*; the t4-t5 fold is formed as in the control. **(G-J)** Adult legs of *ap*>UAS-*GFP* **(G)**, *ap*>UAS-*Rho1^{N19}* **(H)**, *ap*>UAS-*Rho1^{N19}*, UAS-*miRHG* **(I)** and *ap*>UAS-*miRHG* **(J)**. The activity of the *ap-Gal4* driver was restricted to 48 hrs (encompassing late larva and early pupal development) with the *tubulin-Gal80^{ts}* technique, except in **G** and **J** that was continuously active (see Material and Methods). In **H** and **I** the t4-t5 joint is lost, despite some indentations in the cuticle could still be observed. Note that in *ap*>UAS-*miRHG* legs **(J)** the fourth and fifth tarsi are slightly thickened compared to the control **(G)**. Arrows indicate formation of the t4-t5 joint, while asterisks indicate its loss.

positive cells being extruded or exhibiting aberrant morphologies (Figure 30B and C). Moreover, according to our observations and to the literature, *Rho1^{N19}* expression leads to increased cell death (Neisch et al., 2010). Therefore, we decided to inhibit apoptosis in our experimental setting to try to avoid these side effects on epithelial integrity. In *ap>miRHG; Rho1^{N19}* prepupal leg discs (expressed for 24 hrs and dissected 3 hrs APF) the

formation of the t4-t5 fold is completely abolished, and no accumulation of apical F-actin was detected. Meanwhile, epithelial integrity (as assessed by correct Dlg localization) does not seem to be affected (Figure 30D and E). As a control, expression of UAS-*miRHG* in the *ap* domain for the whole development eliminated apoptosis but do not cause any effect in F-actin accumulation nor fold formation (Figure 30F).

After assessing the requirement of Rho1 during epithelial fold formation, we asked whether Rho1 activity is also required for adult joint formation. To answer this, we knocked down Rho1 function for 48 hrs, through late third instar to early pupation, expressing *ap>Rho1^{N19}* and then letting the flies recover until pharate (see Material and Methods). We observed a range of phenotypes, from complete loss of the t4-t5 joint to cuticular indentations that may correspond with incomplete joint formation (Figure 30H). As *Rho1^{N19}* expression may likely affect tissue integrity in this experimental setting, we decided to simultaneously inhibit cell death. In these conditions, we observed similar loss of the t4-t5 joint, and in some cases the presence of cuticular indentations (Figure 30I). Importantly, the loss of the joint is not caused by the elimination of apoptosis, as in *ap>miRHG* the t4-t5 joint develops normally (Figure 30J). Taken together, our results indicate that the activity of Rho1 is required to coordinate the cell shape changes necessary to form the prepupal tarsal folds and the adult joints.

4.5 Rho1 downstream effectors are required for tarsal fold and joint formation

Rho1 exerts its cellular functions by regulating the activity of a subset of downstream targets, including the kinases Rok and Drak, which have overlapping functions in Sqh phosphorylation, acto-myosin contractility and cytoskeleton remodeling (RIENTO AND RIDLEY 2003; NEUBUESER AND HIPFNER 2010). To study the specific contribution of each effector to tarsal joint development, we used mutant alleles and interference RNA to generate loss of function of Rok and Drak and evaluate their effects on adult tarsal joint formation. Legs that are completely mutant for *rok* (see Materials and Methods) are shorter and present a consistently mild defect in joint formation (~80% of the legs lacking one to two joints) (Figure 31A and I). *Drak* mutants have smaller wings and twisted legs (NEUBUESER AND HIPFNER 2010), although the four tarsal joints are correctly formed in ~95% of the legs (Fig 31B and I). Nevertheless, double mutant clones for *rok* and *Drak* were small and hardly recovered even if cell death is inhibited (Figure 32E). Therefore, we decided to use RNAi mediated depletion of Rok and Drak as a less drastic loss of function condition. We used the *Dll^{212}-Gal4* driver that display by its own a subtle leg phenotype, causing defects in the formation of one tarsal joint in less than 8% of the legs (Fig 31C and I). As a positive control, we used the *Dll^{212}>dysfRNAi* condition that abolish tarsal joint formation in more than 95% of the cases (quantified in Figure 31I). When both Drak and Rok were simultaneously knocked down, we found stronger phenotypes than in the independent downregulation of each gene (Figure 31D-F and I). In ~50% of *Dll^{212}>DrakRNAi, rokRNAi* legs, several distal segments were lost and the legs considered as truncated, while the

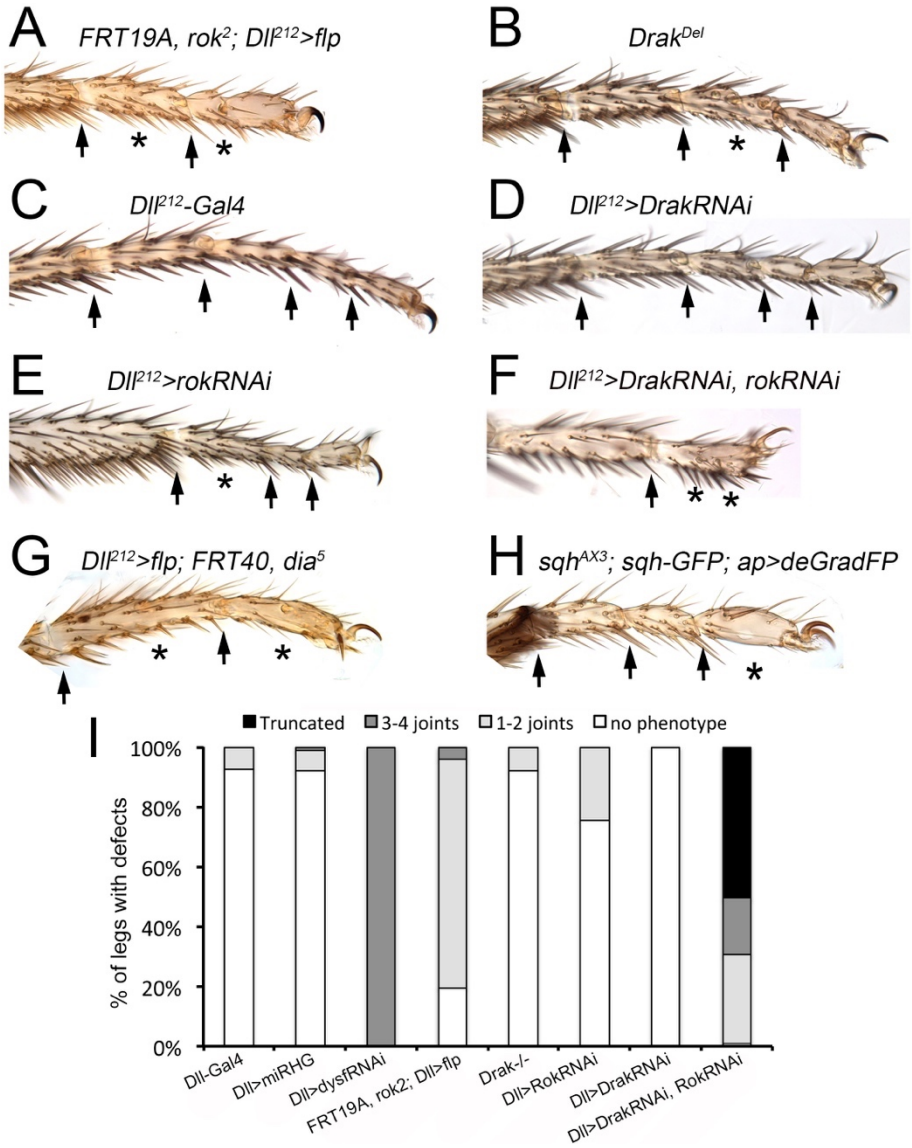

Figure 31. Loss of function analysis of Rho1 downstream effectors in adult joint formation. (A-H) Tarsal region of adult legs of the following genotypes: *FRT19A, rok2; Dll^{212}>UAS-flp* **(A)**, *Drak^{Del}* **(B)**, *Dll^{212}-Gal4* **(C)**, *Dll^{212}>UAS-DrakRNAi* **(D)**, *Dll^{212}>UAS-rokRNAi* **(E)**, *Dll^{212}>UAS-DrakRNAi,* UAS-*rokRNAi* **(F)**, *Dll^{212}>UAS-flp; FRT40, dia^{5}* **(G)** and *sqh^{AX3}; sqh-GFP; ap>*UAS-*deGradFP* **(H)**. See Materials and Methods for details. Arrows indicate normal joint formation, and asterisks point to loss of joints. **(I)** Quantification of leg joint defects observed in the genotypes above. Individual legs were grouped according to severity of joint defects: *no phenotype*, *1-2 joints* and *3-4 joints* and *truncated*. Dll-Gal4 (n=55); Dll>miRHG (n=89); Dll>dysfRNAi (n=47); FRT19A, rok^{2}; Dll>flp (n=72); Drak$^{-/-}$ (n=100); Dll>rokRNAi (n=86); Dll>DrakRNAi (n=60) and Dll>DrakRNAi, rokRNAi (n=85).

rest of the legs presented a reduction in length and defects in joint formation (31F and I). Dia is another downstream target of Rho1, implicated in F-actin assembly and its connection with adherens junctions (HOMEM AND PEIFER 2008; MASON *et al.* 2013). *dia* mutant clones cause the loss of joints in the adult legs, even though the lack of cuticular markers does not allow us to further characterize these clones (Figure 31G).

We then analyzed the phenotypes caused by the different loss of function conditions of Rho1 effectors in prepupal leg discs. *rok* mutants presented an altered morphology characterized by the loss of several tarsal folds, a phenotype reminiscent of the tarsal joint defects observed in the corresponding adult legs (compare Figure 32A and Figure 31A). Generation of mutant *dia* clones also inhibited fold formation, as predicted by adult joint phenotypes (compare Figure 32B and Figure 31G). Double knockdown of Rok and Drak caused the disruption of several tarsal folds, along with a reduction in tarsal size and an increase in cell death (Figure 32D and control in C). These phenotypes are consistent with the range of joint defects observed in the adult legs.

To directly test the requirement of acto-myosin contractility in fold formation, we depleted the MyoII regulatory light chain, Sqh, from the tarsal epithelium. We used mutant *sqh* flies carrying a rescue transgene expressing *sqh-GFP* under the control of the *sqh* promoter (*sqh^{AX3}; sqh-GFP*). In these flies, a UAS-*deGradFP* was expressed using the *Dll^{212}-Gal4* driver to degrade the Sqh-GFP fusion protein, and therefore depleting Sqh from the epithelium (CAUSSINUS *et al.* 2011). In control leg discs Sqh-GFP is accumulated at the adherens junctions of the epithelial cells (Figure 32F). Sqh-GFP depletion for 24 hrs caused the inhibition of fold formation throughout the *Dll* domain (Figure 32G). To analyze MyoII depletion effects on adult joint formation we used the same approach directed by the *ap-Gal4* driver, and observed the loss the t4-t5 joint (Figure 31H). Nevertheless, these phenotypes might respond to severe defects in epithelial integrity caused by Sqh depletion, rather than to the inhibition of acto-myosin contractility.

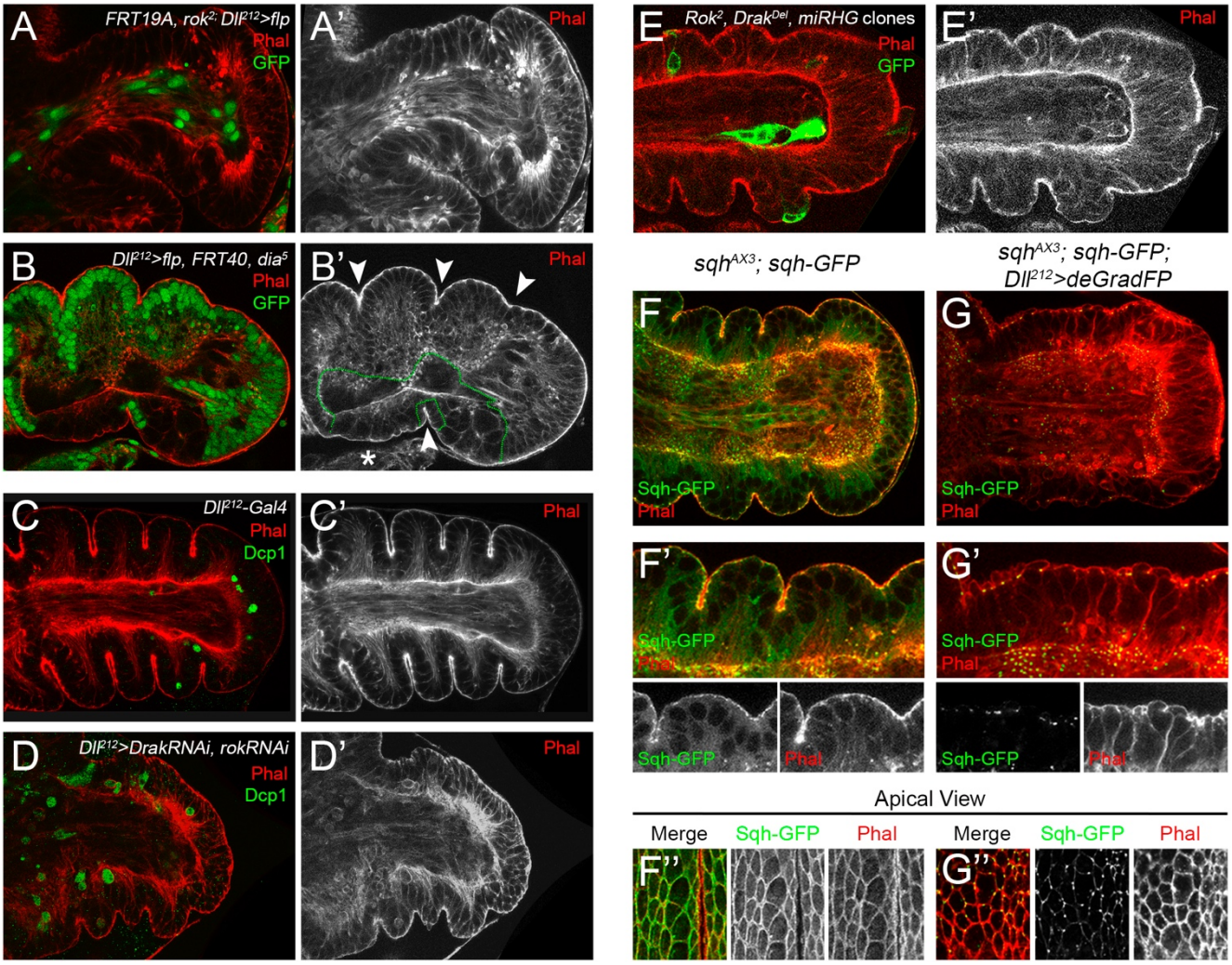

Figure 32. Loss of function analysis of Rho1 downstream effectors in prepupal fold formation. (A and B) *rok^{2}* and *dia^{5}* mutant clones (marked by loss of GFP expression in **A** and **B**, respectively) generated in the distal domain of prepupal leg discs, using the *Minute* technique. Note that the *rok^{2}* clones covered the entire distal leg disc, while *dia^{5}* mutant clones were much smaller. **(C and D)** *Dll^{212}-Gal4* control **(C)** and *Dll^{212}*>UAS-*DrakRNAi,* UAS-*rokRNAi* **(D)** prepupal leg discs stained for Dcp1 (green, Z-stacks are shown). Cell death is increased and fold formation altered in **D**. **(E)** Double *rok^{2}* and *Drak^{Del}* mutant clones expressing UAS-*miRHG* (see Materials and Methods for details). Clones are very small and present aberrant integration in the epithelium. Phal is in red in **A-E** and separate channels in **A'-E'**. **(F and G)** Control *sqh^{AX3}; sqh-GFP* **(F)** and *sqh^{AX3}; sqh-GFP; Dll^{212}*>UAS-*deGradFP* **(G)** prepupal leg discs. *Dll^{212}-Gal4* expression was restricted for 24 hrs prior to dissection using *tubGal80^{ts}* (see Materials and Methods for details). Sqh-GFP is in green and separate channels in **F'**, **F''**, **G'** and **G''**, and Phal is in red and separate channels in **F'**, **F''**, **G'** and **G''**. Close up views of **F** and **G** are shown in **F'** and **G'**, and apical views of the same genotypes are shown in **F''** and **G''**. Note that Sqh-GFP depletion is almost complete in **G-G''**, impairing apical constriction and fold formation, and causing aberrant cell morphologies.

Taken together, these results indicate that precise regulation of Rho1 effectors is required for correct fold and tarsal joint formation. The functional redundancy of several effectors and the structural roles played by the Rho1 pathway in epithelial organization and maintenance makes difficult to separate these requirements from their function in fold formation.

4.6 Expression of *dysf*, *Rho1* and Rho1 effectors cause ectopic fold formation in the wing disc

We have shown previously in this work that the misexpression of *dysf* causes the formation of ectopic epithelial folds and joint-like indentations in the adult leg (Figure 4). Nevertheless, the folded structure of the leg disc makes it difficult to observe the features of the induced fold. For better visualization, we used the pouch of the third instar larval wing disc, a relatively flat epithelium, to describe the effect of *dysf* misexpression in the *ptc* domain for increasing time periods (Figure 33B-E and Figure 34B-D). After 24 hrs of *dysf* ectopic expression, cells in the *ptc* domain start to constrict apically (arrows in Figure 33B and detail in Figure 34B and F) and cause indentations in the epithelium that are more visible at the proximal domain of the wing pouch (arrowheads in Figure 33B). After 36 hrs the apical surface of *dysf* expressing cells is clearly constricted along the *ptc* domain, and a fold starts to be evident (Figure 33C and Figure 34C and G). When *dysf* is expressed for 48 hrs or longer, we could clearly observe the formation of a cleft that divides the wing pouch and that is characterized by the accumulation of apical F-actin (Figure 33D and E and detail in Figure 34D and H). As previously described, expression of *dysf* cause elevated levels of cell death (compare Figure 33B''-E'' with A''). Nevertheless, apoptosis does not seem to be required, as a fold is still formed when *dysf* is ectopically expressed in a *dronc* mutant background where levels of apoptosis are highly reduced (Figure 33F''). To test whether the formation of Dysf-induced ectopic folds is cell autonomous, we generated 'flip-out' UAS-*dysf* clones in the wing pouch (see Materials and Methods). In the center of each clone a sharp and deep fold could be observed, that is characterized by an increase in apical F-actin (Figure 35A and B).

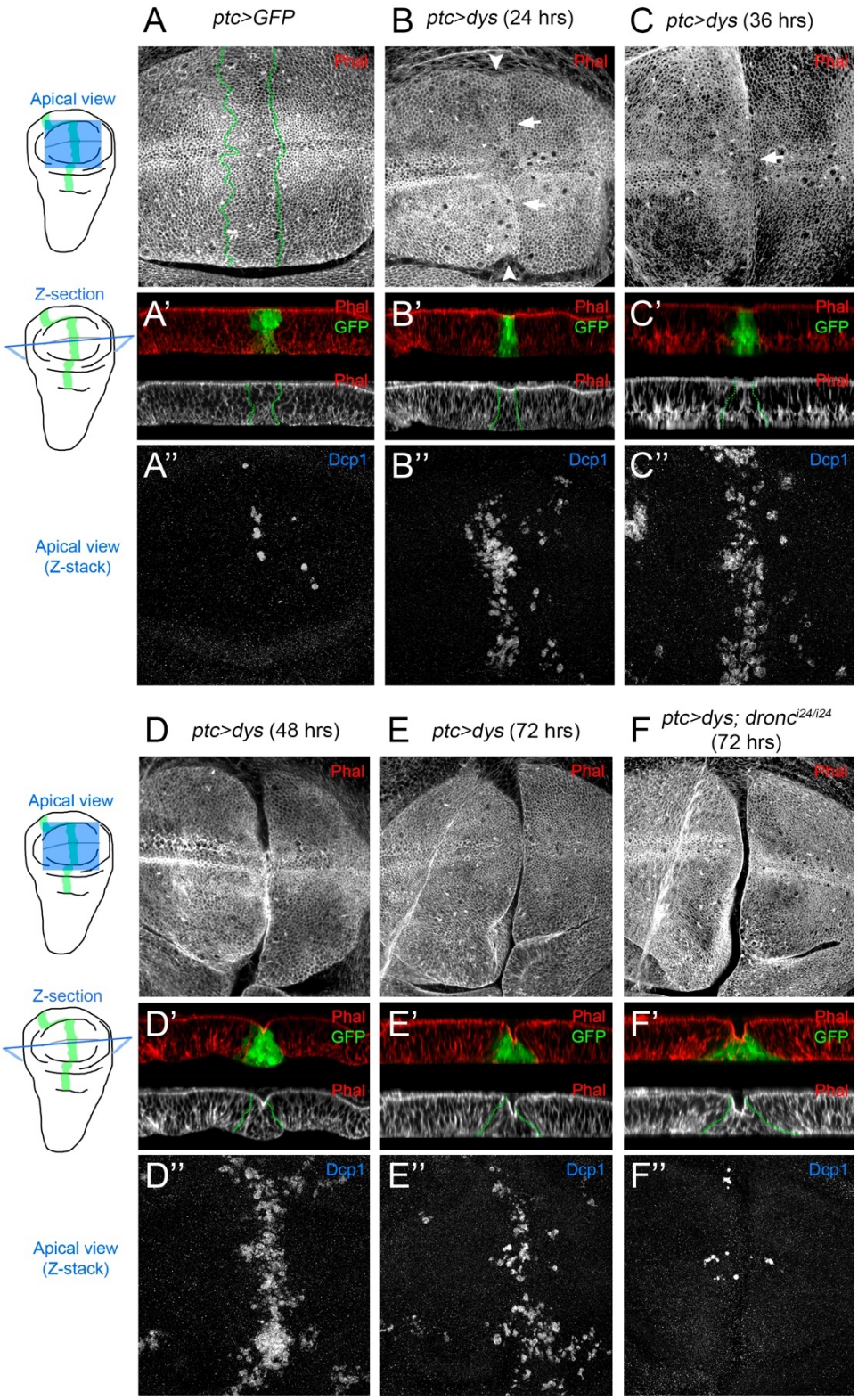

Figure 33. *dysf* ectopic expression cause fold formation in the wing disc. (A-F) Apical view of the pouch region of third instar larva wing discs. The *ptc-Gal4* driver is used to express UAS-*dysf* for different time periods **(B-E)**, or UAS-*GFP* as a control **(A)**, in a band of cells of the anterior compartment (marked by GFP expression, green in **A'-F'** and dotted lines). Apical view of the wing pouch is shown in **A-F**, and Z-sections are shown in **A'-F'**. Phal is in red in **A'-F'** and separate channels in **A-F** and **A'-F'** (lower panels), and Dcp1 is used to visualize cell death (single channel in **A''-F''** display the sum of all cell death observed in Z-stack imaging across the wing pouch). *dysf* misexpression for 24-36 hrs result in apical narrowing of the *ptc* domain (arrows) and visible indentations in the borders of the pouch (arrowheads), but do not cause significant folding of the epithelium. From 48 hrs onwards **(D-E)**, a clear fold is seen accompanied by the accumulation of apical F-actin. **(F)** Ectopic expression of *dysf* for 72 hrs in the *ptc* domain in a *dronc*$^{i24/i24}$ mutant background. Cell death is dramatically increased upon *dysf* misexpression, but is almost completely reverted in a *dronc* mutant background, while the fold formation is maintained **(F-F'')**.

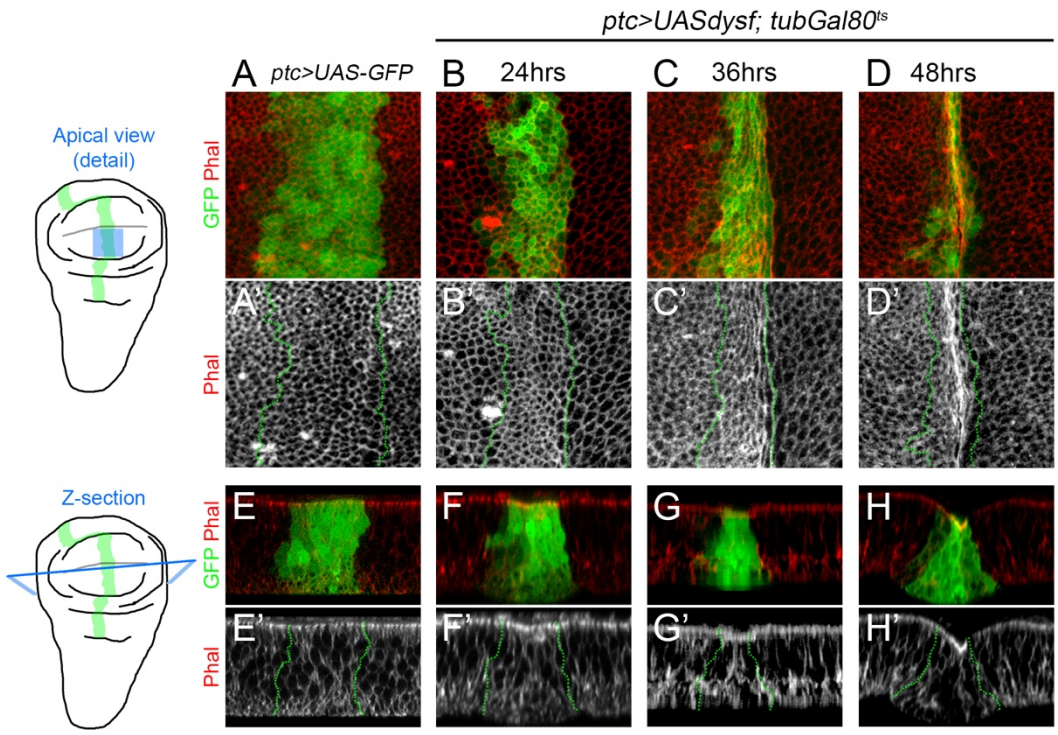

Figure 34. Time course of *dysf*-induced epithelial folding in the wing disc. (A-D) Apical view of a region of the wing pouch (blue square in the schematic wing disc) of control *ptc*>UAS-*GFP* **(A)**, and different times of *ptc*>UAS-*dysf* expression **(B-D)**. *ptc* domain is marked by GFP expression (green and dotted line in **A'-D'**). Phal is in red and separate channels in **A'-D'**). The *dysf*-expressing cells undergo apical constriction and consequently the *ptc* domain becomes narrower. By 48 hrs, accumulation of F-actin is clearly visible. **(E-H)** Sagittal sections of the genotypes described above. Note the progressive narrowing of the GFP positive cells in their apical region and the formation of a fold that is completely formed by 48 hrs.

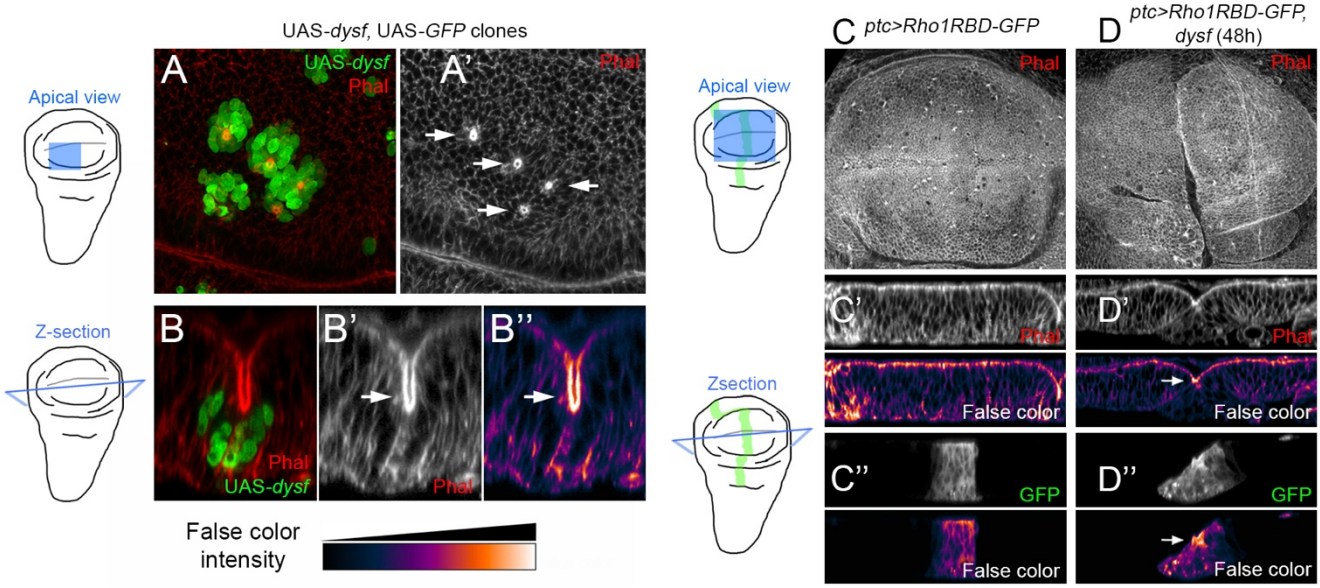

Figure 35. Ectopic *dysf* expression forms folds cell-autonomously and activates Rho1. (A) Apical view of the pouch region of a wing disc showing *'flip-out'* clones of UAS-*dysf* marked positively by GFP expression. In the center of each clone accumulation of F-actin could be observed (arrows in **A'**). A Z-section of one of the clones is shown in **B**, where the formation of a deep fold could be observed, accompanied by the accumulation of apical F-actin in the fold-forming cells (arrows in **B'** and **B''**). Phal is in red in **A** and **B**, in separated channels in **A'** and **B'** and in false color to enhance contrast in **B''**. GFP is in green in **A** and **B**. **(C and D)** Wing disc pouch (apical view) of *ptc*>UAS-*Rho1RBD-GFP* **(C)** and *ptc*>UAS-*Rho1RBD-GFP,* UAS-*dysf* **(D)**, transferred to 29°C 48 hrs before dissection. Z-sections of the control **(C' and C'')** and UAS-*dysf* **(D' and D'')** wing discs are shown below. F-actin is visualized by Phal staining (grey channel in **C**, **C'**, **D** and **D'** and false color to enhance contrast in **C'** and **D'**, lower panels). Rho1RBD-GFP is in grey channel in **C''** and **D''** and false color to enhance contrast in **C''** and **D''**, lower panels. Note that ectopic fold formation in **(D)** is accompanied by apical accumulation of F-actin (arrow in **D'**) and enhanced Rho1 activity in the apical region of the fold-forming cells (arrow in **D''**).

Dysf regulates Rho1 activity during endogenous tarsal fold formation in the leg. Therefore, we explored if Dysf could analogously activate Rho1 activity to form ectopic folds in the wing pouch. Coexpression of UAS-*dysf* with the Rho1 activity biosensor (UAS-*Rho1RBD-GFP*) for 48 hrs cause Rho1RBD-GFP accumulation in the apical region of the fold forming cells (Figure 35D), which is reminiscent of Rho1 activity pattern in endogenous prepupal tarsal folds (compare with Figure 20I). These results indicate that ectopic Dysf is capable of forming cell-autonomous folds in the wing disc, probably through the activation of Rho1. Moreover, *dysf* expression cause increased apoptosis that nonetheless is dispensable to form ectopic folds.

We reasoned that if the formation of ectopic folds by Dysf is mediated by Rho1 activity, then misexpression of *Rho1* or its downstream effectors could reproduce the phenotype of ectopic *dysf* expression. The expression of a wild type form of Rho1 in the *ptc* domain is sufficient to form a deep fold in the wing pouch epithelium, and only generates moderate levels of cell death compared to *dysf* misexpression (Figure 36A). Nevertheless, the formation of these folds is independent of cell death (Figure 37C and D). Consistently, the expression of a constitutively active form of Rok (UAS-rok^{CAT}) also causes the folding of the epithelium and the accumulation of F-actin, with no evident cell death induction (Figure 36B). Similar phenotypes are observed when MyoII contractility is directly activated using a phosphomimetic form of Sqh (UAS-sqh^{EE}) (Figure 36C). The expression of a constitutively activated form of Dia also forms a cleft in the wing pouch, although in this case F-actin is accumulated all around the plasma membrane of the *ptc* cells and not restricted to the apical region (Figure 36D). Also, high levels of cell death could be seen in this case. In contrast, ectopic expression of the pro-apoptotic gene *rpr* for 6 or 24 hrs does not cause any visible fold in the wing pouch epithelium (Figure 36E and F). Therefore, the activation of Rho1 or its downstream targets is sufficient to reproduce, to some extent, the ectopic fold phenotype caused by Dysf. Importantly, these folds form independently of apoptosis, and this phenotype cannot be reproduced by the induction of localized cell death.

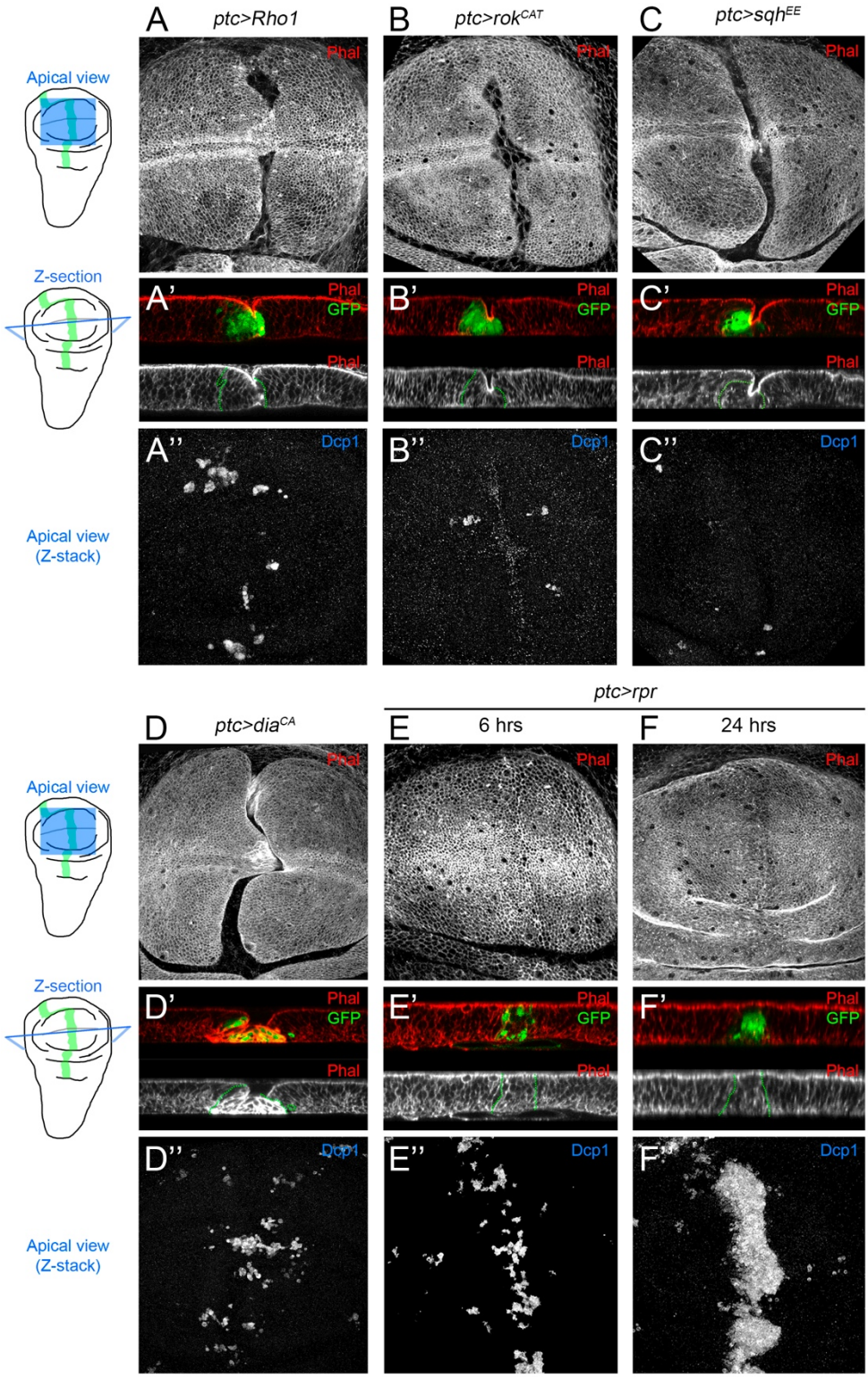

Figure 36. Misexpression of *Rho1* and *Rho1* downstream effectors is sufficient to form ectopic folds in the wing disc. (A-D) Third instar larva wing discs (wing puch, apical view). Different UAS constructions are expressed under the control of the *ptc-Gal4* driver: UAS-*Rho1* **(A)**, UAS-*Rok*^{CAT} **(B)**, UAS-*sqh*^{EE} **(C)**, UAS-*Dia*^{CA} **(D)** and UAS-*rpr* (**E** and **F**; 6 and 24 hrs of expression, respectively). Z-sections of each genotype are shown in **A'-E'**. Phal is in red in **A'-E'** and separate channels in **A-E** and **A'-E'** (lower panels). *ptc* domain is marked by GFP expression, green in **A'-E'** and dotted line in lower panels. Note that in the apical views in **A-D** a cleft is formed in the center of the wing pouch, but not in **D-E**. The membranes that can be observed in the center of the fold **(A-D)** correspond to the peripodial membrane of the wing disc, as can be observed in **A'-D'**. F-actin is accumulated apically in the *ptc* cells that form the fold **(A-C)**. In **D**, a fold is also formed, but the cells in the *ptc* domain accumulate F-actin all around their surface, and not restricted to their apical side. To monitor cell death, Z-stacks of Dcp1 staining are shown in **A''-E''** (grey channel). UAS-*Rho1* and UAS-*dia*^{CA} expression increase levels of cell death, while UAS-*rok*^{CAT} and UAS-*sqh*^{EE} expression have no apparent effect on apoptosis. UAS-*rpr* expression dramatically increases cell death without folding the wing disc epithelium.

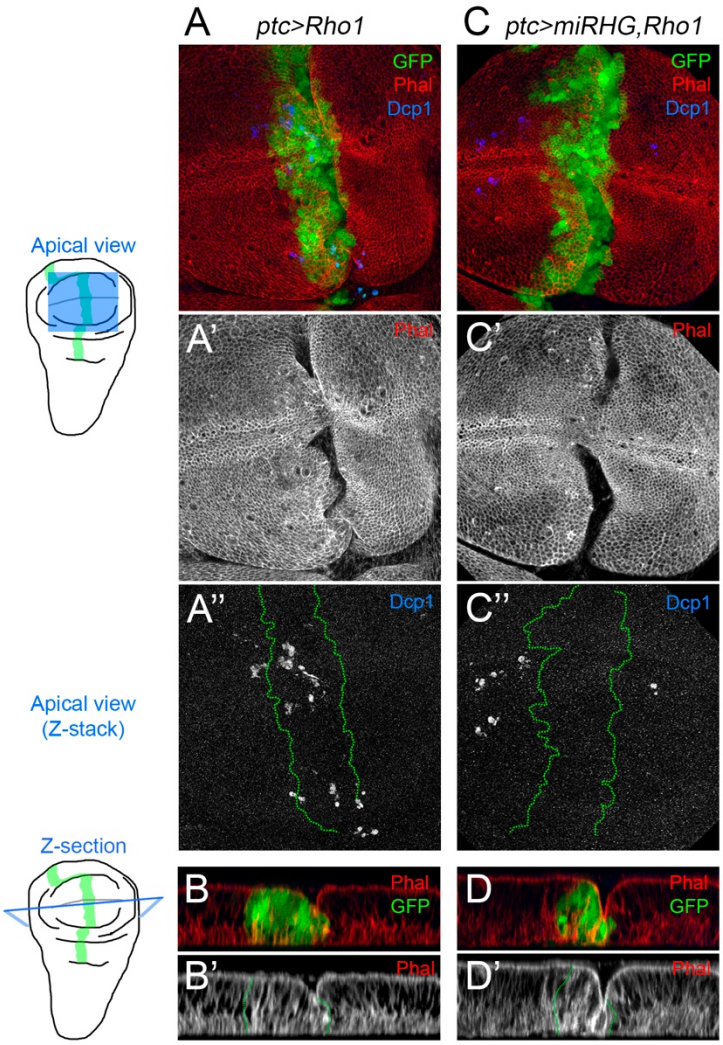

Figure 37. Cell death is not required for Rho1-dependent fold formation. (A and C) Third instar larva wing discs (apical view) of ptc>UAS-Rho1 **(A)** and ptc>UAS-Rho1, UAS-miRHG **(C)**. ptc domain is marked by GFP expression (green and dotted lines in **A''** and **C''**). Phal is in red and separate channels in **A'** and **C'**, and Z-stacks of Dcp1 staining to visualize cell death are shown in **A''** and **C''**. **(B and D)** Z-section of the wing discs above. ptc domain is marked by GFP expression (green in **B** and **D** and dotted lines in **B'** and **D'**). Phal is in red in **B** and **D** and separate channels in **B'** and **D'**. Note that fold formation is maintained when cell death is inhibited in the ptc domain.

DISCUSSION

In the present work we have analyzed the regulation and function of the bHLH-PAS transcription factor Dysf during leg joint formation in *Drosophila melanogaster*. The study of Dysf function has allowed us to investigate the link between pattern formation in the leg and the morphogenetic mechanisms that direct the cellular behaviors that sculpt the joints. Localized *dysf* expression is directly dependent on Notch activity and is restricted specifically to the tarsal domain. We identified and molecularly analyzed a dedicated *cis*-regulatory module (CRM) that integrates this information to regulate *dysf* expression. In turn, Dysf activity is completely required for the development of the tarsal joints and the epithelial folds that prefigure them during prepupal stage, and is sufficient to generate epithelial folds and joint-like structures when ectopically expressed. This control of epithelial morphogenesis is carried out mainly through the regulation of Rho1 GTPase activity that organizes the process of apical constriction at the folds.

1. Genetic regulation of *dysf* expression

Drosophila leg segmentation depends on the spatially organized expression of transcription factors that direct the activation of Notch at the presumptive leg joints. However, Notch requirement for the formation of every leg joint cannot explain the anatomical, evolutionary and developmental divergence observed among 'true' and tarsal joints: there must be another layer of genetic regulation that distinguish between proximal and distal joints. The expression of the *odd-skipped* TF family members *odd*, *drm* and *sob* is restricted to the presumptive 'true' joints, however their requirement for proximal joint formation in *Drosophila* has not been studied in depth (HAO *et al.* 2003). Combined loss of function of these three TFs in the flour beetle (*Tribolium castaneum*) abrogates 'true' joint formation, pointing to a functional redundancy between them, while their ectopic expression cause folding of the leg (HAO *et al.* 2003; ANGELINI *et al.* 2012). Another member of the *odd-skipped* family, *bowl*, participates in a feedback loop with *lines* to refine Notch activity pattern in the 'true' joints (GREENBERG AND HATINI 2009; SUZANNE 2016). In this work we have identified a direct target of Notch activity, *dysf*, which expression is restricted to the tarsal presumptive joints. *dysf* is completely required for tarsal joint development and is capable of inducing joint-like formation when ectopically expressed. Importantly, *dysf* mutants retain a correct tarsal P-D patterning and Notch activation, indicating that *dysf* mutant phenotypes are not primarily caused by defects in Notch function. Nevertheless, we cannot completely rule out a possible feedback mechanism by which Dysf reinforce Notch activity, as *dysf* knockdown slightly downregulates *E(spl)mβ* expression, and the borders of Ser and E(spl)mβ domains are slightly diffuse in *dysf* mutants.

To understand *dysf* regulation we set out to identify the CRM that governs its expression in the tarsal region of the leg. The CRMs that direct *dysf* expression in the context of tracheal development were already described (JIANG *et al.* 2010). We identified a different regulatory region, *dysf640* that faithfully reproduces *dysf* expression in the tarsal region, and responds to Notch activity in the same manner that the endogenous *dysf* gene. Notch regulates *dysf* expression directly through, at least, two specific binding sites for Su(H) located

within this sequence. Mutation of the predicted Su(H) sites suppress peak levels of reporter expression at the presumptive joints while a derepression, despite at lower levels, is observed within the tarsal region of the leg. These results fits into the model of 'default repression' proposed for Su(H) function (BAROLO *et al.* 2002): in the absence of intracellular Notch, Su(H) bind to its target sites and forms complexes with Co-Repressors, inhibiting the transcription of Notch downstream genes. Conversely, upon Notch activation, Notch^{ICD} binding to Su(H) displaces Co-Repressors, and recruits Co-Activators to form a complex that induce target gene transcription (Figure D-1). Therefore, in this context Notch activation plays an *instructive* role, as it is required not only to overcome the repression exerted by Su(H), but also to induce high levels of *dysf* expression at the presumptive tarsal joints (BRAY AND FURRIOLS 2001; LAI 2002).

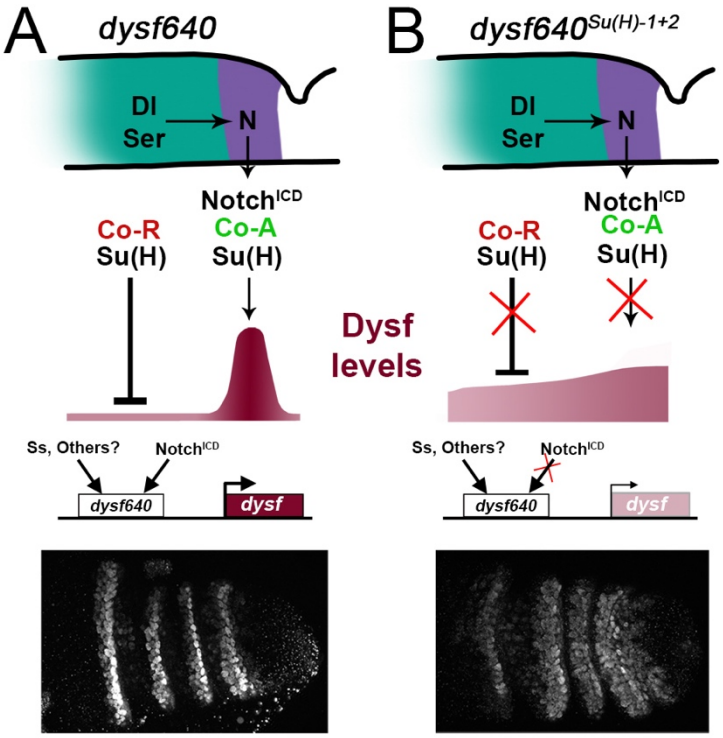

Figure D-1: Proposed model for direct regulation of dysf expression by Notch. (A) Schematic representation of a wild type (*dysf640*) leg. In the interjoint region, Su(H) associates with co-repressors to keep dysf expression off in the absence of Notch activation. In the presumptive joint, Dl/Ser binding to Notch receptor and the release of Notch^{ICD}, that enters the nucleus and associates with Su(H) and co-activators, to induce high levels of *dysf* expression. The tarsal-specific TF Ss, and probably others, is required together with Notch^{ICD} to restrict *dysf* expression to the tarsal domain of the leg. **(B)** In *dysf640*$^{Su(H)-1+2}$ legs, Su(H) cannot bind to the *dysf* CRM, and therefore is unable to repress *dysf* in the interjoint region and to activate high levels of *dysf* expression in the presumptive joints. The observed *dysf* expression in this context may result from a positive input arising from tarsal TFs, including Ss and maybe others

Interestingly, the derepression observed in *dysf640*$^{Su(H)-1+2}$*-lacZ* unveils a second regulatory input for *dysf* expression distinct from Notch activity, which would be responsible for *dysf* restriction to the tarsal domain. This regulation is paramount, as it makes possible the implementation of a specific developmental program for tarsal joints directed by Dysf. Notch outcome depends on the cellular context where it is activated. Therefore, the signal that restricts *dysf* expression has to be present in the tarsal domain, and act in parallel with Notch for *dysf* regulation. We observed that Ss loss of function inhibits the expression of *dysf640-lacZ*. Nevertheless, Ss function is earlier required for the determination of the tarsal region (DUNCAN *et al.* 1998; EMMONS *et al.* 1999; KOZU *et al.* 2006), and so it is possible that the loss of *dysf* reporter expression would be caused by the loss of tarsal fate rather than the lack of *dysf* activation. Moreover, ectopic expression of *ss* does not activate *dysf* at proximal joints (data not shown), as would be predicted by the proposed model of combined positive inputs from Notch and a distal TF for regulation of *dysf* expression. Other possibility is that *dysf* restriction to the tarsal region would be exerted through a negative regulation by other TFs such as Dac or members of the *odd* family

that would inhibit *dysf* activation outside the tarsal region. Therefore, the regulatory network that restricts *dysf* expression to the tarsal domain is yet to be fully elucidated.

2. Dysf transcriptional regulation of tarsal joint formation

The formation of tarsal joints implies the precise coordination of morphogenetic mechanisms to shape the prepupal folds and the adult joints. Dysf protein, a bHLH-PAS transcription factor is completely necessary for tarsal fold and joint formation. Therefore, we reasoned that its control of this process should be exerted through transcriptional regulation of target genes. Two mechanisms, regulation of Rho GTPase activity and cell death have been previously described to take part in tarsal joint development (MANJON *et al.* 2007; GREENBERG AND HATINI 2011; MONIER *et al.* 2015).

Several Rho GTPase regulators, including GEFs and GAPs are expressed in the presumptive leg joints, and a subset of them are restricted to the tarsal region and cause joint defects when downregulated (GREENBERG AND HATINI 2011). Interestingly, Rho GTPase regulators have been previously implicated in processes of apical constriction and epithelial folding. In *Drosophila*, RhoGEF2 dependent activation of Rho1 seems to be a conserved mechanism to induce acto-myosin contractility in different contexts; RhoGEF2 is necessary for correct apical constriction during ventral furrow formation (BARRETT *et al.* 1997; HACKER AND PERRIMON 1998; FOX AND PEIFER 2007; KOLSCH *et al.* 2007), and for the formation of segmental grooves during embryogenesis (MULINARI *et al.* 2008). A similar role in acto-myosin contractility activation has been described for its mammalian ortholog ARHGEF11 (NISHIMURA *et al.* 2012; SAI *et al.* 2014). Counter-intuitively, the inhibition of Rho1 activity appears to be necessary in some cases; RhoGAP71E (also referred to as C-GAP) controls pulsed acto-myosin activity that is required for ventral furrow morphogenesis (MASON *et al.* 2016). The restriction of Rho1 activity by RhoGAPs is also necessary for correctly localized apical constriction during salivary gland formation, and RhoGAP88C (also known as Cv-c) interacts specifically with Rho1 and is required for F-actin reorganization in different morphogenetic processes (DENHOLM *et al.* 2005; BRODU AND CASANOVA 2006; KOLESNIKOV AND BECKENDORF 2007). Moreover, combined activity of RhoGEFs and RhoGAPs is necessary to modulate Rho1 function in posterior spiracle morphogenesis in *Drosophila* embryos (SIMOES *et al.* 2006). This evidence indicate that a precise balance between activating and inhibiting signals is required to regulate Rho1 activity during morphogenesis, and a similar regulation could be necessary for tarsal joint development.

The pro-apoptotic genes *rpr* and *hid* are expressed in rings at the presumptive tarsal joints and are coincident with increased levels of cell death. Together with the joint phenotypes observed in certain conditions of cell death inhibition, these findings lead to the hypothesis that apoptosis might regulate the formation of prepupal folds and adult joint morphogenesis (MANJON *et al.* 2007; MONIER *et al.* 2015). Accordingly, *rpr*-dependent cell death is necessary to form a fold between several cephalic segments of the *Drosophila* embryo

(LOHMANN *et al.* 2002). Cell death participation in morphogenesis has been historically considered as a sculptor that simply removes excess cells, as exemplified by the individualization of the digits in mammals (HERNANDEZ-MARTINEZ AND COVARRUBIAS 2011). However, new evidence points to a more active role of apoptosis in development, by which dying cells can affect the neighboring tissue in processes such as dorsal closure and male genital rotation in *Drosophila* or neural tube closure in mice (TOYAMA *et al.* 2008; SUZANNE *et al.* 2010; YAMAGUCHI *et al.* 2011; and reviewed in SUZANNE AND STELLER 2013). Recently, a mechanistic model has been proposed that links apoptosis and MyoII activation in the context of tarsal fold and joint formation (MONIER *et al.* 2015).

Therefore, Dysf might regulate both Rho GTPase activity and localized apoptosis to globally control joint formation. Accordingly, *dysf* knockdown abolish the expression of *lacZ* reporters of the Rho GTPase regulators *RhoGEF2* and *RhoGAP71E*, and of the pro-apoptotic genes *rpr* and *hid*, while forced *dysf* expression cause their autonomous ectopic expression in the tarsal region of the leg. Therefore, Dysf transcriptionally regulates the expression of several genes potentially involved in tarsal epithelial fold and joint development. Oddly, *dysf* and its putative targets respective expression patterns are not completely coincident. *dysf* expression is more proximal, overlaps in a couple rows of cells with its targets, and targets' expression is shifted distally two or three more rows towards the fold. This discrepancy suggests that the mechanism through which Dysf regulates their expression is not straightforward and may not be direct (schematic representation in Figure D-2C). Several hypotheses could be brought up to explain these results.

Dpp graded activity and specifically the formation of sharp boundaries of Dpp activation at the presumptive tarsal joints has been implicated in the formation of epithelial folds and adult joints through the regulation of JNK-dependent *rpr* activity and cell death (MANJON *et al.* 2007). Thus, it is possible that Dysf regulation of target genes, including *rpr*, would be mediated by its regulation of Dpp graded activity. Accordingly, *dysf* knockdown disrupts the pattern of P-Mad, a readout of the activation of the Dpp pathway. Therefore, it is possible that Dysf would be required to generate the sharp borders of Dpp activity that are responsible for the activation of Dysf target genes (ADACHI-YAMADA AND O'CONNOR 2002; MANJON *et al.* 2007). Interestingly, groups of cells that fail to activate the Dpp pathway are extruded from the wing disc epithelium, in a process that involves Rho1 and acto-myosin contractility (GIBSON AND PERRIMON 2005; SHEN AND DAHMANN 2005; WIDMANN AND DAHMANN 2009). The initial steps of this process include apical constriction and apico-basal shortening of the cells, which keeps a certain similarity with endogenous tarsal fold formation in the leg disc. Could be hypothesized that a similar mechanism, harnessed and tightly regulated could occur in the presumptive tarsal joints, where Dpp activity levels drop in the cells that form the folds (our results and MANJON *et al.* 2007). Nonetheless, the induction of target gene expression through boundaries of Dpp activity would only explain the activation of targets in the borders of ectopic Dysf activity. Contrary to this prediction, targets expression is cell autonomous within the domain of *dysf* misexpression and is not restricted to the boundaries (Figure 10 and 11). Additionally, *dysf* expression itself is affected when Dpp is ectopically activated in the *ap* domain. These results,

and the ectopic expression of *E(Spl)mβ* induced by *tkv*^{QD} clones (MANJON *et al.* 2007), indicate that the role of Dpp in the tarsal region might be related to refinement of precise borders of Notch activity, rather than the direct regulation of Dysf targets. This possible role of Dpp has not been previously described, and would be another mechanism to ensure correct Notch signaling in the tarsal domain of the leg. Future experiments would be required to distinguish between both possibilities.

Another possible explanation for Dysf regulation of its tarsal effectors transcription in the leg involves a similar mechanism to the one operating in embryonic ventral furrow formation. There, the TFs Twi and Sna activate the expression of *fog*, which encodes for a secreted protein that act as a short range signal, and *mist*, that encodes the GPCR receptor of Fog. Transduction of Fog signaling localizes RhoGEF2 towards the apical domain of the ventral furrow cells and induces Rho1-dependent acto-myosin contractility and eventually apical constriction (reviewed in MANNING AND ROGERS 2014). If a similar model applies during tarsal fold formation, the role of Dysf would be to activate the expression of a secretable protein that would act as an extracellular signal to activate target gene expression in the adjacent fold-forming cells. Importantly, this model would require a directional component to move this predicted signal (or restrict its reception) to the cells distal to *dysf* expression that will form the fold. Another important difference is that transcriptional regulation of *RhoGEF2*, *RhoGAP71E*, *rpr* and *hid* is taking place in the tarsal leg, whereas RhoGEF2 presence is ubiquitous in the embryo and its activity is controlled by regulating its subcellular localization (BARRETT *et al.* 1997; HACKER AND PERRIMON 1998; KOLSCH *et al.* 2007). This would imply a second step of transcriptional regulation in the tarsal folds that could not be mediated by Dysf, and that at this point is completely unknown to us.

A third hypothesis would imply direct regulation of tarsal effectors by Dysf, followed by a proximal shift of *dysf* expression during late tarsal leg development. In this hypothesis, cells at the joints that have been exposed to Dysf and activated expression of the tarsal effectors would maintain their expression when *dysf* pattern moves proximally. Hence, an epigenetic mechanism would be required to maintain the expression of *dysf* target genes in the fold cells. Candidates to regulate this process are the Trithorax-group proteins (TrxG), implicated in maintaining the 'on' state of gene expression (STEFFEN AND RINGROSE 2014). Nevertheless, downregulation of Trx activity by RNAi does not affect *rpr-lacZ* expression at the tarsal folds (data not shown).

To summarize, we have demonstrated that Dysf is necessary and sufficient for the expression of a set of target genes previously implicated in the morphogenesis of tarsal joints. Unfortunately, we cannot offer yet a molecular explanation of how this transcriptional regulation is exerted, due to the differences in the expression patterns of Dysf and its putative targets. An analysis of the transcriptome by RNA-seq or the analysis of the chromatin accessibility by ATAC-seq of *dysf* mutants could help identify direct targets of Dysf (and their regulatory regions) to solve this question.

As was described for Dysf function in embryonic tracheal development and for its mammalian ortholog Npas4, Dysf forms heterodimers with the bHLH-PAS protein Tgo (Arnt in mammals) to regulate target gene expression and joint development (JIANG AND CREWS 2007). In the leg disc, Tgo is excluded from the nucleus if Dysf is not present, while ectopic Dysf mobilizes Tgo to the nucleus. Unlike its mammalian ortholog, Tgo protein lacks an N-terminal nuclear localization sequence, and therefore relies on its bHLH-PAS partners (Dysf in this case) for nuclear localization (CREWS 2003). Tgo in turn is required for activation of Dysf targets *bib* and *rpr*, and ultimately for the development of tarsal joints. Nevertheless, despite Tgo knockdown inhibits joint formation we still observed Dysf nuclear localization, a result that was not previously described in tracheal development. This should be further investigated, but could indicate the ability of Dysf to independently translocate into the nucleus, while still depends on Tgo to activate target gene expression and regulate joint morphogenesis (JIANG AND CREWS 2007).

The mode of action of the complex Dysf-Tgo is maintained in their mammalian orthologs Npas4-Arnt, even to the point of conservation of the specificity of their DNA binding sites (JIANG AND CREWS 2007). Even an analogy could be stablished between Dysf function in tracheal formation and Npas4 role in sprouting angiogenesis in mammals (JIANG AND CREWS 2006; ESSER *et al.* 2017). Nevertheless, no implication has been described yet for Npas4 during vertebrate limb formation. Interestingly, a search in the MGI database (http://www.informatics.jax.org/) shows *Npas4* expression in the limbs of mice embryos (GRAY *et al.* 2004). Little is known about joint development in mammals, but the requirement of *Gdf5*, a TGF-β ligand, at the sites of joint formation has been reported (DECKER *et al.* 2014). Nevertheless, the genetic specification of the presumptive joint cells that express *Gdf5* and the morphogenetic mechanisms that shape them in vertebrates are yet to be described. It would be interesting to explore if *Npas4* plays any role in the regulation of vertebrate joint development, even though arthropod and vertebrate joints are not homologous structures.

3. Morphogenesis of the tarsal joints

So far, we have discussed the genetic regulation that directs *dysf* expression at the presumptive tarsal joints and identified several genes that are transcriptionally regulated by Dysf and could account for tarsal fold formation and adult joint development. We then decided to further analyze the process of fold formation at the cellular level, and study the cytoskeletal and regulatory components that could be regulated by Dysf.

Apical constriction is a fundamental process in epithelial morphogenesis that allows the generation of three-dimensional shapes from a flat epithelial sheet. Its participation in morphogenesis has been widely documented in vertebrate and invertebrate model organisms alike and in many developmental contexts (SAWYER *et al.* 2010; GILMOUR *et al.* 2017; PEARL *et al.* 2017). Although the details in the molecular dynamics may differ in each case, apical constriction is characterized by the shrinkage of the apical domain of the cell caused by

increased contractility of the acto-myosin cytoskeleton (ESCUDERO *et al.* 2007; MARTIN *et al.* 2009; LEE AND HARLAND 2010; ROH-JOHNSON *et al.* 2012; MARTIN AND GOLDSTEIN 2014). During *Drosophila* embryogenesis, apical constriction could lead to delamination of individual neuroblasts (AN *et al.* 2017) or the invagination of the epithelium when groups of cells constrict coordinately to form new embryonic layers or tubules (LEPTIN AND GRUNEWALD 1990; BRODU AND CASANOVA 2006; GIRDLER AND ROPER 2014).

In leg development, apical constriction is used to form the four highly stereotyped epithelial folds in the prepupal leg disc that prefigure the adult tarsal joints (GREENBERG AND HATINI 2011; MONIER *et al.* 2015; SUZANNE 2016). *dysf* mutants fail to form tarsal folds and lack the corresponding adult joints. As we have shown, these phenotypes are not due to defects in tarsal segmentation or apico-basal polarity defects of the epithelial cells. Therefore, most likely the loss of tarsal folds is caused by the lack of an instructive signal to activate the molecular mechanisms that direct apical constriction in response to Dysf activity. Is intriguing that, while the formation of four correctly patterned and shaped tarsal folds is disrupted in *dysf* mutants, the apical constriction and epithelial folding of isolated groups of cells could be observed (data not shown). Importantly, this folding never results in adult joint formation, but raises some important questions about apical constriction in the leg disc. First, it shows that an external force might contribute to the folding of the tarsal region. This force could be exerted by the peripodial membrane, which generates a resistance against eversion of the leg disc during prepupal stages (PROAG *et al.* 2018). Second, it might respond to an intrinsic Dysf-independent force that helps folding the epithelium. Interestingly, some authors propose a role for apical constriction as a guide for correct tissue invagination, rather than being completely required in tracheal tube formation (LLIMARGAS AND CASANOVA 2010; CHUNG *et al.* 2017). In this view, Dysf would be required to direct the precise timing and localization of apical constriction and subsequent tissue folding.

Despite apical constriction is a common theme in morphogenesis, fold formation in the tarsal leg present some characteristics that make this model worthy of a detailed analysis. In contrast to most models (LEPTIN AND GRUNEWALD 1990; SIMOES *et al.* 2006; XU *et al.* 2008), apical constriction in the leg disc does not result in tissue invagination and the basal lamina remains flat during the process. Instead, it results in stable fold formation through the apico-basal shortening of the fold-forming cells and the intense accumulation of apical F-actin in mature folds.

Importantly, we have not observed apical accumulation of MyoII (visualized by Zip-GFP or Sqh-GFP) in sagittal sections of the developing folds. Instead, we found Zip and Sqh localized at the level of the adherens junctions, where it remains throughout the process of apical constriction. This MyoII localization is not altered in *dysf* loss of function. In contrast, Rho1-GFP is accumulated in the apical region of the fold cells. Accordingly, activation of Rho1 visualized with the Rho1RBD-GFP biosensor increases towards the apical region of the fold-forming cells, and specifically at the level of the adherens junctions. When *dysf* is knocked down, Rho1 fails to

be apically localized and activated, which could account for the observed defects in apical constriction. From these observations, we propose a model where Dysf dependent activation of Rho1 GTPase in the apical region of the fold-forming cells promotes apical constriction by activating a preexisting MyoII network localized preferentially at the level of the adherens junctions. This mechanism would be different from the accumulation of apical MyoII described for other models of apical constriction (DAWES-HOANG *et al.* 2005; MARTIN *et al.* 2009; MASON *et al.* 2013; WENG AND WIESCHAUS 2016; AN *et al.* 2017; CHUNG *et al.* 2017). A more detailed analysis, including live imaging of fold formation, would be required to unambiguously determine the dynamics of the acto-myosin cytoskeleton and the components of the Rho1 regulatory pathway during apical constriction in this model.

Additionally, we have observed active Rho1 accumulation in small clusters that may correspond with trafficking vesicles, suggesting a possible role of Rho1 in vesicular transport in the leg epithelium (SYMONS AND RUSK 2003). Interestingly, endocytosis plays a role downstream of acto-myosin contraction to ensure efficient apical constriction in *Xenopus laevis* (LEE AND HARLAND 2010), and more recently RhoGAP68F has been implicated in the regulation of endocytosis and epithelial remodeling during tarsal fold formation in *Drosophila* (DE MADRID *et al.* 2015). Therefore, regulation of endocytic activity by Rho1 is potentially another mechanism that could impact epithelial morphogenesis.

4. Regulation of apical constriction in the tarsal folds

Our data demonstrate that Dysf function directs apical constriction in the tarsal folds. This regulation is likely implemented through the localization and activation of the Rho1 GTPase and the regulation of morphogenetic cell death at the presumptive joints. Nevertheless, how these two mechanisms are coordinated to regulate epithelial dynamics and what is their specific contribution and requirements for apical constriction is mostly unknown (SUZANNE 2016).

4.1. Cell death contribution to tarsal joint development

Recently, localized apoptosis at the folds has been proposed to generate a mechanical force that would cause increased acto-myosin contractility and lead to fold formation (MONIER *et al.* 2015; SUZANNE 2016). Apoptosis involves extensive cytoskeletal remodeling both in the dying cells and in their immediate neighbors, which require Rho GTPase activity and acto-myosin contractility for the correct extrusion of the dying cells (ROSENBLATT *et al.* 2001; COLEMAN AND OLSON 2002; SLATTUM *et al.* 2009; and reviewed in MONIER AND SUZANNE 2015). Theoretically, this relationship between cell death and cytoskeletal dynamics might be harnessed and exploited for epithelial morphogenesis during tarsal fold formation. Surprisingly, cell death can still be detected in *dysf* loss of function at similar levels than in wild type discs, despite the expression of the pro-apoptotic genes

rpr and *hid* is abolished. This could indicate either that cell death is triggered by RHG-independent mechanisms in the leg disc, or that our *rpr*- and *hid-lacZ* reporters are not completely reliable in this context. Importantly, the distribution of cell death around the tarsal folds is altered in *dysf* loss of function, where it is no longer preferentially localized at the folds. According to the model proposed by Monier and colleagues, a random distribution of cell death would abort fold formation, which might explain the lack of tarsal folds observed in *dysf* loss of function conditions.

We reasoned then that localized apoptosis at the presumptive joints could regulate Rho1 function upstream of MyoII activation to control apical constriction and fold formation. Surprisingly, we do not observe any defect on Rho1 activation pattern and apical constriction proceeds normally when cell death is inhibited. This result strongly opposes previous findings that place apoptosis as the main driver of tarsal fold development (MANJON *et al.* 2007; MONIER *et al.* 2015).

Given the implications of the latter result, we decided to thoroughly study the role of cell death in tarsal development using multiple genetic conditions to inhibit apoptosis. We blocked cell death at four levels of the apoptotic pathway: at the level of the pro-apototic genes (by *miRHG* expression and generating *DfH99* mutant legs), at the level of the Inhibitor of apoptosis protein (by overexpressing *Diap1*), at the level of initiator caspases (using *dronc* mutants) and blocking the function of executioner caspases (by expressing *p35*). In every case we observed efficient inhibition of cell death, but no defects (or minimal) on prepupal fold or adult joint formation.

These results strongly indicate that apoptosis does not play an instructive role in epithelial morphogenesis in this context, and that it is dispensable for tarsal fold and joint formation. However, we cannot discard a role of apoptosis in the dynamics of fold formation, regulating the speed or the efficiency of the process. Interestingly, cell death is not required for dorsal closure during *Drosophila* embryogenesis, but its inhibition delays completion of the process (TOYAMA *et al.* 2008). The morphogenetic role of cell death has also been debated in other developmental events such as vertebrate neural tube closure. In this model a strong association between apoptosis and closing of the neural tube has been observed (HARRIS AND JURILOFF 2007); however this cell death increases the efficiency of the process but is not essential for neural closure (MASSA *et al.* 2009; YAMAGUCHI *et al.* 2011). It would be interesting to study if apoptosis plays a similar role in tarsal joint formation.

4.2. Rho1 and downstream effectors function in tarsal joint development

Rho1 localization and activity are altered in *dysf* loss of function, which correlates with failure in apical constriction, tarsal fold formation and adult joint development. Rho1 is known to regulate acto-myosin contractility through activation of the Rok kinase, which in turn phosphorylates the regulatory light chain of

MyoII, Sqh. This functional relationship between Rho1-Rok-Sqh (RhoA-ROCK-MRLC, for their orthologues in vertebrates) is found to regulate morphogenesis in many animal models, and its appearance might have been very early in evolution, as evidenced by Rho1 regulation of cell constriction in the basal animal *Hydra* (RIENTO AND RIDLEY 2003; ZIMMERMAN *et al.* 2010; SAI *et al.* 2014; GILMOUR *et al.* 2017; HOLZ *et al.* 2017). In *Drosophila* Sqh is also phosphorylated by another kinase, Drak (NEUBUESER AND HIPFNER 2010; ROBERTSON *et al.* 2012). In parallel, Rho1 regulates F-actin cytoskeleton organization and its coupling to adherens junctions to promote force transmission across the epithelium (CITI *et al.* 2014; MARTIN AND GOLDSTEIN 2014; VASQUEZ AND MARTIN 2016). This Rho1 function is mediated by the activation of the formin Dia, and is also conserved in vertebrates (WATANABE *et al.* 1997; HOMEM AND PEIFER 2008; MASON *et al.* 2013; KUHN AND GEYER 2014). To elucidate the requirements of Rho1 and its effectors in the leg disc, we performed a comprehensive loss of function analysis of each element of the pathway and searched for tarsal fold and adult joint defects.

Direct blocking of Rho1 function expressing a dominant negative form of Rho1 disrupted fold and joint formation but also caused severe defects, including increased cell death and loss of epithelial integrity (BLOOR AND KIEHART 2002; NEISCH *et al.* 2010). This result was expected, as Rho1 activity is required for basic cellular functions besides morphogenesis, including cell adhesion, apico-basal polarity and cytokinesis (BAUSEK AND ZEIDLER 2014; CITI *et al.* 2014; MACK AND GEORGIOU 2014). Interestingly, simultaneous Rho1 blocking and cell death inhibition reverted most of the epithelial integrity phenotypes, while fold formation remained impaired. As previously discussed, Rho1 function is required for extrusion of apoptotic cells (COLEMAN AND OLSON 2002; MONIER AND SUZANNE 2015). Is possible that blocking Rho1 activity initiates a feedback loop of incorrectly extruded apoptotic cells that lead to more apoptosis and the accumulation of epithelial integrity defects. Therefore, by preventing the onset of apoptosis we can preserve epithelial integrity while clearly observe Rho1 requirements in tarsal joint development.

Interestingly, *rok* mutants display only mild defects in fold and adult joint formation. This result, however, is consistent with the functional redundancy previously described between Rok and Drak (NEUBUESER AND HIPFNER 2010; ROBERTSON *et al.* 2012). Consistently, *Drak* mutants present even milder leg phenotypes, but simultaneous RNAi-mediated knockdown of Rok and Drak strongly enhanced epithelial fold and adult joint defects. Nevertheless, the phenotype caused by the complete elimination of both Rok and Drak functions was impossible to analyze, as the double mutant clones did not grow properly. In a similar fashion, knockdown of *dia* also disrupted fold and joint formation, but aberrant cell morphology could be observed within mutant clones. Direct elimination of Sqh from the epithelium for a short period of time also abolished fold formation. Nevertheless, given the strong epithelial integrity defects observed in this condition, we cannot easily assign the loss of adult joints to defects in acto-myosin contractility. Both regulation of cell adhesion and acto-myosin cytoskeleton contraction are processes regulated by Rho1. As these processes are coupled, it is not possible to

separate these two Rho1 functions. Therefore, the requirement of Rho1 and its effectors in epithelial integrity and other basic cellular functions hinders a more precise analysis of their specific role during joint development.

5. Ectopic expression of Dysf, Rho1 and Rho1 effectors mimic endogenous fold formation

In the present work we show evidence to support that Dysf exerts its instructive function on tarsal fold and joint formation through the regulation of Rho1 mediated apical constriction. Thus, we explored whether missexpression of Dysf, Rho1 or Rho1 effectors is sufficient to reproduce endogenous fold and joint formation.

Using the relatively flat wing imaginal disc to perform gain of function experiments we were able to follow the process of fold formation caused by *dysf* expression. Interestingly, we observed an initial step of apical constriction by 24 hrs that was later followed by increasing accumulation of apical F-actin, activation of Rho1 and the formation of a deep fold that is already visible after 48 hrs of *dysf* expression. In contrast, direct expression of Rho1 or activated forms of Rok, Dia and Sqh caused a much more rapid fold formation, already visible after 24 hrs of ectopic expression. This delay is expected, as Dysf promotion of epithelial folding would require an intermediate step of transcriptional regulation. During leg development, fold formation is observed in cells distal to *dysf* expression. However, ectopic expression of *dysf* in the wing disc whether in the *ptc* domain or in clones, fold formation is induced in a cell autonomous manner. This discrepancy could be due to the experimental setting, as ectopic expression is performed in a different developmental context. It was recently described a mechanism that cause aberrantly fated cells within the wing epithelium to form cysts through activation of acto-myosin contractility (BIELMEIER *et al.* 2016). It is possible that *dysf* expressing cells in the wing disc undergo a similar mechanism triggered by their abnormal cell fate in the context of the wing disc.

Dysf ectopic expression causes the formation of cuticular indentations in the adult leg that resemble joints. Interestingly, this phenotype was not reproduced by the ectopic activation of either Rho1 or its effectors Rok, Dia and Sqh (data not shown). These results may indicate that Rho1 activity needs to be tightly regulated by Dysf throughout development. Conversely, it may evidence the requirement of other Dysf effectors that function in folding the adult cuticle and that are different from the Rho1-related effectors that shape the prepupal folds.

Importantly, despite high levels of cell death are observed upon *dysf* ectopic expression, its inhibition does not prevent fold formation. Cell death inhibition neither affect Rho1-induced ectopic folds. Moreover, induction of cell death alone does not form folds in the wing epithelium. These experiments are consistent with our previous findings showing that apoptosis is dispensable for normal fold development. Moreover, ectopic folds caused by *dysf* expression display increased Rho1RBD-GFP signal around the apical domain of the cells, arguing in favor of a similar mechanism for ectopic joint formation and endogenous tarsal fold development.

To summarize, in this work we have identified a link between the genetic patterning of the leg and the morphogenetic mechanisms that shape tarsal joints in *Drosophila*. We found that this link is exerted by Dysf, a transcription factor which expression is directly regulated by Notch activity and restricted to the tarsal region of the leg. In turn, Dysf is capable of coordinating the developmental machinery that leads to fold and joint formation. We have shown that the regulation of Rho1 activity is ultimately controlled by Dysf in this context, and is a key event for apical constriction and subsequent joint development. We propose that Dysf control of Rho1 activity is exerted through the transcriptional regulation of RhoGEFs and RhoGAPs, although the precise molecular mechanism of this control is yet to be clarified. In contrast with previous studies, we have not observed any requirement for cell death in joint development, although the expression of pro-apoptotic genes is observed at the presumptive joints and is regulated by *dysf* (Figure D-2).

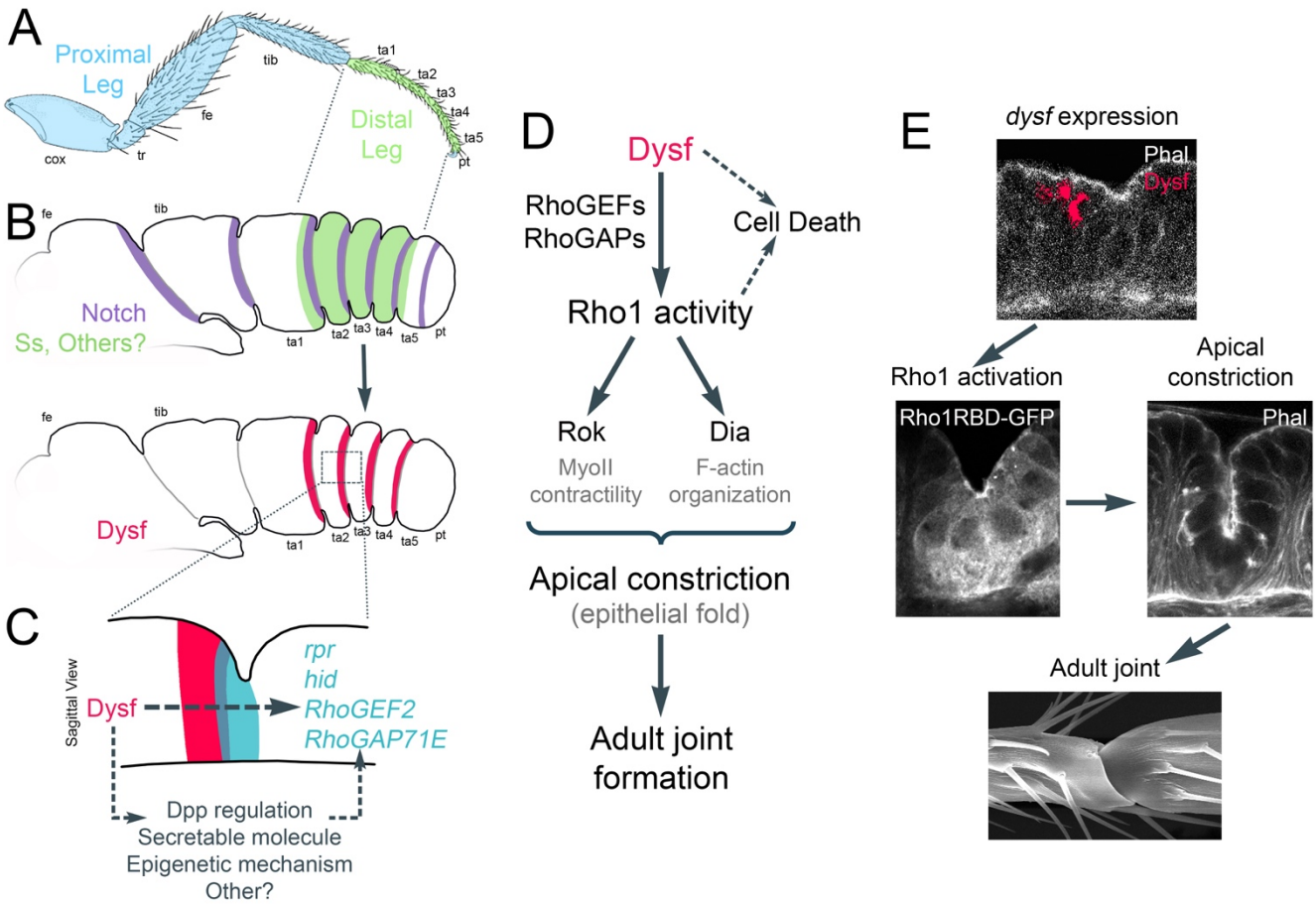

Figure D-2: Proposed model for Dysf regulation of tarsal joint development. (A) Schematic representation of a *Drosophila* adult leg where the distal and proximal regions are indicated. **(B)** Activation of the Notch pathway (purple) is localized at each presumptive joint in a prepupal leg disc. Combination of the regulatory inputs from Notch activity and a tarsal-specific TF (Ss, green, and possibly others) restrict the expression of *dysf* to the presumptive joints within the tarsal region. **(C)** Schematic representation of a tarsal epithelial fold, showing Dysf localization just proximal to the fold forming cells (red). The expression domain of the transcriptional targets of Dysf (*rpr*, *hid*, *RhoGEF2* and *RhoGAP71E*) is shown in blue. Note that the expression patterns of *dysf* and its targets is not completely coincident, which makes difficult to propose a direct regulation of target expression by Dysf. Some hypotheses that could explain Dysf regulation of target gene expression are listed below. **(D and E)** Dysf localization in the presumptive tarsal joints is required for Rho1 activity. This regulation is probably exerted through the control of *RhoGEFs* and *RhoGAPs* localized expression. Cell death is observed upon *dysf* expression, which could be either directly activated by Dysf or could emerge as the result of the increased levels of Rho1 activity in the fold forming cells. Rho1 in turn coordinates MyoII contractility through the regulation of Rok activity and F-actin assembly through Dia function, to efficiently promote apical constriction and the formation of epithelial folds. Epithelial folds in the tarsal region prefigure the formation of adult tarsal joints.

CONCLUSIONS

1. *dysf* encodes for a bHLH-PAS containing transcription factor, that is expressed in a ring-like pattern in the four tarsal segments of the leg.

2. *dysf* mutants present complete absence of the four tarsal joints, while proximal or 'true' joints are maintained. Consequently, the formation of deep epithelial folds in the prepupal leg disc that precede adult joint development is also lost. Conversely, *dysf* misexpression is sufficient to induce ectopic folding of the leg disc epithelium and generate joint-like indentations in the cuticle of the adult leg.

3. Notch activity is necessary and sufficient for *dysf* expression in the tarsal domain of prepupal leg discs. Additionally, Dysf function is epistatic to Notch for adult joint formation.

4. We have identified a *cis*-regulatory module, *dysf640*, which faithfully reproduces endogenous *dysf* expression. The Notch pathway directly regulates *dysf640* activity through, at least, two Su(H) binding sites. A distally localized transcription factor, possibly Ss, is required in combination with Notch for restricted *dysf640* activity in the tarsal domain.

5. Dysf is necessary and sufficient to regulate the expression of a subset of target genes in the presumptive tarsal joints. These targets include Rho GTPase regulators and pro-apoptotic genes. Nevertheless, the molecular mechanism through which Dysf regulates the expression of these targets remains elusive.

6. Dysf regulation of target gene expression and joint development requires its dimerization with the bHLH-PAS protein Tgo.

7. Apical constriction is the process that shapes the tarsal epithelial folds, and in this model is characterized by the intense accumulation of apical F-actin and Rho1, while MyoII remains localized at the level of adherens junctions. Apical constriction, F-actin accumulation and Rho1 localization at the developing folds are dependent on Dysf.

8. The activity of Rho1 is preferentially localized towards the apical region of the cells that undergo apical constriction to form the epithelial folds. This stereotyped pattern of Rho1 activity is dependent on Dysf.

9. The requirement of Rho1 and its downstream effectors, Rok, Drak and Dia, analyzed by loss of function experiments suggest an important function for them in prepupal fold and tarsal joint formation. However, the double requirements of the Rho1 pathway for regulation of basic cellular functions and apical constriction hinders a more detailed analysis of Rho1 specific function in joint development.

10. Exhaustive analysis of the role of cell death rule out a fundamental contribution of this process in the formation of prepupal folds and tarsal joints.

11. Ectopic induction of Dysf activity in the flat epithelium of the wing disc cause ectopic fold formation, which reproduces the F-actin accumulation and the Rho1 activity pattern observed during endogenous fold formation in the leg. Direct activation of Rho1, its effectors Rok and Dia, or activation of MyoII activity also yield ectopic fold formation, while induced cell death does not cause epithelial folding in the wing disc.

1. *dysf* codifica para un factor de transcripción de tipo bHLH-PAS, que se expresa en un patrón en forma de anillos en los cuatro segmentos tarsales de la pata.

2. Los mutantes *dysf* presentan complete ausencia de las cuatro articulaciones tarsales, mientras que mantienen las articulaciones proximales o 'verdaderas'. Consecuentemente, la formación de los pliegues epiteliales en el disco prepupal de pata, que preceden la formación de las articulaciones adultas, también se pierde. Al contrario, la expresión ectópica de *dysf* es suficiente para inducir pliegues en el epitelio del disco de pata y para generar indentaciones en la cutícula de la pata adulta.

3. La actividad de Notch es necesaria y suficiente para la expresión de *dysf* en el dominio tarsal de discos prepupales de pata. Además, la función de Dysf es epistática respecto a Notch para la formación de articulaciones adultas.

4. Hemos identificado un módulo regulador en *cis*, *dysf640*, que reproduce fielmente la expresión endógena de *dysf*. La ruta de Notch regula directamente la actividad de *dysf640* a través de, al menos, dos sitios de unión para Su(H). Un factor de transcripción localizado distalmente, posiblemente Ss, es necesario en combinación con Notch para la expresión de *dysf640* restringida al dominio tarsal.

5. Dysf es necesario y suficiente para regular la expresión de un subgrupo de genes diana en las articulaciones tarsales presuntivas. Estos genes diana incluyen reguladores de GTPasas y genes pro-apoptóticos. Sin embargo, el mecanismo molecular a través del cual Dysf regula la expresión de estos genes no está aún definido.

6. La regulación por parte de Dysf de la expresión de genes diana y del desarrollo de las articulaciones requiere su dimerización con la proteína Tgo, de tipo bHLH-PAS.

7. La constricción apical es el proceso que conforma los pliegues epiteliales de los tarsos, y en este modelo se caracteriza por la intensa acumulación apical de F-actina y Rho1, mientras que la MyoII se mantiene localizada al nivel de las uniones adherentes. La constricción apical, la acumulación de F-actina y la localización de Rho1 en las articulaciones en desarrollo dependen de Dysf.

8. La actividad de Rho1 se localiza preferentemente hacia la región apical de las células que experimentan constricción apical para formar los pliegues. Este patrón estereotipado de activación de Rho1 depende de Dysf.

9. El requerimiento de Rho1 y sus efectores derivados, Rok, Drak y Dia, analizado mediante experimentos de pérdida de función sugiere una función importante de los mismos en la formación de los pliegues prepupales y la formación de articulaciones tarsales adultas. Sin embargo, el doble requerimiento de la ruta Rho1 para la regulación de funciones celulares básicas y de la constricción apical previene un análisis más detallado de la función específica de Rho1 en el desarrollo de las articulaciones.

10. El análisis exhaustivo del papel de la muerte celular descarta una contribución fundamental de la misma en la formación de los pliegues prepupales y de las articulaciones tarsales adultas.

11. La inducción ectópica de la actividad de Dysf en el epitelio plano del disco de ala causa la formación ectópica de pliegues, que reproducen la acumulación de F-actina y el patrón de actividad de Rho1 observado durante la formación endógena de pliegues en la pata. La activación directa de Rho1, de sus efectores Rok y Dia, o la activación de la actividad de MyoII también resulta en la formación ectópica de pliegues, mientras la inducción de muerte celular no produce el plegamiento del epitelio del disco de ala.

BIBLIOGRAPHY

Abu-Shaar, M., and R. S. Mann, 1998 Generation of multiple antagonistic domains along the proximodistal axis during Drosophila leg development. Development 125: 3821-3830.

Adachi-Yamada, T., and M. B. O'Connor, 2002 Morphogenetic apoptosis: a mechanism for correcting discontinuities in morphogen gradients. Dev Biol 251: 74-90.

Adams, M. D., S. E. Celniker, R. A. Holt, C. A. Evans, J. D. Gocayne *et al.*, 2000 The genome sequence of Drosophila melanogaster. Science 287: 2185-2195.

Ahn, Y., J. Zou and P. J. Mitchell, 2011 Segment-specific regulation of the Drosophila AP-2 gene during leg and antennal development. Dev Biol 355: 336-348.

Aldaz, S., L. M. Escudero and M. Freeman, 2010 Live imaging of Drosophila imaginal disc development. Proc Natl Acad Sci U S A 107: 14217-14222.

An, Y., G. Xue, Y. Shaobo, D. Mingxi, X. Zhou *et al.*, 2017 Apical constriction is driven by a pulsatile apical myosin network in delaminating Drosophila neuroblasts. Development 144: 2153-2164.

Anderson, K. V., 1998 Pinning down positional information: dorsal-ventral polarity in the Drosophila embryo. Cell 95: 439-442.

Angelini, D. R., F. W. Smith and E. L. Jockusch, 2012 Extent With Modification: Leg Patterning in the Beetle Tribolium castaneum and the Evolution of Serial Homologs. G3 (Bethesda) 2: 235-248.

Awasaki, T., and K. Kimura, 2001 Multiple function of poxn gene in larval PNS development and in adult appendage formation of Drosophila. Dev Genes Evol 211: 20-29.

Baanannou, A., L. H. Mojica-Vazquez, G. Darras, J. L. Couderc, D. L. Cribbs *et al.*, 2013 Drosophila distal-less and Rotund bind a single enhancer ensuring reliable and robust bric-a-brac2 expression in distinct limb morphogenetic fields. PLoS Genet 9: e1003581.

Barolo, S., T. Stone, A. G. Bang and J. W. Posakony, 2002 Default repression and Notch signaling: Hairless acts as an adaptor to recruit the corepressors Groucho and dCtBP to Suppressor of Hairless. Genes Dev 16: 1964-1976.

Barrett, K., M. Leptin and J. Settleman, 1997 The Rho GTPase and a putative RhoGEF mediate a signaling pathway for the cell shape changes in Drosophila gastrulation. Cell 91: 905-915.

Basler, K., and G. Struhl, 1994 Compartment boundaries and the control of Drosophila limb pattern by hedgehog protein. Nature 368: 208-214.

Bate, M., and A. M. Arias, 1991 The embryonic origin of imaginal discs in Drosophila. Development 112: 755-761.

Bausek, N., and M. P. Zeidler, 2014 Galpha73B is a downstream effector of JAK/STAT signalling and a regulator of Rho1 in Drosophila haematopoiesis. J Cell Sci 127: 101-110.

Beira, J. V., and R. Paro, 2016 The legacy of Drosophila imaginal discs. Chromosoma 125: 573-592.

Bellen, H. J., C. Tong and H. Tsuda, 2010 100 years of Drosophila research and its impact on vertebrate neuroscience: a history lesson for the future. Nat Rev Neurosci 11: 514-522.

Bielmeier, C., S. Alt, V. Weichselberger, M. La Fortezza, H. Harz *et al.*, 2016 Interface Contractility between Differently Fated Cells Drives Cell Elimination and Cyst Formation. Curr Biol 26: 563-574.

Bishop, S. A., T. Klein, A. M. Arias and J. P. Couso, 1999 Composite signalling from Serrate and Delta establishes leg segments in Drosophila through Notch. Development 126: 2993-3003.

Bloor, J. W., and D. P. Kiehart, 2002 Drosophila RhoA regulates the cytoskeleton and cell-cell adhesion in the developing epidermis. Development 129: 3173-3183.

Boettner, B., and L. Van Aelst, 2002 The role of Rho GTPases in disease development. Gene 286: 155-174.

Brand, A. H., and N. Perrimon, 1993 Targeted gene expression as a means of altering cell fates and generating dominant phenotypes. Development 118: 401-415.

Bray, S., and M. Furriols, 2001 Notch pathway: making sense of suppressor of hairless. Curr Biol 11: R217-221.

Bray, S. J., 2006 Notch signalling: a simple pathway becomes complex. Nat Rev Mol Cell Biol 7: 678-689.

Brodu, V., and J. Casanova, 2006 The RhoGAP crossveinless-c links trachealess and EGFR signaling to cell shape remodeling in Drosophila tracheal invagination. Genes Dev 20: 1817-1828.

Campbell, G., 2002 Distalization of the Drosophila leg by graded EGF-receptor activity. Nature 418: 781-785.

Campbell, G., 2005 Regulation of gene expression in the distal region of the Drosophila leg by the Hox11 homolog, C15. Dev Biol 278: 607-618.

Campbell, G., T. Weaver and A. Tomlinson, 1993 Axis specification in the developing Drosophila appendage: the role of wingless, decapentaplegic, and the homeobox gene aristaless. Cell 74: 1113-1123.

Capilla, A., R. Johnson, M. Daniels, M. Benavente, S. J. Bray *et al.*, 2012 Planar cell polarity controls directional Notch signaling in the Drosophila leg. Development 139: 2584-2593.

Casares, F., and R. S. Mann, 2001 The ground state of the ventral appendage in Drosophila. Science 293: 1477-1480.

Caussinus, E., O. Kanca and M. Affolter, 2011 Fluorescent fusion protein knockout mediated by anti-GFP nanobody. Nat Struct Mol Biol 19: 117-121.

Chung, S., S. Kim and D. J. Andrew, 2017 Uncoupling apical constriction from tissue invagination. Elife 6.

Ciechanska, E., D. A. Dansereau, P. C. Svendsen, T. R. Heslip and W. J. Brook, 2007 dAP-2 and defective proventriculus regulate Serrate and Delta expression in the tarsus of Drosophila melanogaster. Genome 50**:** 693-705.

Citi, S., D. Guerrera, D. Spadaro and J. Shah, 2014 Epithelial junctions and Rho family GTPases: the zonular signalosome. Small GTPases 5**:** 1-15.

Cohen, B., A. A. Simcox and S. M. Cohen, 1993 Allocation of the thoracic imaginal primordia in the Drosophila embryo. Development 117**:** 597-608.

Cohen, S. M., 1990 Specification of limb development in the Drosophila embryo by positional cues from segmentation genes. Nature 343**:** 173-177.

Coleman, M. L., and M. F. Olson, 2002 Rho GTPase signalling pathways in the morphological changes associated with apoptosis. Cell Death Differ 9**:** 493-504.

Cordoba, S., D. Requena, A. Jory, A. Saiz and C. Estella, 2016 The evolutionarily conserved transcription factor Sp1 controls appendage growth through Notch signaling. Development 143**:** 3623-3631.

Corrigall, D., R. F. Walther, L. Rodriguez, P. Fichelson and F. Pichaud, 2007 Hedgehog signaling is a principal inducer of Myosin-II-driven cell ingression in Drosophila epithelia. Dev Cell 13**:** 730-742.

Couderc, J. L., D. Godt, S. Zollman, J. Chen, M. Li *et al.*, 2002 The bric a brac locus consists of two paralogous genes encoding BTB/POZ domain proteins and acts as a homeotic and morphogenetic regulator of imaginal development in Drosophila. Development 129**:** 2419-2433.

Crews, S. T., 2003 *Drosophila bHLH-PAS Developmental Regulatory Proteins. In: PAS Proteins: Regulators and Sensors of Development and Physiology. Chapter IV*. Springer US.

Dawes-Hoang, R. E., K. M. Parmar, A. E. Christiansen, C. B. Phelps, A. H. Brand *et al.*, 2005 folded gastrulation, cell shape change and the control of myosin localization. Development 132**:** 4165-4178.

de Celis Ibeas, J. M., and S. J. Bray, 2003 Bowl is required downstream of Notch for elaboration of distal limb patterning. Development 130**:** 5943-5952.

de Celis, J. F., 2003 Pattern formation in the Drosophila wing: The development of the veins. Bioessays 25**:** 443-451.

de Celis, J. F., and S. Bray, 1997 Feed-back mechanisms affecting Notch activation at the dorsoventral boundary in the Drosophila wing. Development 124**:** 3241-3251.

de Celis, J. F., D. M. Tyler, J. de Celis and S. J. Bray, 1998 Notch signalling mediates segmentation of the Drosophila leg. Development 125**:** 4617-4626.

de Madrid, B. H., L. Greenberg and V. Hatini, 2015 RhoGAP68F controls transport of adhesion proteins in Rab4 endosomes to modulate epithelial morphogenesis of Drosophila leg discs. Dev Biol 399: 283-295.

Decker, R. S., E. Koyama and M. Pacifici, 2014 Genesis and morphogenesis of limb synovial joints and articular cartilage. Matrix Biol 39: 5-10.

del Valle Rodriguez, A., D. Didiano and C. Desplan, 2012 Power tools for gene expression and clonal analysis in Drosophila. Nat Methods 9: 47-55.

Denholm, B., S. Brown, R. P. Ray, M. Ruiz-Gomez, H. Skaer *et al.*, 2005 crossveinless-c is a RhoGAP required for actin reorganisation during morphogenesis. Development 132: 2389-2400.

Diaz-Benjumea, F. J., B. Cohen and S. M. Cohen, 1994 Cell interaction between compartments establishes the proximal-distal axis of Drosophila legs. Nature 372: 175-179.

Duncan, D. M., E. A. Burgess and I. Duncan, 1998 Control of distal antennal identity and tarsal development in Drosophila by spineless-aristapedia, a homolog of the mammalian dioxin receptor. Genes Dev 12: 1290-1303.

Emmons, R. B., D. Duncan, P. A. Estes, P. Kiefel, J. T. Mosher *et al.*, 1999 The spineless-aristapedia and tango bHLH-PAS proteins interact to control antennal and tarsal development in Drosophila. Development 126: 3937-3945.

Engel, M. S., 2015 Insect evolution. Curr Biol 25: R868-872.

Escudero, L. M., M. Bischoff and M. Freeman, 2007 Myosin II regulates complex cellular arrangement and epithelial architecture in Drosophila. Dev Cell 13: 717-729.

Esser, J. S., A. Charlet, M. Schmidt, S. Heck, A. Allen *et al.*, 2017 The neuronal transcription factor NPAS4 is a strong inducer of sprouting angiogenesis and tip cell formation. Cardiovasc Res 113: 222-223.

Estella, C., and A. Baonza, 2015 Cell proliferation control by Notch signalling during imaginal discs development in Drosophila. AIMS Genetics 2: 70-96.

Estella, C., and R. S. Mann, 2008 Logic of Wg and Dpp induction of distal and medial fates in the Drosophila leg. Development 135: 627-636.

Estella, C., and R. S. Mann, 2010 Non-redundant selector and growth-promoting functions of two sister genes, buttonhead and Sp1, in Drosophila leg development. PLoS Genet 6: e1001001.

Estella, C., D. J. McKay and R. S. Mann, 2008 Molecular integration of wingless, decapentaplegic, and autoregulatory inputs into Distalless during Drosophila leg development. Dev Cell 14: 86-96.

Estella, C., G. Rieckhof, M. Calleja and G. Morata, 2003 The role of buttonhead and Sp1 in the development of the ventral imaginal discs of Drosophila. Development 130: 5929-5941.

Estella, C., R. Voutev and R. S. Mann, 2012 A dynamic network of morphogens and transcription factors patterns the fly leg. Curr Top Dev Biol 98: 173-198.

Fox, D. T., and M. Peifer, 2007 Abelson kinase (Abl) and RhoGEF2 regulate actin organization during cell constriction in Drosophila. Development 134: 567-578.

Fuchs, Y., and H. Steller, 2015 Live to die another way: modes of programmed cell death and the signals emanating from dying cells. Nat Rev Mol Cell Biol 16: 329-344.

Galindo, M. I., S. A. Bishop and J. P. Couso, 2005 Dynamic EGFR-Ras signalling in Drosophila leg development. Dev Dyn 233: 1496-1508.

Galindo, M. I., S. A. Bishop, S. Greig and J. P. Couso, 2002 Leg patterning driven by proximal-distal interactions and EGFR signaling. Science 297: 256-259.

Garcia-Bellido, A., P. Ripoll and G. Morata, 1973 Developmental compartmentalisation of the wing disk of Drosophila. Nat New Biol 245: 251-253.

Gavrieli, Y., Y. Sherman and S. A. Ben-Sasson, 1992 Identification of programmed cell death in situ via specific labeling of nuclear DNA fragmentation. J Cell Biol 119: 493-501.

Gibson, M. C., and N. Perrimon, 2005 Extrusion and death of DPP/BMP-compromised epithelial cells in the developing Drosophila wing. Science 307: 1785-1789.

Gilmour, D., M. Rembold and M. Leptin, 2017 From morphogen to morphogenesis and back. Nature 541: 311-320.

Giorgianni, M. W., and R. S. Mann, 2011 Establishment of medial fates along the proximodistal axis of the Drosophila leg through direct activation of dachshund by Distalless. Dev Cell 20: 455-468.

Girdler, G. C., and K. Roper, 2014 Controlling cell shape changes during salivary gland tube formation in Drosophila. Semin Cell Dev Biol 31: 74-81.

Godt, D., J. L. Couderc, S. E. Cramton and F. A. Laski, 1993 Pattern formation in the limbs of Drosophila: bric a brac is expressed in both a gradient and a wave-like pattern and is required for specification and proper segmentation of the tarsus. Development 119: 799-812.

Gonzalez-Crespo, S., M. Abu-Shaar, M. Torres, A. C. Martinez, R. S. Mann *et al.*, 1998 Antagonism between extradenticle function and Hedgehog signalling in the developing limb. Nature 394: 196-200.

González-Crespo, S., and G. Morata, 1996 Genetic evidence for the subdivision of the arthropod limb into coxopodite and telopodite. 122: 3921-3928.

Gordon, R., 1985 A review of the theories of vertebrate neurulation and their relationship to the mechanics of neural tube birth defects. J Embryol Exp Morphol 89 Suppl: 229-255.

Goyal, L., K. McCall, J. Agapite, E. Hartwieg and H. Steller, 2000 Induction of apoptosis by Drosophila reaper, hid and grim through inhibition of IAP function. EMBO J 19: 589-597.

Gray, P. A., H. Fu, P. Luo, Q. Zhao, J. Yu *et al.*, 2004 Mouse brain organization revealed through direct genome-scale TF expression analysis. Science 306: 2255-2257.

Greenberg, L., and V. Hatini, 2009 Essential roles for lines in mediating leg and antennal proximodistal patterning and generating a stable Notch signaling interface at segment borders. Dev Biol 330: 93-104.

Greenberg, L., and V. Hatini, 2011 Systematic expression and loss-of-function analysis defines spatially restricted requirements for Drosophila RhoGEFs and RhoGAPs in leg morphogenesis. Mech Dev 128: 5-17.

Grether, M. E., J. M. Abrams, J. Agapite, K. White and H. Steller, 1995 The head involution defective gene of Drosophila melanogaster functions in programmed cell death. Genes Dev 9: 1694-1708.

Guarner, A., C. Manjon, K. Edwards, H. Steller, M. Suzanne *et al.*, 2014 The zinc finger homeodomain-2 gene of Drosophila controls Notch targets and regulates apoptosis in the tarsal segments. Dev Biol 385: 350-365.

Hacker, U., and N. Perrimon, 1998 DRhoGEF2 encodes a member of the Dbl family of oncogenes and controls cell shape changes during gastrulation in Drosophila. Genes Dev 12: 274-284.

Hao, I., R. B. Green, O. Dunaevsky, J. A. Lengyel and C. Rauskolb, 2003 The odd-skipped family of zinc finger genes promotes Drosophila leg segmentation. Dev Biol 263: 282-295.

Harris, M. J., and D. M. Juriloff, 2007 Mouse mutants with neural tube closure defects and their role in understanding human neural tube defects. Birth Defects Res A Clin Mol Teratol 79: 187-210.

Hay, B. A., T. Wolff and G. M. Rubin, 1994 Expression of baculovirus P35 prevents cell death in Drosophila. Development 120: 2121-2129.

Heisenberg, C. P., and Y. Bellaiche, 2013 Forces in tissue morphogenesis and patterning. Cell 153: 948-962.

Hernandez-Martinez, R., and L. Covarrubias, 2011 Interdigital cell death function and regulation: new insights on an old programmed cell death model. Dev Growth Differ 53: 245-258.

Holz, O., D. Apel, P. Steinmetz, E. Lange, S. Hopfenmuller *et al.*, 2017 Bud detachment in hydra requires activation of fibroblast growth factor receptor and a Rho-ROCK-myosin II signaling pathway to ensure formation of a basal constriction. Dev Dyn 246: 502-516.

Homem, C. C., and M. Peifer, 2008 Diaphanous regulates myosin and adherens junctions to control cell contractility and protrusive behavior during morphogenesis. Development 135: 1005-1018.

Hulskamp, M., and D. Tautz, 1991 Gap genes and gradients--the logic behind the gaps. Bioessays 13: 261-268.

Ishihara, S., and K. Sugimura, 2012 Bayesian inference of force dynamics during morphogenesis. J Theor Biol 313: 201-211.

Jaffe, A. B., and A. Hall, 2005 Rho GTPases: biochemistry and biology. Annu Rev Cell Dev Biol 21: 247-269.

Jiang, C., A. F. Lamblin, H. Steller and C. S. Thummel, 2000 A steroid-triggered transcriptional hierarchy controls salivary gland cell death during Drosophila metamorphosis. Mol Cell 5: 445-455.

Jiang, L., and S. T. Crews, 2003 The Drosophila dysfusion Basic Helix-Loop-Helix (bHLH)-PAS Gene Controls Tracheal Fusion and Levels of the Trachealess bHLH-PAS Protein. Molecular and Cellular Biology 23: 5625-5637.

Jiang, L., and S. T. Crews, 2006 Dysfusion transcriptional control of Drosophila tracheal migration, adhesion, and fusion. Mol Cell Biol 26: 6547-6556.

Jiang, L., and S. T. Crews, 2007 Transcriptional specificity of Drosophila dysfusion and the control of tracheal fusion cell gene expression. J Biol Chem 282: 28659-28668.

Jiang, L., J. C. Pearson and S. T. Crews, 2010 Diverse modes of Drosophila tracheal fusion cell transcriptional regulation. Mech Dev 127: 265-280.

Jockusch, E. L., 2017 Developmental and Evolutionary Perspectives on the Origin and Diversification of Arthropod Appendages. Integr Comp Biol 57: 533-545.

Johnston, L. A., and G. Schubiger, 1996 Ectopic expression of wingless in imaginal discs interferes with decapentaplegic expression and alters cell determination. Development 122: 3519-3529.

Jory, A., C. Estella, M. W. Giorgianni, M. Slattery, T. R. Laverty *et al.*, 2012 A survey of 6,300 genomic fragments for cis-regulatory activity in the imaginal discs of Drosophila melanogaster. Cell Rep 2: 1014-1024.

Karess, R. E., X. J. Chang, K. A. Edwards, S. Kulkarni, I. Aguilera *et al.*, 1991 The regulatory light chain of nonmuscle myosin is encoded by spaghetti-squash, a gene required for cytokinesis in Drosophila. Cell 65: 1177-1189.

Keller, R., 2012 Developmental biology. Physical biology returns to morphogenesis. Science 338: 201-203.

Kerber, B., I. Monge, M. Mueller, P. J. Mitchell and S. M. Cohen, 2001 The AP-2 transcription factor is required for joint formation and cell survival in Drosophila leg development. 128: 1231-1238.

Kiehart, D. P., C. G. Galbraith, K. A. Edwards, W. L. Rickoll and R. A. Montague, 2000 Multiple forces contribute to cell sheet morphogenesis for dorsal closure in Drosophila. J Cell Biol 149: 471-490.

Kojima, T., 2017 Developmental mechanism of the tarsus in insect legs. Curr Opin Insect Sci 19: 36-42.

Kojima, T., M. Sato and K. Saigo, 2000 Formation and specification of distal leg segments in Drosophila by dual Bar homeobox genes, BarH1 and BarH2. Development 127: 769-778.

Kolesnikov, T., and S. K. Beckendorf, 2007 18 wheeler regulates apical constriction of salivary gland cells via the Rho-GTPase-signaling pathway. Dev Biol 307: 53-61.

Kolsch, V., T. Seher, G. J. Fernandez-Ballester, L. Serrano and M. Leptin, 2007 Control of Drosophila gastrulation by apical localization of adherens junctions and RhoGEF2. Science 315: 384-386.

Kornberg, T. B., and M. A. Krasnow, 2000 The Drosophila genome sequence: implications for biology and medicine. Science 287: 2218-2220.

Kozu, S., R. Tajiri, T. Tsuji, T. Michiue, K. Saigo *et al.*, 2006 Temporal regulation of late expression of Bar homeobox genes during Drosophila leg development by Spineless, a homolog of the mammalian dioxin receptor. Dev Biol 294: 497-508.

Kuhn, S., and M. Geyer, 2014 Formins as effector proteins of Rho GTPases. Small GTPases 5: e29513.

Lai, E. C., 2002 Keeping a good pathway down: transcriptional repression of Notch pathway target genes by CSL proteins. EMBO Rep 3: 840-845.

Lawrence, P. A., and G. Morata, 1977 The early development of mesothoracic compartments in Drosophila. An analysis of cell lineage and fate mapping and an assessment of methods. Dev Biol 56: 40-51.

Le Dreau, G., and E. Marti, 2012 Dorsal-ventral patterning of the neural tube: a tale of three signals. Dev Neurobiol 72: 1471-1481.

Lecuit, T., and S. M. Cohen, 1997 Proximal-distal axis formation in the Drosophila leg. Nature 388: 139-145.

Lee, J. Y., and R. M. Harland, 2010 Endocytosis is required for efficient apical constriction during Xenopus gastrulation. Curr Biol 20: 253-258.

Leptin, M., and B. Grunewald, 1990 Cell shape changes during gastrulation in Drosophila. Development 110: 73-84.

Liu, R., E. V. Linardopoulou, G. E. Osborn and S. M. Parkhurst, 2010 Formins in development: orchestrating body plan origami. Biochim Biophys Acta 1803: 207-225.

Llimargas, M., and J. Casanova, 2010 Apical constriction and invagination: a very self-reliant couple. Dev Biol 344: 4-6.

Lohmann, I., N. McGinnis, M. Bodmer and W. McGinnis, 2002 The Drosophila Hox gene deformed sculpts head morphology via direct regulation of the apoptosis activator reaper. Cell 110: 457-466.

Mack, N. A., and M. Georgiou, 2014 The interdependence of the Rho GTPases and apicobasal cell polarity. Small GTPases 5: 10.

Manjon, C., E. Sanchez-Herrero and M. Suzanne, 2007 Sharp boundaries of Dpp signalling trigger local cell death required for Drosophila leg morphogenesis. Nat Cell Biol 9: 57-63.

Mann, R. S., and G. Morata, 2000 The developmental and molecular biology of genes that subdivide the body of Drosophila. Annu Rev Cell Dev Biol 16: 243-271.

Manning, A. J., and S. L. Rogers, 2014 The Fog signaling pathway: insights into signaling in morphogenesis. Dev Biol 394: 6-14.

Martin, A. C., and B. Goldstein, 2014 Apical constriction: themes and variations on a cellular mechanism driving morphogenesis. Development 141: 1987-1998.

Martin, A. C., M. Kaschube and E. F. Wieschaus, 2009 Pulsed contractions of an actin-myosin network drive apical constriction. Nature 457: 495-499.

Martinez-Arias, A., and P. A. Lawrence, 1985 Parasegments and compartments in the Drosophila embryo. Nature 313: 639-642.

Mason, F. M., M. Tworoger and A. C. Martin, 2013 Apical domain polarization localizes actin-myosin activity to drive ratchet-like apical constriction. Nat Cell Biol 15: 926-936.

Mason, F. M., S. Xie, C. G. Vasquez, M. Tworoger and A. C. Martin, 2016 RhoA GTPase inhibition organizes contraction during epithelial morphogenesis. J Cell Biol 214: 603-617.

Massa, V., D. Savery, P. Ybot-Gonzalez, E. Ferraro, A. Rongvaux *et al.*, 2009 Apoptosis is not required for mammalian neural tube closure. Proc Natl Acad Sci U S A 106: 8233-8238.

McKay, D. J., C. Estella and R. S. Mann, 2009 The origins of the Drosophila leg revealed by the cis-regulatory architecture of the Distalless gene. Development 136: 61-71.

Mirth, C., and M. Akam, 2002 Joint development in the Drosophila leg: cell movements and cell populations. Dev Biol 246: 391-406.

Monier, B., M. Gettings, G. Gay, T. Mangeat, S. Schott *et al.*, 2015 Apico-basal forces exerted by apoptotic cells drive epithelium folding. Nature 518: 245-248.

Monier, B., and M. Suzanne, 2015 The Morphogenetic Role of Apoptosis. Curr Top Dev Biol 114: 335-362.

Morata, G., and P. Ripoll, 1975 Minutes: mutants of drosophila autonomously affecting cell division rate. Dev Biol 42: 211-221.

Morimura, S., L. Maves, Y. Chen and F. M. Hoffmann, 1996 decapentaplegic overexpression affects Drosophila wing and leg imaginal disc development and wingless expression. Dev Biol 177: 136-151.

Mulinari, S., M. P. Barmchi and U. Hacker, 2008 DRhoGEF2 and diaphanous regulate contractile force during segmental groove morphogenesis in the Drosophila embryo. Mol Biol Cell 19: 1883-1892.

Muqit, M. M., and M. B. Feany, 2002 Modelling neurodegenerative diseases in Drosophila: a fruitful approach? Nat Rev Neurosci 3: 237-243.

Natori, K., R. Tajiri, S. Furukawa and T. Kojima, 2012 Progressive tarsal patterning in the Drosophila by temporally dynamic regulation of transcription factor genes. Dev Biol 361: 450-462.

Neisch, A. L., O. Speck, B. Stronach and R. G. Fehon, 2010 Rho1 regulates apoptosis via activation of the JNK signaling pathway at the plasma membrane. J Cell Biol 189: 311-323.

Neubueser, D., and D. R. Hipfner, 2010 Overlapping roles of Drosophila Drak and Rok kinases in epithelial tissue morphogenesis. Mol Biol Cell 21: 2869-2879.

Nishimura, T., H. Honda and M. Takeichi, 2012 Planar cell polarity links axes of spatial dynamics in neural-tube closure. Cell 149: 1084-1097.

Nusslein-Volhard, C., and E. Wieschaus, 1980 Mutations affecting segment number and polarity in Drosophila. Nature 287: 795-801.

Pastor-Pareja, J. C., F. Grawe, E. Martin-Blanco and A. Garcia-Bellido, 2004 Invasive cell behavior during Drosophila imaginal disc eversion is mediated by the JNK signaling cascade. Dev Cell 7: 387-399.

Pearl, E. J., J. Li and J. B. Green, 2017 Cellular systems for epithelial invagination. Philos Trans R Soc Lond B Biol Sci 372.

Perez-Garijo, A., and H. Steller, 2015 Spreading the word: non-autonomous effects of apoptosis during development, regeneration and disease. Development 142: 3253-3262.

Presente, A., S. Shaw, J. S. Nye and A. J. Andres, 2002 Transgene-mediated RNA interference defines a novel role for notch in chemosensory startle behavior. Genesis 34: 165-169.

Proag, A., B. Monier and M. Suzanne, 2018 Physical and functional cell-matrix uncoupling in a developing tissue under tension. bioRxiv 306696.

Pueyo, J. I., and J. P. Couso, 2008 The 11-aminoacid long Tarsal-less peptides trigger a cell signal in Drosophila leg development. Dev Biol 324: 192-201.

Pueyo, J. I., and J. P. Couso, 2011 Tarsal-less peptides control Notch signalling through the Shavenbaby transcription factor. Dev Biol 355: 183-193.

Pueyo, J. I., M. I. Galindo, S. A. Bishop and J. P. Couso, 2000 Proximal-distal leg development in Drosophila requires the apterous gene and the Lim1 homologue dlim1. Development 127: 5391-5402.

Quintin, S., C. Gally and M. Labouesse, 2008 Epithelial morphogenesis in embryos: asymmetries, motors and brakes. Trends Genet 24**:** 221-230.

Rauskolb, C., 2001 The establishment of segmentation in the Drosophila leg. Development 128**:** 4511-4521.

Rauskolb, C., T. Correia and K. D. Irvine, 1999 Fringe-dependent separation of dorsal and ventral cells in the Drosophila wing. Nature 401**:** 476-480.

Rauskolb, C., and K. D. Irvine, 1999 Notch-mediated segmentation and growth control of the Drosophila leg. Dev Biol 210**:** 339-350.

Reeves, G. T., and A. Stathopoulos, 2009 Graded dorsal and differential gene regulation in the Drosophila embryo. Cold Spring Harb Perspect Biol 1**:** a000836.

Ridley, A. J., M. A. Schwartz, K. Burridge, R. A. Firtel, M. H. Ginsberg *et al.*, 2003 Cell migration: integrating signals from front to back. Science 302**:** 1704-1709.

Riento, K., and A. J. Ridley, 2003 Rocks: multifunctional kinases in cell behaviour. Nat Rev Mol Cell Biol 4**:** 446-456.

Robertson, F., N. Pinal, P. Fichelson and F. Pichaud, 2012 Atonal and EGFR signalling orchestrate rok- and Drak-dependent adherens junction remodelling during ommatidia morphogenesis. Development 139**:** 3432-3441.

Roh-Johnson, M., G. Shemer, C. D. Higgins, J. H. McClellan, A. D. Werts *et al.*, 2012 Triggering a cell shape change by exploiting preexisting actomyosin contractions. Science 335**:** 1232-1235.

Rosenblatt, J., M. C. Raff and L. P. Cramer, 2001 An epithelial cell destined for apoptosis signals its neighbors to extrude it by an actin- and myosin-dependent mechanism. Curr Biol 11**:** 1847-1857.

Royou, A., C. Field, J. C. Sisson, W. Sullivan and R. Karess, 2004 Reassessing the role and dynamics of nonmuscle myosin II during furrow formation in early Drosophila embryos. Mol Biol Cell 15**:** 838-850.

Rubin, G. M., and E. B. Lewis, 2000 A brief history of Drosophila's contributions to genome research. Science 287**:** 2216-2218.

Sai, X., S. Yonemura and R. K. Ladher, 2014 Junctionally restricted RhoA activity is necessary for apical constriction during phase 2 inner ear placode invagination. Dev Biol 394**:** 206-216.

San-Juan, B. P., and A. Baonza, 2011 The bHLH factor deadpan is a direct target of Notch signaling and regulates neuroblast self-renewal in Drosophila. Dev Biol 352**:** 70-82.

Sawyer, J. M., J. R. Harrell, G. Shemer, J. Sullivan-Brown, M. Roh-Johnson *et al.*, 2010 Apical constriction: a cell shape change that can drive morphogenesis. Dev Biol 341**:** 5-19.

Schock, F., and N. Perrimon, 2002 Molecular mechanisms of epithelial morphogenesis. Annu Rev Cell Dev Biol 18: 463-493.

Shellenbarger, D. L., and J. D. Mohler, 1978 Temperature-sensitive periods and autonomy of pleiotropic effects of l(1)Nts1, a conditional notch lethal in Drosophila. Dev Biol 62: 432-446.

Shen, J., and C. Dahmann, 2005 Extrusion of cells with inappropriate Dpp signaling from Drosophila wing disc epithelia. Science 307: 1789-1790.

Shepard, R., K. Heslin and L. Coutellier, 2017 The transcription factor Npas4 contributes to adolescent development of prefrontal inhibitory circuits, and to cognitive and emotional functions: Implications for neuropsychiatric disorders. Neurobiol Dis 99: 36-46.

Shubin, N., C. Tabin and S. Carroll, 1997 Fossils, genes and the evolution of animal limbs. Nature 388: 639-648.

Siegrist, S. E., N. S. Haque, C. H. Chen, B. A. Hay and I. K. Hariharan, 2010 Inactivation of both Foxo and reaper promotes long-term adult neurogenesis in Drosophila. Curr Biol 20: 643-648.

Sim, S., S. Antolin, C. W. Lin, Y. Lin and C. Lois, 2013 Increased cell-intrinsic excitability induces synaptic changes in new neurons in the adult dentate gyrus that require Npas4. J Neurosci 33: 7928-7940.

Simoes, S., B. Denholm, D. Azevedo, S. Sotillos, P. Martin *et al.*, 2006 Compartmentalisation of Rho regulators directs cell invagination during tissue morphogenesis. Development 133: 4257-4267.

Slattum, G., K. M. McGee and J. Rosenblatt, 2009 P115 RhoGEF and microtubules decide the direction apoptotic cells extrude from an epithelium. J Cell Biol 186: 693-702.

Snodgrass, R., 1935 Principles of Insect Morphology. New York: McGraw-Hill: pp. 83-99.

Somogyi, K., and P. Rorth, 2004 Evidence for tension-based regulation of Drosophila MAL and SRF during invasive cell migration. Dev Cell 7: 85-93.

Sosinsky, A., C. P. Bonin, R. S. Mann and B. Honig, 2003 Target Explorer: An automated tool for the identification of new target genes for a specified set of transcription factors. Nucleic Acids Res 31: 3589-3592.

Steffen, P. A., and L. Ringrose, 2014 What are memories made of? How Polycomb and Trithorax proteins mediate epigenetic memory. Nat Rev Mol Cell Biol 15: 340-356.

Stern, D. L., and E. Sucena, 2012 Rapid mounting of adult Drosophila structures in Hoyer's medium. Cold Spring Harb Protoc 2012: 107-109.

Struhl, G., and K. Basler, 1993 Organizing activity of wingless protein in Drosophila. Cell 72: 527-540.

Strutt, D. I., U. Weber and M. Mlodzik, 1997 The role of RhoA in tissue polarity and Frizzled signalling. Nature 387: 292-295.

Suzanne, M., 2016 Molecular and cellular mechanisms involved in leg joint morphogenesis. Semin Cell Dev Biol 55: 131-138.

Suzanne, M., A. G. Petzoldt, P. Speder, J. B. Coutelis, H. Steller *et al.*, 2010 Coupling of apoptosis and L/R patterning controls stepwise organ looping. Curr Biol 20: 1773-1778.

Suzanne, M., and H. Steller, 2013 Shaping organisms with apoptosis. Cell Death Differ 20: 669-675.

Svendsen, P. C., J. R. Ryu and W. J. Brook, 2015 The expression of the T-box selector gene midline in the leg imaginal disc is controlled by both transcriptional regulation and cell lineage. Biol Open 4: 1707-1714.

Symons, M., and N. Rusk, 2003 Control of vesicular trafficking by Rho GTPases. Curr Biol 13: R409-418.

Tajiri, R., K. Misaki, S. Yonemura and S. Hayashi, 2010 Dynamic shape changes of ECM-producing cells drive morphogenesis of ball-and-socket joints in the fly leg. Development 137: 2055-2063.

Tajiri, R., K. Misaki, S. Yonemura and S. Hayashi, 2011 Joint morphology in the insect leg: evolutionary history inferred from Notch loss-of-function phenotypes in Drosophila. Development 138: 4621-4626.

Tajiri, R., T. Tsuji, R. Ueda, K. Saigo and T. Kojima, 2007 Fate determination of Drosophila leg distal regions by trachealess and tango through repression and stimulation, respectively, of Bar homeobox gene expression in the future pretarsus and tarsus. Dev Biol 303: 461-473.

Tan, J. L., S. Ravid and J. A. Spudich, 1992 Control of nonmuscle myosins by phosphorylation. Annu Rev Biochem 61: 721-759.

Theisen, H., T. E. Haerry, M. B. O'Connor and J. L. Marsh, 1996 Developmental territories created by mutual antagonism between Wingless and Decapentaplegic. Development 122: 3939-3948.

Toyama, Y., X. G. Peralta, A. R. Wells, D. P. Kiehart and G. S. Edwards, 2008 Apoptotic force and tissue dynamics during Drosophila embryogenesis. Science 321: 1683-1686.

Van Aelst, L., and M. Symons, 2002 Role of Rho family GTPases in epithelial morphogenesis. Genes Dev 16: 1032-1054.

Vasquez, C. G., and A. C. Martin, 2016 Force transmission in epithelial tissues. Dev Dyn 245: 361-371.

von Kalm, L., D. Fristrom and J. Fristrom, 1995 The making of a fly leg: a model for epithelial morphogenesis. Bioessays 17: 693-702.

Wangler, M. F., S. Yamamoto and H. J. Bellen, 2015 Fruit flies in biomedical research. Genetics 199: 639-653.

Ward, M. P., J. T. Mosher and S. T. Crews, 1998 Regulation of bHLH-PAS protein subcellular localization during Drosophila embryogenesis. Development 125: 1599-1608.

Watanabe, N., P. Madaule, T. Reid, T. Ishizaki, G. Watanabe *et al.*, 1997 p140mDia, a mammalian homolog of Drosophila diaphanous, is a target protein for Rho small GTPase and is a ligand for profilin. EMBO J 16**:** 3044-3056.

Weng, M., and E. Wieschaus, 2016 Myosin-dependent remodeling of adherens junctions protects junctions from Snail-dependent disassembly. J Cell Biol 212**:** 219-229.

White, K., M. E. Grether, J. M. Abrams, L. Young, K. Farrell *et al.*, 1994 Genetic control of programmed cell death in Drosophila. Science 264**:** 677-683.

Widmann, T. J., and C. Dahmann, 2009 Dpp signaling promotes the cuboidal-to-columnar shape transition of Drosophila wing disc epithelia by regulating Rho1. J Cell Sci 122**:** 1362-1373.

Wilder, E. L., and N. Perrimon, 1995 Dual functions of wingless in the Drosophila leg imaginal disc. Development 121**:** 477-488.

Wilson, R., L. Goyal, M. Ditzel, A. Zachariou, D. A. Baker *et al.*, 2002 The DIAP1 RING finger mediates ubiquitination of Dronc and is indispensable for regulating apoptosis. Nat Cell Biol 4**:** 445-450.

Winter, C. G., B. Wang, A. Ballew, A. Royou, R. Karess *et al.*, 2001 Drosophila Rho-associated kinase (Drok) links Frizzled-mediated planar cell polarity signaling to the actin cytoskeleton. Cell 105**:** 81-91.

Wolpert, L., and C. Tickle, 2011 *Principles of Development. Fourth edition*. Oxford University Press.

Xu, D., Y. Li, M. Arcaro, M. Lackey and A. Bergmann, 2005 The CARD-carrying caspase Dronc is essential for most, but not all, developmental cell death in Drosophila. Development 132**:** 2125-2134.

Xu, D., S. E. Woodfield, T. V. Lee, Y. Fan, C. Antonio *et al.*, 2009 Genetic control of programmed cell death (apoptosis) in Drosophila. Fly (Austin) 3**:** 78-90.

Xu, N., B. Keung and M. M. Myat, 2008 Rho GTPase controls invagination and cohesive migration of the Drosophila salivary gland through Crumbs and Rho-kinase. Dev Biol 321**:** 88-100.

Yamaguchi, Y., N. Shinotsuka, K. Nonomura, K. Takemoto, K. Kuida *et al.*, 2011 Live imaging of apoptosis in a novel transgenic mouse highlights its role in neural tube closure. J Cell Biol 195**:** 1047-1060.

Yoshihara, S., H. Takahashi, N. Nishimura, M. Kinoshita, R. Asahina *et al.*, 2014 Npas4 regulates Mdm2 and thus Dcx in experience-dependent dendritic spine development of newborn olfactory bulb interneurons. Cell Rep 8**:** 843-857.

Young, P. E., A. M. Richman, A. S. Ketchum and D. P. Kiehart, 1993 Morphogenesis in Drosophila requires nonmuscle myosin heavy chain function. Genes Dev 7**:** 29-41.

Zegers, M. M., and P. Friedl, 2014 Rho GTPases in collective cell migration. Small GTPases 5**:** e28997.

Zimmerman, S. G., L. M. Thorpe, V. R. Medrano, C. A. Mallozzi and B. M. McCartney, 2010 Apical constriction and invagination downstream of the canonical Wnt signaling pathway require Rho1 and Myosin II. Dev Biol 340**:** 54-66.

ACKNOWLEDGEMENTS

Apologizing to the English reader that might reach these pages, this section of the Thesis is going to be written in Spanish, as Spanish is most of the people that should be acknowledged for making possible this work.

Esta Tesis, como supongo que todas las demás, es fruto de un largo y laborioso proceso, y difícilmente puede ser entendida como el trabajo individual de una sola persona. Al contrario, que yo haya sido capaz de llegar hasta aquí ha sido gracias a la ayuda de muchas personas, tanto en el ámbito científico como en el personal.

En primer lugar, me gustaría darle las gracias Carlos, mi director de Tesis y el primer responsable de que este trabajo haya salido adelante. Realmente creo que he tenido mucha suerte de haber llegado al sitio al que llegué y en el momento en el que lo hice. Ha sido un auténtico placer poder trabajar contigo y aprender de ti durante estos años de formación. Me llevo de esta etapa varias lecciones importantes y que estoy seguro de que me van a ser muy útiles en mi futura carrera en este mundo tan complicado. Creo que has sabido inculcarme la autoexigencia y el rigor que hacen falta para poder afrontar con garantías el trabajo científico. Ser el primer crítico de mi propio trabajo es la principal enseñanza que me llevo en el zurrón, y espero tenerla muy presente ahora y siempre. Además un trabajo como el nuestro, que exige tanto tiempo y dedicación, sería un auténtico dolor de muelas si no estuviéramos rodeados de buena gente, y me alegra poder decir que en eso también he tenido una enorme suerte al haber tenido el jefe que he tenido. Y por último, pero no por ello menos importante, me gustaría señalar que mi gusto musical se ha visto muy mejorado durante estos años de estancia bajo la dirección del Dr. Estella.

Tengo que agradecer también a José Félix y a Antonio, que siempre han estado cerca como referencia y como apoyo, y que han ayudado a curtir mi joven pellejo científico en los seminarios de grupo que he tenido la suerte de compartir con ellos. No quiero olvidarme tampoco de Mar Ruiz, Sonsoles y Quim. Ha sido un privilegio tener a mano tantos puntos de vista experimentados y capaces, que han ayudando a pulir mi trabajo y me han obligado a estar siempre alerta al mostrar mis resultados. También tengo que destacar las aportaciones fundamentales de Ernesto Sánchez-Herrero a este trabajo, por guiar nuestra vista hacia la morfogénesis de las articulaciones y por las siempre edificantes y honestas discusiones sobre nuestro modelo.

Como decía antes, este trabajo ya tiene de por sí sus complicaciones, y todo hubiera sido mucho más aburrido y complicado si no hubiera tenido los compañeros que he tenido a lo largo del camino. Por supuesto los que están presentes ahora; pero también los que han pasado por el laboratorio y por el centro durante estos años, y a los que ha sido un placer haber conocido y una pena haber despedido. De todos he aprendido cosas, y todos han hecho que ir al laboratorio sea una motivación para levantarse cada mañana.

Llegué el primero al grupo de Carlos, pero por suerte eso duró poco. Un recuerdo para todas las incorporaciones que fueron animando el cotarro, y las que seguirán llevando esto adelante ahora que llega mi momento de decir hasta luego. A Almudena, que al final entendió que su lugar estaba en un campo de rugby. A José Andrés y David, que llegaron a la vez y, la verdad, a mí me supo a poco. Son el tipo de gente que uno desea tener siempre alrededor, que está siempre ahí para ayudar o para dar unas palabras de ánimo. A los dos Cristian, al sevillano al que conocí menos de lo que me gustaría y al vallecano al que vi esforzarse siempre por hacerlo bien. A Hugo por ser siempre una fuente de alegría y buen rollo, y que espero que lo siga siendo cuando tenga que ir a trabajar de traje y corbata. A Pablete, que vale muchísimo aunque a veces tenga la cabeza por las nubes, como su dron. Y por último a los que están en el laboratorio en este momento: a Mireya, que sé que es mucho mejor científica de lo que ella misma se piensa, y que pronto nos llevará de sarao a Jerez; a David, al que he conocido muy poquito pero le deseo toda la suerte del mundo y al nuevo Pablo, del que lo único que puedo decir (y no es poco) es que parece que viene con ganas y la mejor actitud.

Por supuesto quiero también agradecer a la gente de nuestros dos grupos hermanos. Han cambiado mucho las caras desde que llegué, pero siempre he estado rodeado de buenos amigos. A Ana López y a Nuria, que son las primeras caras que veo cada mañana (¿quién va a deciros ahora '*buongiorno*'?) y a las que se me va a hacer muy raro dejar de ver. A Ana Ruiz, que ha sido mi proveedora de cafeína en cápsulas durante estos años y una más que paciente profesora de la alquimia que es la bioquímica. Por supuesto a Cris, mi camarada de la Complutense, que me hace preguntarme cómo es que no conocí a tal encanto de muchacha cuando estábamos en la carrera. Me alegro de veras que nuestros caminos se hayan juntado después, eres una compañera de diez. Me acuerdo mucho en estos momentos de Mer, que me ha dado innumerables horas de conversación en la Fly Room, y con la que comparto la querencia por las palabras súper súper bonicas de la lengua de Cervantes. Quiero agradecer también a Cova, que tiene las cosas siempre tan claras que más de una vez me ha ayudado a aclararme a mí. Y también a María y a Cris Molnar, que tanto me ayudaron durante los primeros años. Y claro, no puedo olvidarme de las chicas de Ana Ruiz, de Julia que siempre tenía una sonrisa en la boca y de Patri, que sigue la misma línea de compañerismo y amabilidad, y que poco a poco vencerá a su timidez para demostrar lo que vale. A Inés, Tamara y Alberto, que estos últimos meses han compartido conmigo las penurias de sus respectivos TFs.

Del laboratorio de Baonza fue un placer compartir espacio pre-mudanza con las tres históricas; Bea, Sandra e Irene, que siempre me han tratado con un enorme cariño y a quienes admiro de veras. Espero que

algún día volváis de la diáspora y nos podamos tomar una buena cerveza juntos. A Javiercete, que aunque haya dejado el boxeo tenemos pendiente una sesión de sparring (pero flojito). Temo que sin tu ayuda voy a perderme gran cantidad de memes y vídeos virales, mantenme al corriente por favor. Benjas, a ver si dentro de unos meses y con tu flamante ciudadanía chipriota estamos celebrando la tuya con unas chelas bien padres. Y a Sara, que seguro que no se toma una chela sino una buena manzanilla bien fresquita. Va a ser difícil enumerar a toda la gente que ha pasado por el laboratorio 412, así que por favor, daros por recordados todos los que estáis o habéis estado por allí, porque todos me habéis aportado algo. Ha sido un placer conoceros, y un verdadero reto cada día encontrar mesa en el comedor para tres laboratorios al completo.

Y en fin, al resto de compañeros del Departamento con los que he compartido charlas científicas y no tan científicas, risas y alguna que otra cervecita (aunque me hubiera gustado compartir más). Gracias en especial a Ana Guarner, que me enseñó algo tan fundamental para esta Tesis como diseccionar pupas, y a apreciar la suerte que tuve al toparme con *dysf*. Y a Nuria, que ha tenido más paciencia que un santo explicándole punto por punto a un zote como yo cómo hacer los papeles de una Tesis sin perecer en el camino.

A Magali, que me acogió en su laboratorio de Toulouse, y a todo su equipo. A Arnaud, Amsha y Lucie, a los que considero de verdad amigos y que hicieron que nunca me sintiera solo a mil kilómetros de casa.

Por último, dentro del ámbito laboral, me gustaría dar las gracias al servicio de transgénesis, a Eva, Mar Casado (precioso apellido) y Lorena, porque siempre trabajan duro pero con una sonrisa, y al servicio de cocina porque sin ellas nuestro trabajo sería simplemente imposible. También al servicio de microscopía confocal, donde he pasado gran parte de esta Tesis y donde siempre me han ayudado con enorme amabilidad.

Por supuesto, no estaría escribiendo los agradecimientos de una Tesis Doctoral si no tuviera una familia como la que tengo detrás. Le dedico esta Tesis a mis padres, que me han dado siempre su amor incondicional y sobre todo su apoyo. En casa siempre me animaron a hacer la carrera que de verdad me llenara, y eso lo he tenido muy presente siempre. Gracias porque me lo habéis dado todo, no se os puede pedir más. Me han dado, incluso, un hermano mellizo, que es mi otra mitad y con el que comparto la vida desde, precisamente, el desarrollo embrionario. A mi segunda madre, que fue mi tía Araceli, que capeó siempre el temporal con una alegría y una fuerza inquebrantables. A mi abuela, que espero esté muy orgullosa de su nieto, y no sólo por hacerse doctor. Y a todos mis tíos y primos, que hacen que la palabra ‘familia’ sea mucho más que una mera formalidad.

A Ana, mi compañera y mi apoyo. Sin ti sería otra persona, menos completa y mucho menos feliz. Gracias por estar ahí, por hacerme reír y por aguantarme cuando estoy de mal humor. Y prepárate porque me tendrás que aguantar aún mucho tiempo. Espero darte siempre más alegrías que penas, y ser merecedor de que te quedes a mi lado. Y gracias también a tus padres y tu hermano, que me hacen sentir que tengo una segunda familia en levante. Ánimo, fuerza y optimismo.

A la gente que conocí en la universidad cuando éramos unos biólogos verdes y pimpollos. A Alba, a la que por suerte sigo teniendo cerca después de tantos años, y a Cris y Jesús, que saben bien lo que se sufre y se disfruta de una Tesis. A Geo, que todavía me hace emocionarme una vez al año con un balón ovalado en las manos, y que me enseñaron que hay que levantarse siempre a por el siguiente *ruck*. A Mr. Tirado, que me acompañó durante el mejor año de mi vida y que espero que algún día saque un ratito para tomarse una caña con un viejo amigo. A Xabi, que me llevó a Eibar a disfrutar del fútbol de siempre y a Miguel, que no sé ni dónde estará ahora. A todos los amigos que me traje de Århus, porque aquello fue irrepetible.

A los amigos que de verdad merecen tal nombre. Soy un amigo pésimo, descuidado y medio ausente, y sin embargo siempre estáis ahí. Vosotros sabréis por qué, pero yo os lo agradezco de corazón. A Guille, que tira cobetes desde Alicante y a Andrea, que lleva dentro el espíritu ilustrado de la Guardia Civil. A Sara, que es talento puro y tiene una capacidad de trabajo que a mi me asombra. A Keyvan y Clara, que me dejaron al cuidado de su piso londinense y de su gato. Pero ahora volved, chicos, ya toca. A Nachete que va a ser doctor de galaxias, y a Adri que todavía me recuerda la pasión del arte en pequeñito. Y quién lo iba a decir, también doy las gracias a un puñado de ingenieros, aunque sigan creyendo que sirvo patatas en un McDonalds.

Lo peor es que, a pesar del tostón que acabo de soltar, más de uno se ha quedado sin nombrar. Mis disculpas. Y mi sincero agradecimiento a todo el que, de una manera u otra, ha hecho de mí la persona y el científico que soy ahora.